DEVELOPMENT OF POLYPYRROLE/NAFION COMPOSITE MEMBRANES AND A DYNAMIC HYDROGEN REFERENCE ELECTRODE FOR DIRECT METHANOL FUEL CELLS

JUN ZHU

NOTE TO USERS

Development of Polypyrrole/Nafion Composite Membranes and a Dynamic Hydrogen Reference Electrode for Direct Methanol Fuel Cells

by

Jun Zhu

A thesis submitted to the School of Graduate Studies in partial fulfillment of the requirements for the degree of Master of Science.

Department of Chemistry
Memorial University of Newfoundland
St. John's, Newfoundland, Canada
August 2004

Your file Votre référence
ISBN: 0-494-02396-1
Our file Notre référence
ISBN: 0-494-02396-1

Abstract

One major goal of this research was to increase the fuel efficiency and cell performance of direct methanol fuel cells (DMFCs) by decreasing the methanol crossover from the anode to the cathode. Polypyrrole/Nafion composite membranes were prepared, and factors influencing the modification procedures were studied. An optimized, reproducible modification procedure was developed. The composite membranes outperformed pure Nafion 115 but need a longer activation time. The polarization and electrochemical impedance spectroscopy measurements showed that the activation process was due to two main factors: slow membrane hydration and slow cathode activation. The composite membranes showed an over 40% reduction in methanol crossover and a 70% increase in membrane resistance relative to Nafion 115. To further decrease the membrane resistance, counter ions were provided in the modification process. Poly[3-(pyrrole-1-yl)propanesulfonate]/Nafion composite membranes were also prepared to address this problem.

Another major goal was to develop and characterize a micro reference electrode to resolve the anode and cathode behavior in a fuel cell. An edge type Pt wire Dynamic Hydrogen Electrode (DHE) reference electrode was developed and used in a hydrogen proton exchange membrane fuel cell and a DMFC. The advantage of this DHE is that it is easy to use and does not require modification of the fuel cell hardware. This reference electrode provided good qualitative information. However, potential drift over long times makes it inappropriate for long-term measurements.

Acknowledgements

I would like to express my sincere appreciation to Dr. Peter Pickup for his supervision and guidance throughout the duration of the degree program. I would also like to thank my supervisory committee, Dr. M. Mackey and Dr. G. Bodwell for their comments and advice throughout the course of my studies.

A special thanks to all the members of the Pickup research group for their help and the wonderful time spent together over the past two years. In particular, I would like to thank Dr. Chaojie Song, Dr. Brad Easton and Guangchun Li for their helpful discussions.

Financial support from the School of Graduate Studies, the Chemistry Department, NSERC are gratefully acknowledged.

Finally, I would like to thank my family, my wife and friends for all their support and encouragement throughout my studies.

Table of Contents

List of Abbreviations and Symbols

AC – Alternating current

AFC – Alkaline fuel cell

ATR-FTIR – Attenuated total reflection Fourier transfer infrared

CV – Cyclic voltammetry or cyclic voltammogram

CFP – Carbon fiber paper

DHE – Dynamic hydrogen electrode

DMFC – Direct methanol fuel cell

EIS – Electrochemical impedance spectroscopy

MCFC – Molten carbonate fuel cell

MEA – Membrane electrode assembly

NMR – Nuclear magnetic resonance

ORR – Oxygen reduction reaction

OCP – Open circuit potential

PAFC – Phosphoric acid fuel cell

PBI – polybenzimidazole

PEEK – poly(etheretherketone)

PEM – Proton exchange membrane

PEMFC – Proton exchange membrane Fuel cell

PP – Polyphenylene

PTFE – Polytetrafluoroethylene

PVA – Poly(vinyl alcohol)

RHE – Reversible hydrogen electrode

SOFC – Solid oxide fuel cell

C_m – Methanol concentration

d – Membrane thickness

D_m – Methanol diffusion coefficient

E – Potential

F – Faraday constant

I – Current

J_{lim} – Limiting methanol crossover current density

k_{dl} – Drag coefficient

R – Resistance

Z' – Real resistance

Z'' – Imaginary resistance

ξ – Electro-osmetic drag coefficient

ε – Membrane porosity

List of Tables

List of Figures

Chapter 1

Chapter 2

Chapter 3

Chapter 4

Chapter 5

Chapter 1

General Review of Fuel Cells

1.1 Introduction to Fuel Cells

A fuel cell can be defined as an instrument that can continuously convert chemical energy to electrical energy and heat,[1] without combustion. Unlike a battery, the fuel cell does not need recharging. As long as fuel (such as hydrogen, methanol, propane, etc.) and an oxidizing agent (pure oxygen or air) are supplied, it can continue to supply an electrical current indefinitely.

The fuel cell is not a new device. More than one and a half centuries ago, the British chemist Sir William Robert Grove first demonstrated a hydrogen-air fuel cell (what he called a "gas battery") in 1839.[2] But the fuel cell did not begin to reach a fraction of its potential because of economic factors and materials problems. Almost a century later, in 1932, Francis Bacon produced a successful device in the first major fuel cell project. Subsequently, fuel cells were applied as power sources for NASA space flights in the Gemini and Apollo space programs in the 1960s.[3] It was then that fuel cells were pulled out of the lab and into the mainstream of modern technology.

The key advantages of the fuel cell are high efficiency and the lack of emissions. The high efficiency arises from the electrochemical nature of energy conversion. A fuel cell converts the chemical energy of the fuel directly into electricity without going through an intermediate combustion step for internal combustion and other heat engines. It therefore is not limited by the Carnot cycle. Fuel cells can also significantly reduce carbon dioxide emission, and are also free from other harmful emissions, such as No_x,

SO_x and airborne particles.[4,5] Moreover, fuel cells have no moving parts and noise pollution can be reduced.[6]

These numerous advantages make fuel cells the perfect candidates for an alternative energy source. With their high efficiency, low maintenance, and low pollution production, fuel cells will make a valuable contribution to future power generation facilities.

1.2. Principles of Fuel Cells

The basic structure of all fuel cells is similar. The cell consists of an anode (negatively charged electrode) and a cathode (a positively charged electrode) which are separated by an electrolyte (a conductor of ions) and which are connected by an external circuit. In a hydrogen cell, the hydrogen gas separates into protons and electrons at the anode under the activation of a catalyst, and the electrons are conducted through a wire, forming an electrical current. The protons move through the electrolyte, where they combine with oxygen and electrons at the cathode to produce heat and water as byproducts.

Since the fuel cell operates isothermally, all the free energy (ΔG) associated with this reaction should in principle be converted to electrical energy. The cell voltage is related to the Gibbs free energy change of the fuel oxidation via:[7]

$$\Delta G = -nF\Delta E^0 \qquad (1.1)$$

where n is the number of electrons involved in the reaction, F is the Faraday constant, and

ΔE^0 is the thermodynamic equilibrium voltage of the cell.

For the case of a hydrogen/oxygen fuel cell, the overall reaction is:

$$H_2 + 1/2\ O_2 \rightarrow H_2O, \text{ with } \Delta G = -273kJ/mol \text{ at } 25\ ^\circ C \qquad (1.2)$$

The thermodynamic equilibrium voltage for standard conditions is $\Delta E^0 = 1.23V$.

However, slow kinetics mean that the equilibrium value is never achieved. The real cell potential ΔE is always lower than the equilibrium voltage described by the Nernst equation and decreases as current is drawn from the cell due to the mass transfer hindrance within both electrode reactions together with the net resistive components of the cell. ΔE is expressed in Equation 1.3:

$$\Delta E = E_{cathode} - E_{anode} - iR \qquad (1.3)$$

The potential of the each electrode is determined by:

$$E_{cathode\ or\ anode} = E_{eq} - \eta_{kinetic} - \eta_{conc.} \qquad (1.4)$$

Where E_{eq} is the equilibrium potential of the electrode, $\eta_{kinetic}$ is the kinetic overpotential, and $\eta_{conc.}$ is the concentration overpotential.

$E_{eq.}$ is given by the Nernst equation:

$$E_{eq.} = E^\circ + RT/nF\ln(a_O/a_R) \qquad (1.5)$$

$\eta_{kinetic}$ is due to slow charge transfer at the electrode and it can be expressed as the Tafel equation at large overpotentials.

$$\eta_{kinetic} = a + b\log(i) \qquad (1.6)$$

where a is a constant, b is the Tafel slope, and i is the current density.

$\eta_{conc.}$ is due to slow mass transport of fuel or oxygen in the cell and it dominates the cell's performance at high current densities.

The ohmic resistance drop is due to the resistance of the electrolyte and cell contacts and is mainly determined by the resistance of the electrolyte.

1.3 Types of Fuel Cells

There are numerous types of fuel cells that have been made. According to the electrolyte employed, a fuel cell can be classified as a Phosphoric Acid Fuel Cell, Molten Carbonate Fuel Cell, Solid Oxide Fuel Cell, Alkaline Fuel Cell or Proton Exchange Membrane Fuel Cell (PEMFC).[8,9,10] Fuel cells are also classified based on the fuel employed. In a Direct Methanol Fuel Cell (DMFC), for example, methanol is directly fed into the fuel cells without the intermediate step of reforming into hydrogen.[11] DMFCs based on PEMFC technology are the focus of this thesis and are therefore reviewed in detail in 1.4. The other types are briefly reviewed below.

1.3.1 Alkaline Fuel Cells (AFCs)

Alkaline fuel cells were one of the first fuel cell technologies developed, and they were the first type of fuel cell to be used by NASA on space missions. These fuel cells use a solution of potassium hydroxide in water as the electrolyte and can use a variety of non-precious metals as a catalyst at the anode and cathode.

One main advantage of AFCs is the faster kinetics of the oxygen reduction reaction in base. Their efficiency can up to 70 percent. However, this type of fuel cell is easily poisoned by trace amounts of carbon dioxide (CO_2), which makes it necessary to purify both the hydrogen and oxygen used in the cell. This purification process is costly. Also, susceptibility to poisoning shortens lifetimes. Moreover, hydrogen oxidation kinetics are slower in base than in acid.

1.3.2 Phosphoric Acid Fuel Cells (PAFCs).

PAFCs are commercially available today. The electrolyte is liquid phosphoric acid which is usually soaked into a SiC-based matrix. Recently, polybenzimidazole (PBI) membranes doped with phosphoric acid have been produced. PAFCs are typically operated in the range of 150-200 $°C$. At lower temperatures, phosphoric acid is a poor ionic conductor, and carbon monoxide (CO) poisoning of the Platinum (Pt) electro-catalyst in the anode becomes severe.

One of the main advantages of this type of fuel cell is that it can use impure hydrogen as a fuel. PAFCs can tolerate a CO concentration of about 2%, which broadens the choice of fuels they can use.

1.3.3 Molten Carbonate Fuel Cells (MCFCs).

MCFCs use a liquid solution of lithium, sodium and/or potassium carbonates as the

electrolyte. The molten carbonate is stabilized in a reinforced matrix (such as a Al_2O_3 supported $LiAlO_2$ matrix). The use of a molten carbonate as the electrolyte solves the electrolyte carbonation problem for AFCs. They operate at about $650\,°C$ to achieve sufficient conductivity of the electrolyte. The high operating temperature serves as a big advantage because this allows the flexibility to use more types of fuels and inexpensive catalysts. A disadvantage to this, however, is that high temperatures enhance corrosion and the breakdown of cell components.

1.3.4 Solid Oxide Fuel Cells (SOFCs)

SOFCs use a solid ceramic of yttria-stabilized zirconia as the electrolyte, which is an excellent conductor of negatively charged oxygen (oxide) ions at high temperatures. Solid Oxide Fuel Cells (SOFCs) are the highest-temperature fuel cells in development currently and can be operated above 1000°C.[12] The high temperature enables them to tolerate relatively impure fuels. However, the high temperatures require more expensive construction materials.

1.3.5 Proton Exchange Membrane Fuel Cells (PEMFCs)

Proton exchange membrane fuel cells (PEMFCs), also called polymer electrolyte membrane fuel cells, use a thin proton exchange membrane, mainly Nafion by DuPont,[13] as the electrolyte. The PEM separates the anode and cathode and also serves as the proton

conductor between these two electrodes. Compared to other fuel cells, PEMFCs deliver high power density and offer the advantages of low weight and volume. They need only hydrogen, oxygen or air, and water to operate and do not require corrosive fluids like the other fuel cells. Typically, PEMFCs are fueled with pure hydrogen supplied from storage tanks or with a H_2/CO_2 mixture from a reformer.

PEMFCs are generally operated at 80-100°C because of the limitations imposed by the thermal properties of the PEM. That makes it quick to bring the cell to its operating temperature. However, recent research has been focused on high temperature PEMFCs.[14] The operating temperature is supposed to be up to 200°C, so that the fuel cell is more resistant to carbon monoxide impurities in the hydrogen, and water and heat management are simpler and more cost-effective.

Direct methanol fuel cells are often based on proton exchange membrane fuel cells. Compared with a hydrogen PEMFC, direct methanol fuel cells have tremendous advantages. Operating a fuel cell with a liquid fuel is considered to be essential for transport applications. Methanol can be safely stored, transported and supported from the existing gasoline distribution network.[15] Moreover, DMFCs also have some system design advantages over hydrogen PEMFCs. For instance, DMFCs eliminate the heavy and bulky fuel processor (or reformer) for the hydrogen reformer cell.[16,17] The DMFC system doesn't need the complex humidification and heat management hardware used in hydrogen PEMFC systems.

1.4 Direct Methanol Fuel Cells

1.4.1 Introduction to Direct Methanol Fuel Cells

Direct Methanol Fuel Cells represent an exciting area of fuel cell research because of their high energy density, simple system design and operation. People began to study DMFCs early in the 1960s.[18] As methanol and other small organic molecules are more reactive in basic media than in acid media, an alkaline electrolyte was used at that time. As in the AFC, carbonation of the electrolyte (caused by the complete oxidation of methanol to carbon dioxide) decreased the cell efficiency by decreasing the electrolyte conductivity and cathode electrode depolarization.[19] Thereafter, researchers studied the use of concentrated sulfuric acid as an electrolyte.[20] The recent rapid development of DMFCs is thanks to the introduction of proton exchange membranes, an electronic insulator that allows protons to migrate through it. The best available PEM to date is the Nafion perflurosulfonic acid series of membranes. Nafion was invented by Dupont in the 1960s, and initially used as a separator in electrolysis cells.[21,22] However, Nafion membranes began to gain popularity as solid polymer electrolytes in fuel cells until 1990.[23] Although significant performance gains have been achieved using Nafions, many problems, especially methanol crossover, still exist that must be overcome. The properties of Nafion and other alternative PEMs are discussed in detailed in Section 1.5.

1.4.2 Principles of the DMFC

The key part of a DMFC is the membrane electrode assembly (MEA). The components of a MEA are shown in Fig.1.1. It consists of five layers, which include gas and liquid diffusion layers, a catalytic methanol anode and a catalytic oxygen cathode layer, separated by a proton conducting membrane. Generally, the MEA is prepared by hot-pressing the cathode and the anode onto each side of the membrane.

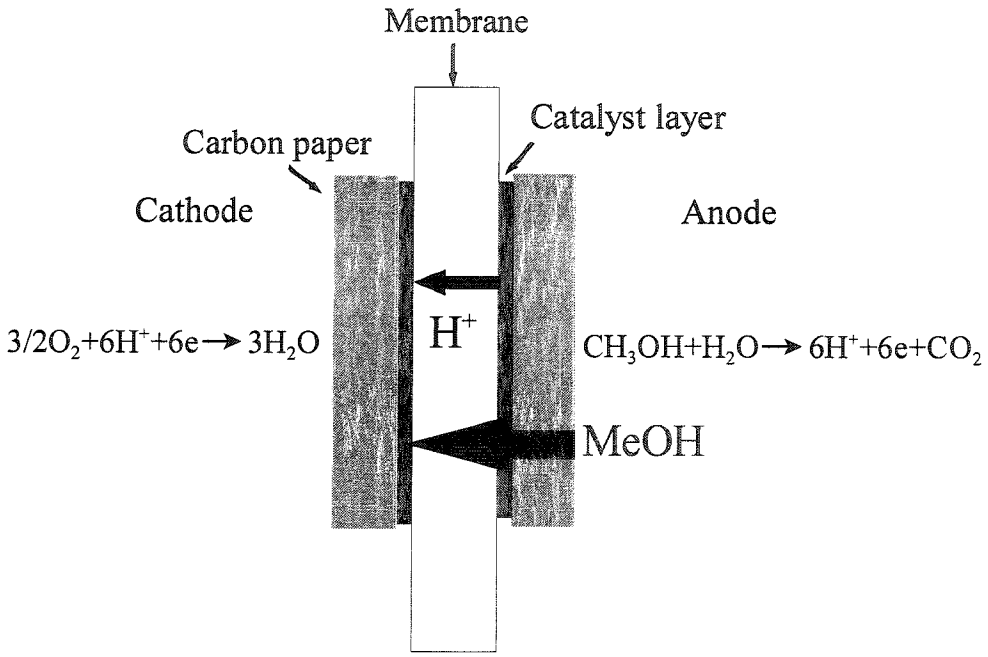

Fig. 1.1. Schematic diagram of a Membrane Electrodes Assembly (MEA) of a DMFC

The main DMFC processes include methanol oxidation on the anode, oxygen reduction on the cathode, liquid transport and oxygen gas permeation through the backing and catalyst layers, proton and water transport in the PEM layer, and the methanol crossover as shown in Figure 1.1.

The DMFC has a thermodynamic voltage of 1.18V at 25 °C, determined by the electrochemical oxidation of methanol (in acid electrolyte):

$$\text{Anode reaction: } CH_3OH + H_2O \rightarrow CO_2 + 6H^+ + 6e^- \quad E_a^0 = 0.046V \qquad (1.7)$$

$$\text{Cathode reaction: } 3/2O_2 + 6H^+ + 6e^- \rightarrow 3H_2O \quad E_c^0 = 1.23V \qquad (1.8)$$

$$\text{Overall reaction: } CH_3OH + 3/2O_2 \rightarrow CO_2 + 2H_2O \quad E_{cell}^0 = 1.18V \qquad (1.9)$$

While the structure and thermodynamic characteristics of DMFCs are similar to those of hydrogen PEMFCs, the performance of each is very different. Like hydrogen PEMFCs, DMFCs are also limited by the poor oxygen reduction activity of the cathode. Unlike the PEMFC, the DMFC anode is also limited by poor methanol electro-oxidation activity. Electro-oxidization of hydrogen is a fast reaction on a low Pt loading catalyst. On the other hand, the methanol oxidation reaction rate is at least 3 to 4 orders magnitude slower, even on an optimized Pt/Ru catalyst.

At present, the two most serious technical problems for DMFCs are poor catalyst activities and methanol crossover to the cathode. The latter issue is due to the fact that methanol from the anode compartment permeates the electrolyte and reacts directly with oxygen at the cathode, significantly decreasing the efficiency of methanol utilization and causing a mixed cathode potential. The main available energy losses of DMFCs are attributed to the poor activities of the cathode and anode and methanol crossover.[24] The cathode overpotential can also be increased by methanol crossover. In order to develop a

practical energy production device, the serious problems of poor anode activity and methanol crossover must be solved.

1.4.3 Anodes for Direct Methanol Fuel Cells

To increase the efficiency of the anode reaction, it is important to understand the reaction mechanism. In the last few years, a large amount of research has been carried out to identify the nature and rate-limiting step of electro-oxidation of methanol.[25,26]

The best single metal catalyst that displays the necessary reactivity and stability to adsorb and break the C-H bond of methanol in an acidic environment is Pt.[27,28] The electrochemical oxidation of methanol on Pt involves several intermediate steps[29,30] and the mechanism can be generally presented as in Fig. 1.2.[31] At first, methanol molecules adsorb onto the Pt surface (step i in Fig. 1.2.). Then a sequence of dehydrogeneration steps and surface rearrangement steps give rise to adsorbed carbon monoxide (step ii-v in Fig. 1.2.).

i) $CH_3OH + Pt \rightarrow Pt - CH_3OH$ (1.10)

ii) $Pt - CH_3OH \rightarrow Pt - CH_2OH + H^+ + 1e^-$ (1.11)

iii) $Pt - CH_2OH + Pt \rightarrow Pt - CHOH + H^+ + 1e^-$ (1.12)

iv) $Pt - CHOH + Pt \rightarrow Pt - CHO + H^+ + 1e^-$ (1.13)

v) $Pt - CHO \rightarrow Pt - CO + H^+ + 1e^-$ (1.14)

However, the CO intermediates strongly adsorb and therefore poison the Pt catalyst.

To remove these CO intermediates, water disassociation occurs at high anodic potentials and forms Pt-OH species on the surface (vi, vii in Fig. 2).

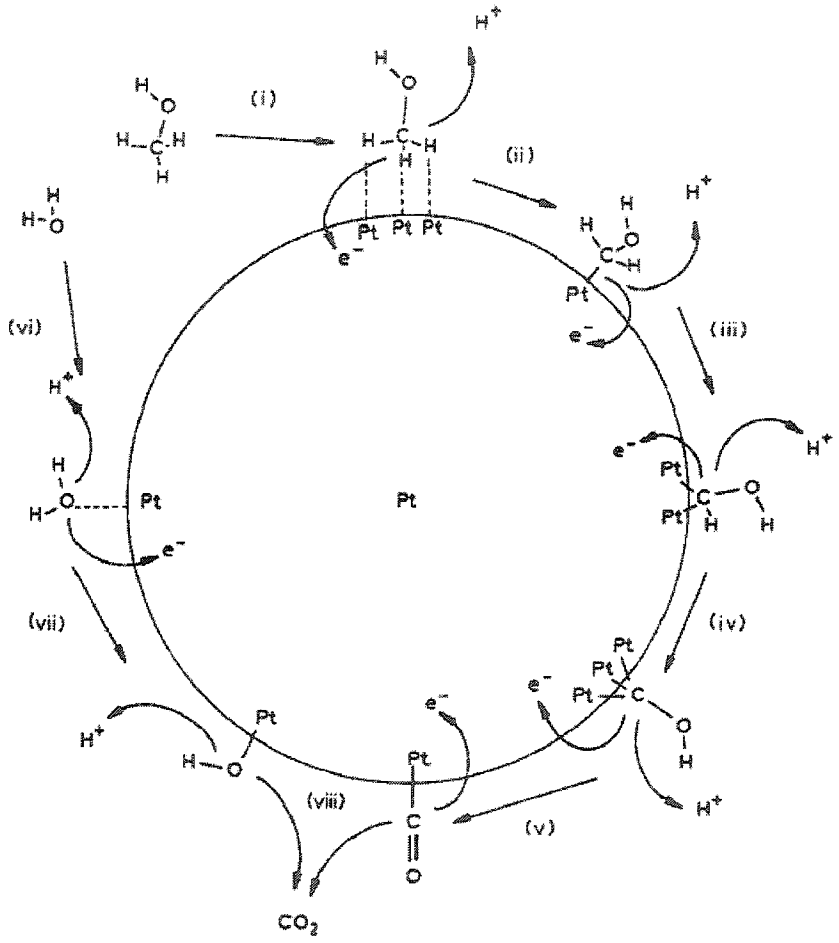

Fig. 1.2. A reaction scheme describing the probable methanol electrooxidation process (Steps i to viii) within a DMFC anode. Only Pt-based electrocatalysts show the necessary reactivity and stability in the acidic environment of the DMFC to be of practical use.

Reprinted from M. P. Hogarth, T. R. Ralph. *Platinum Metals Rev.*, 2002, 46 (4): 146–164

vi, vii) $Pt + H_2O \rightarrow Pt - OH + H^+ + 1e^-$ (1.15)

At last, Pt-OH reacts with Pt-CO to produce carbon dioxide (viii in Fig. 2.).

viii) $Pt - OH + Pt - CO \rightarrow 2Pt + CO_2 + 1e^-$ (1.16)

The overall oxidation process involves six electron transfer and the rate-determination step is the water-discharging step (equation 1.15).[32] On a pure Pt catalyst, the chemisorbed hydroxide group only forms when the potential is greater than 0.5-0.6 V.[33,34,35] This large overpotential relative to the methanol oxidation standard potential causes great performance losses for DMFCs. Researchers have shown that the CO adsorption is less pronounced with increasing temperature.[36,37,38] However, the methanol and water crossover rate greatly increases at high temperature. In general, DMFCs are therefore operated at 60-100 °C.

An active methanol oxidation catalyst should give rise to the hydroxyl group at low potentials and could also catalyze the oxidation of carbon monoxide. Many efforts are devoted towards the development of the binary alloys (Pt with Ru, Sn, Os, Co, Cu, Mo, W, Pd, or Rh),[39,40,41,42] ternary (PtRuW, PtRuMo)[43,44] and quaternary alloys (PtRuIrOs)[45] as highly activity methanol oxidation catalysts. Among them, the Pt-Ru binary catalysts have been extensively investigated and are currently regarded as the most active and durable for methanol and CO electro-oxidation.[46,47,48,49,50]

Although the enhancement effect of ruthenium on methanol oxidation has been used in DMFC for decades, the mechanisms are not well understood. A bi-functional

mechanism is considered to be responsible for the enhancement effect.[51] At lower overpotential (0.25V, compared with pure Pt),[52] water discharging occurs on Ru sites and forms hydroxyl group at the catalyst surface:

$$Ru + H_2O \rightarrow Ru - OH + H^+ + 1e^- \qquad (1.17)$$

Then Ru-OH groups can oxidize the neighbouring Pt-CO and therefore liberate Pt active sites for methanol oxidation.

$$Ru - OH + Pt - CO \rightarrow Ru + Pt + CO_2 + H^+ + 1e^- \qquad (1.18)$$

Moreover, the addition of Ru can weaken the of Pt-CO bond.[53]

There are many factors that affect anode polarization, such as particle size and particle size distribution, oxidation state of the Pt and Ru, the morphology of the catalyst, and its composition, etc.[54,55,56] The composition and especially the surface composition of the Pt-Ru catalyst may be one of the most important factors. [57,58] Gasteiger *et al.* reported that 30% Ru is the optimum ratio,[59] while others claim that 50% Ru is the best.[60] Also, the inconsistency in the literature about the oxidation state of Ru is another issue. Rolison *et al.* indicated that hydrous ruthenium oxide, rather than ruthenium, is more active in the oxidation of methanol on the Pt-Ru catalyst,[61] while other researchers reported that the pure Pt-Ru alloy is preferred for methanol oxidation.[62,63]

1.4.4 Cathodes for Direct Methanol Fuel Cells

The most widely used catalyst employed in DMFCs for oxygen reduction is Pt.[64] As

for hydrogen PEMFCs, the cathode oxygen reduction reaction of a DMFC is very complex and involves a four electron multi-step process.[65] In excess of 300 mV are lost from the thermodynamic potential for oxygen reduction, even at low current densities.

One possible mechanism is presented in Fig. 1.3.[66] In order for the reduction of oxygen reaction to occur, three species (electrons, protons, and oxygen molecules) must meet at the catalyst surface. The catalyst layer is generally a mixture of three different substances: catalyst particles, solid polymer, and a porous carbon support. The solid polymer provides pathways for the protons whereas the carbon and pores allow electrons and oxygen respectively to reach the catalyst sites.

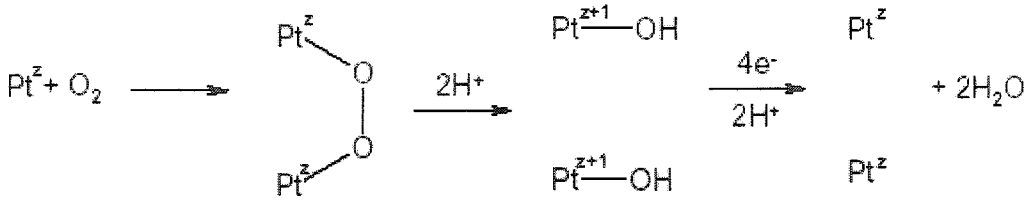

Fig. 1.3. The bridge model of oxygen reduction on Pt

DMFCs are generally fuelled with methanol solution, which will crossover the Nafion-type membrane to reach the cathode side. The crossover methanol is oxidized on the cathode and creates a mixed electrode potential which reduces the cell voltage.[67] Moreover, poisoning of Pt also occurs. CO intermediates form on Pt and reduce the cathode activity over time. Fig. 1.4 shows a cyclic voltammogram of a DMFC cathode

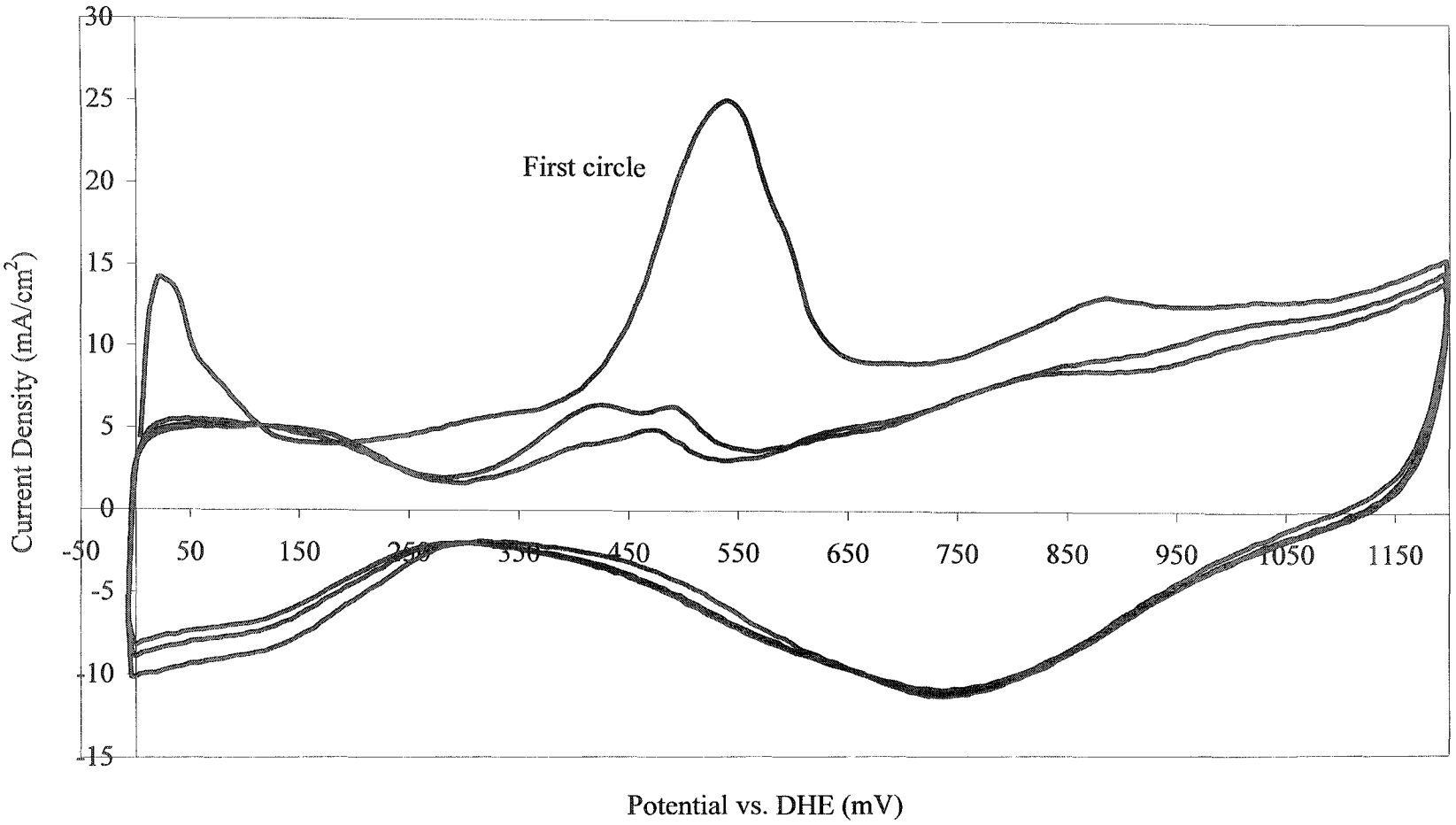

Fig. 1.4. Cyclic voltammogram (20 mV/s) of a Pt cathode after running a DMFC at 60 °C for 2 hours. The CV was measured at 60 °C with H_2 flow through the anode and H_2O through the cathode.

after running with air and methanol for 2 hours. The peak from 400 to 600 mV in the first cycle is attributed to the oxidation of adsorbed CO.

In a DMFC, water management in the cathode compartment also takes on a critical role in the performance. Water builds up readily by three means:[68] 1) diffusion from the methanol solution in the anode; 2) electro-osmotic drag of water molecules along with proton migration;[69,70] and 3) formation of water by oxygen reduction. The high water flux to the cathode may cause flooding of its porous structure even at low currents, thereby limiting oxygen supply to the active catalyst sites. In order to prevent the cathode from flooding, a large excess over stoichiometric airflow is usually employed.[71]

A highly active catalyst, and good electronic and ionic conductivities are three crucial requirements for an ideal cathode. Much effort has been made to increase cathode performance. A number of methanol tolerant cathodes have been developed to suppress the effect of methanol crossover, (i.e. RuSe/C, PtFe/C).[72,73,74,75,76] While Thomas and coworkers claimed that cathode performance losses due to methanol crossover are marginal when the Pt air cathode in a DMFC has a sufficient Pt loading and cell operation conditions are optimized.[77] Increasing the cathode ionic conductivity is another effective way to improve cathode performance. It has been found that the cathode ionic conductivity can be increased by loading Nafion into the Pt catalyst layer[78] and modification the Pt catalyst surface with sulfonated silane.[79] Results in our group showed that the DMFC performance increased with loading Nafion ionomer into the cathode

catalyst layer up to *ca.* 20%, and after which the performance declined with Nafion loading.[80]

1.4.5 Proton Exchange Membranes for Direct Methanol Fuel Cells

A good proton exchange membrane for a DMFC must perform three major functions: 1) high proton conductivity; 2) effective physical separation of the anode and cathode and a barrier for fuel permeation; and 3) insulation for electronic conduction. In addition, good mechanical strength and stability are also required.

The membranes commonly used nowadays in DMFCs, such as Nafion (Dupont) and Dais membrane (sulfonated polystyrene-b-poly(ethylene-r-butylene) block copolymers, Dias-Analytic Co.), were originally developed for hydrogen PEMFC applications. The drawback of their use in DMFCs is that they are not optimal for methanol blocking. These membranes suffer from high methanol crossover rates when methanol is directly passed through the anode. This process is due to the similar properties of methanol and water (e.g., dipole moment). As described before, the presence of methanol on the cathode side not only lowers fuel efficiency but also further polarizes the cathode. Therefore, it is very important to reduce the methanol crossover while maintaining proton conductivity and mechanical strength of the PEM. Many kinds of proton exchange membranes have been developed to decrease the methanol crossover and can be roughly classified into three groups:[81] 1) modified perfluorosulfonic acid membranes, 2) alternatives sulfonated

aromatic polymers, and 3) acid-base polymer membranes.

1.4.5.1 Perfluorosulfonic Acid Membranes

Although several types of perfluorosulfonic acid membranes are commercially available, such as Nafion (DuPont), Flemion (Ashashi Glass), Aciplex (Ashashi Chemicals) or Dow (Dow Chemicals),[82] none is more researched or seen as the standard than the Nafion membranes developed by E. I. DuPont de Nemours & Company.

The chemical structure of Nafion is shown in Fig. 1.5. It consists of a hydrophobic polytetrafluoroethylene (PTFE) like backbone and regularly spaced perfluorovinyl ether side-chains terminated with strong hydrophilic sulfonic acid groups ($-SO_3H$). The Teflon-like main chain gives Nafion excellent mechanical strength, chemical stability and thermal stability, while the sulfonated side chains endow Nafion with high proton conductivity. The x and y values in Fig. 1.5 determined the equivalent weight (EW, as average molecular weight, is defined as the gram of polymer per mole of sulfonate groups) of the membranes. It should be noted that as the EW decreases below 1000 g/equiv, Nafion becomes soluble in water because there is not enough hydrophobic matrix to keep it in a gel-like state.[83]

The configuration and morphologies of Nafion have been intensely studied[84,85,86,87,88] and several models have been proposed to describe how ionic groups aggregate within Nafion membranes. Eisenberg first postulated the existence of ion clusters in Nafion.[89,90]

Based on that, two popular models, Gierke's network model[91,92] and Yeager's three phase model,[93] were proposed. Though the actual morphology of Nafion membranes is still disputed, all research has showed that a well-hydrated membrane contains two phases: a nanometer scale ionic phase (4-5 nm in diameter), which is involved in proton conduction, and a nonionic phase which is associated with the PTFE backbone. Short pathways (1 nm in diameter) connect the ionic clusters and continuous water containing channels are formed.

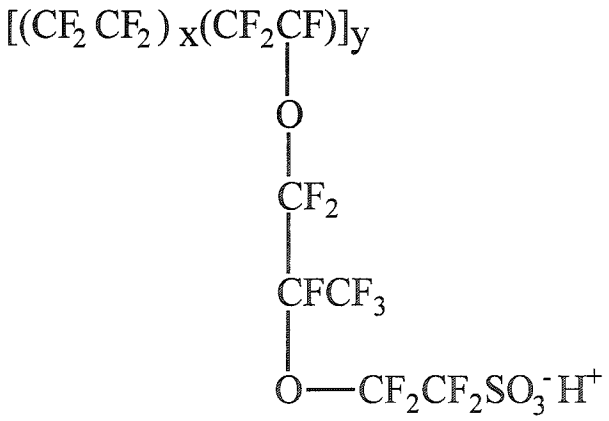

Fig. 1.5. General Chemical Structure of Nafion. X=6-10

As described before, methanol crossover through the Nafion membranes is one of the two major limitations for DMFCs.[94] To reduce methanol crossover, Nafion membranes have been modified by low dose electron beam exposure,[95] by forming sandwich structures with, for example, sulfonated poly(vinyl alcohol) (PVA)[96] or

polybenzimidazole (PBI)[97], or by producing various Nafion based composites.[98]

Mauritz *et al.* developed a sol-gel technique to introduce SiO_2 into the hydrophilic channels of Nafion membranes.[99] Watanabe *et al.* have also applied Nafion/SiO_2 membranes in the fuel cell field.[100] Antonucci *et al.* introduced this type of nanocomposite into DMFCs as a high temperature (145 $°C$) PEM in 1999.[101] The better mechanical strength and self-humidification properties of Nafion/SiO_2 membranes compared with original Nafion membranes, which will degrade and dehydration under high operation temperature, favour their application at high temperatures. After investigating the methanol uptake and permeation as a function of temperature, Miyake *et al.* reported that Nafion/silica hybrid membranes with high silica content (20wt.%) have significantly reduced methanol permeation rates and are potentially useful for both low and high temperature DMFCs.[102] Nafion/TiO_2 membranes were also produced by Uchida et al. recently.[103] These membranes showed increased self-humidification even at low TiO_2 loadings. All the studies of Nafion/inorganic nanocomposites appear to suggest that they are suitable for DMFCs. However, their proton conductivities are substantially lower than for pure Nafion and no better performance results than unmodified Nafion have been reported.

Pickup *et al.* have developed poly(1-methylpyrrole)/Nafion [104, 105] and polypyrrole/Nafion composites membranes.[106, 107, 108] These membranes display a significant reduction of methanol crossover.

1.4.5.2 Alternatives Sulfonated Aromatic Polymer Membranes

The main motivation of development of alternative PEMs is to lower the material cost. From the chemical structure and physical properties point of view, sulfonated polysiloxane is a good candidate for proton exchange membranes. It is very strange that no report concerning its application in fuel cells has been published.

Sulfonated polystyrene (SPS) membranes were the first generation of PEMs. Though this type of membrane suffers severe thermal degradation due to the weak tertiary C-H bonds in the main chain, which are easily oxidized by oxygen, they are still studied in many research groups since it is easy to manipulate the structure to study the relationship between the morphology and ion conductivity.[109,110,111]

Most studies have focused on aromatic polymers with phenylene backbones. However, polymers consisting of pure linked benzene rings, such as polyphenylene (PP), lack flexibility and processability, though their thermal stability is good. Introduction of flexible ether chain links (C-O-C) gives such aromatic polymers good processabilty. Membranes based on sulfonated poly(etheretherketone) (SPEEK) has been actively investigated.[112,113,114,115]

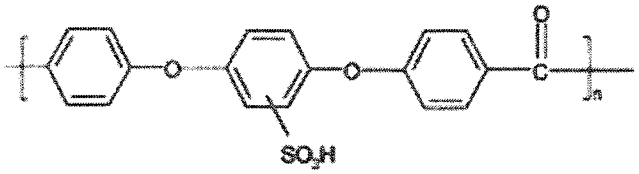

Fig. 1.6. General Chemical Structure of Sulfonated PEEK

The chemical structure of SPEEK is shown in Fig. 1.6. The proton conductivity can be controlled through the degree of sulfonation. As illustrated in Fig. 1.7, SPEEK has a different microstructure than Nafion membranes.[116] When well-hydrated, the hydrophilic channels are narrower and more branched with increased dead-ends in SPEEK compared with Nafion. These characteristics of SPEEK significantly reduce methanol and water permeation. However, the low methanol crossover of SPEEK is always accompanied by lower proton conductivity. An approach to solve this problem is to increase the sulfonation degree[117,118] or use thin membranes, but that always results in poor

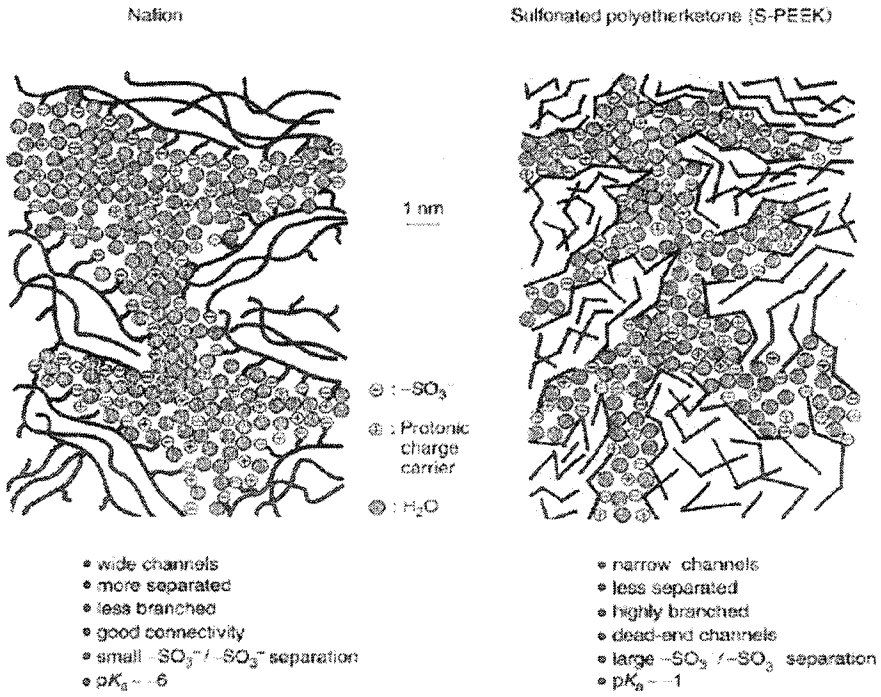

Fig. 1.7. Schematic comparison of the microstructures of Nafion and sulfonated PEEK

Reprinted from K. D. Kreuer. J. Membr. Sci., 2001, 185: 29-39

mechanical properties.[119] Cross-linking the polymer or making composite membranes may be two ways to reinforce the membranes.

1.4.5.3 Acid-base Polymer Membranes

Basic polymers can be doped with an acid, such as phosphoric acid or sulphuric acid, as a donor and an acceptor to conduct protons. Acid-doped polybenzimidazole (PBI) has been well addressed in the past few years.[120,121,122]

PBI (chemical structure showed in Fig. 1.8.) based membranes have good chemical resistance and excellent mechanical strength. Pure PBI is not conducting. The conductivity of acid-doped PBI is strongly dependent on the doping level. The presence of free or unbounded acid is necessary to improve its conductivity. It is reported that these PEMs have high ionic conductivity,[123] low methanol crossover rate,[124] excellent thermal stability,[125] and a nearly zero water drag coefficient.[126] However, the severe problem of small molecular acid (e.g. H_3PO_4) leakage hinders their application in DMFCs. Research in the Pickup group has shown that the performance of phosphoric acid doped PBI membranes deteriorates quickly in the DMFC as the proton conductors are washed out.

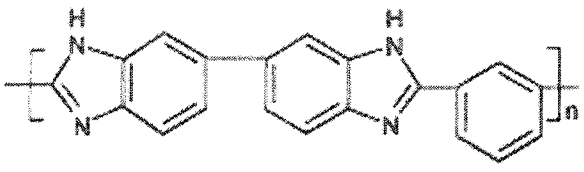

Fig. 1.8. The chemical structure of PBI.

This problem could be solved by substituting the small molecular acid by acid polymers, such as sulfonated polysulfone.[127,128,129] Kerres *et al.* produced a series of sulfonated polyaryl doped PBI composite membranes and applied them to DMFCs.[130,131] This type of membrane greatly decreases methanol crossover with comparable performance to Nafion membranes and shows a promising future for DMFCs.

1.5 Evaluation of DMFC Performance

The most common way to evaluate a fuel cell is a polarization curve measurement (V vs I curve), where cell voltage is plotted as a function of current density. Fig. 1.9 shows a typical polarization curve for a DMFC. A polarization curve can provide information on kinetic, ohmic, and mass transfer losses.[132] A higher current density at an acceptable cell voltage (e.g. 500 mV) indicates better performance.

As described in section 1.2, the kinetic polarization is reflected in the low current density region and can be analyzed with the Tafel equation. Ohmic loss is observed in the linear region at medium current density and governed by Ohm's law. Mass transport can be diagnosed in the high current density region from the typical feature of the steep cell voltage drop.

With the help of a reference electrode (such as the dynamic hydrogen electrode used by Ren *et al.*[133]), the individual electrode polarizations can be resolved. The polarization information of the anode and the cathode is crucial to improving cell performance and

optimizing operation conditions. For a DMFC, a cathode mass transport region is seldom observed due to the low activity of the anode catalyst. Cells cannot reach the high current densities where oxygen mass transfer dominates.

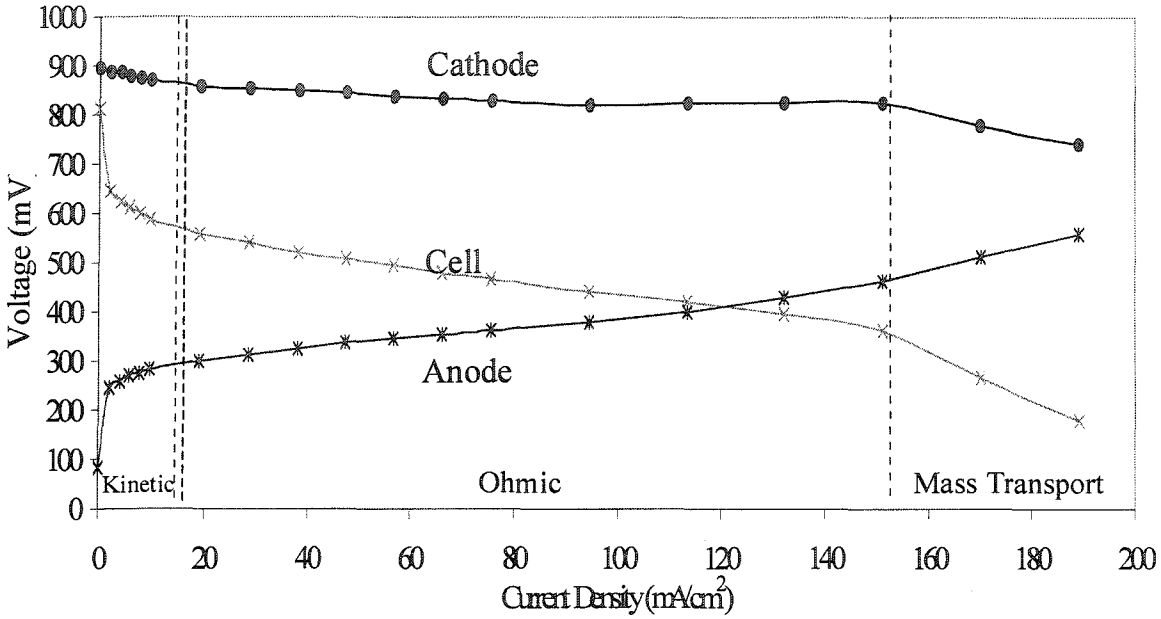

Fig. 1.9. A direct methanol fuel cell polarization, anode polarization and cathode polarization curves, showing kinetic, ohmic loss, and mass transport regions.

Electrochemical impedance spectroscopy (EIS) is another very powerful technique to characterize fuel cells. However, a full discussion of this method is beyond the scope of this thesis. Only a short introduction is presented here. EIS measures the impedance of an electrochemical cell as a function of the frequency of a series of ac excitation signals. As a diagnostic tool, EIS can provide not only the resistance of the PEM, but also more

dynamic information on the interfacial charge transfer resistance, mass transport resistances in the catalyst layer and backing diffusion layer, and ionic and electronic resistances.[134,135,136] Until now, most EIS research has been concerned with hydrogen fuel cells. Few efforts have been dedicated to the EIS study of DMFCs[137,138,139] mainly due to the more complex methanol electrochemical reactions and mass transport properties. The formation of large amounts of CO_2 in the liquid feed anode side make the spectrometry more complex to explain. More research is underway.

1.6 Thesis Objectives

The general goal of the work described in this thesis was to produce polypyrrole modified Nafion membranes to decrease methanol crossover in direct methanol fuel cells and improve DMFC performance.

In Chapter Three, factors affecting the *in situ* polymerization of polypyrrole in Nafion are described. An optimized modification procedure to produce polypyrrole/Nafion composites was determined. The characterization results are displayed in Chapter Four, which shows that the modification procedure has very good reproducibility.

To resolve the anode performance and cathode performance, the development of a more convenient reference electrode is presented in Chapter Five. This reference electrode was examined in both a hydrogen PEMFC and a DMFC.

References

[1] S. Radel, M. Navidi. *Chemistry,* West Publishing Company: New York, 1990.

[2] W. R. Grove. *Philos. Mag.* 1839, 14: 127

[3] W. T. Grubb, L. W. Niedrach. *J. Electrochem. Soc.,* 1960, 107: 131

[4] D. Chu, R. Jiang. *J. Power Sources.* 1999, 80: 226-234

[5] G. Gutmann. *J. Power Sources*, 1999, 84: 275-279

[6] K. T. Adjemian, S. J. Lee, B. Srinivasan, J. Benzigar, A. B. Bocarsly. *J. Electrochem. Soc.*, 2002, 149: A256-A261

[7] P. W. Atkins. Physical Chemistry, 5th ed., Oxford University Press: Oxford, 1994

[8] L. Carrette, K. A. Friedrich, U. Stimming. *ChemPhysChem*, 2000, 1: 162-193

[9] L. Carrette, K. A. Friedrich, U. Stimming. *Fuel Cells*, 2001, 1: 5-39

[10] M. L. Perry, T. F. Fuller. *J. Electrochem. Soc.*, 2002, 149: S59-S67

[11] C. Lamy, J-M. Léger, S. Srinivasan. Direct Methanol Fuel Cells: From a Twentieth Century Electrochemist's Dream to a Twenty-first Century Technology, in Modern Aspects of Electrochemistry, No. 34, Bockris, J. O'M.; Conway, B. E., Eds.; EluwerAcademic/Plenum Publishers: New York, 2001; pp 53-118.

[12] S. P. S. Badwal. *Solid State Ionics*, 2001, 143: 39–46

[13] http://www1.dupont.com/NASApp/dupontglobal/corp/products/prodDetail.jsp?nodeID=3444

[14] Q. Li, R. He, J. O. Jensen, N. J. Bjerrum. *Chem. Mater.*, 2003, 15: 4896-4915

[15] A. K. Shukla, M. K. Ravikumar, K. S. Gandhi. *J. Solid State Electrochem.*, 1998, 2:117-122

[16] M. J. Gonzalez, C. H. Peters, M. S. Wrighton. *J. Phys. Chem. B*, 2001, 105: 5470-5476

[17] H. Uchida, Y. Mizuno, M. Watanabe. *J. Electrochem. Soc.*, 2002, 149: A682-A687

[18] D. B. Boies, A. Dravnieks. *J. Electrochem. Soc.*, 1962, 109: C198

[19] J. N. Murray, P.G. Grimes. In Fuel Cells. American Institute of Chemical Engineers, New York, 1963, P. 57.

[20] R. W. Glazebrook. *J. Power Sources*, 1982, 7: 215

[21] C. J. Hora, D. E. Maloney. *J. Electrochem. Soc.*, 1977, 124: C319

[22] F. Huba, E. B. Yeager, G. A. Olah. *Electrochim. Acta.*, 1979, 24:489

[23] T. E. Springer, T. A. Zawodzinski, S. Gottesfeld. *J. Electrochem. Soc.*, 1991, 138: 2334

[24] D. Chu, R. Jiang. *Solid State Ionics*, 2002, 148: 591-599

[25] R. Parsons, T. Vandernoot. *J. Electroanal. Chem.*, 1988, 257: 9

[26] M. Endo, T. Matasumoto, J. Kubota, K. Domen, C. Hirose. *J. Phys. Chem. B*, 2001, 105: 1573-1577

[27] K. W. Park, J. H, Choi, B. K. Kwon, S. A. Lee, Y. E. Sung, H. Y. Ha, S. A. Hong, H. Kim, A. Wieckowski. *J. Phys. Chem. B*, 2002, 106: 1869

[28] S. Lj. Gojković, T. R. Vidaković. *Electrochimica Acta.*, 2001, 47: 633-642

[29] G.-Q. Lu, W. Chrzanowski, A. Wieckowski. *J. Phys. Chem. B*, 2000, 104: 5566-5572

[30] T. Iwasita. *Electrochimica Acta*, 2002, 47: 3663-3674

[31] M. P. Hogarth, T. R. Ralph. *Platinum Metals Rev.*, 2002, 46: 146–164

[32] A. S. Aricò, S. Srinivasan, V. Antonucci. *Fuel Cells*, 2001, 1: 133-161

[33] B. V. Tilak, B. E. Conway, H. W. Angerstein-Kozlawska. *J. Electroanal. Chem.*, 1973, 48: 1

[34] K. Chandrasekaran, J. C. Wass, J. O'M. Bockris. *J. Electrochem. Soc.*, 1990, 137:518

[35] N. H. Li, S. G. Sun, S. P Chen. *J. Electroanal. Chem.*, 1997, 430: 57.

[36] Thomas H. Madden, Eric M. Stuve. *J. Electrochem. Soc.*, 2003, 150: E571-E577

[37] N. Wakabayashi, Hiroyuki Uchida, M. Watanabe. *Electrochem. and Solid-State Lett.*, 2002, 5: E62-E65

[38] G. Xiao, Q. Li, H. A. Hjuler, N. J. Bjerrum. *J. Electrochem. Soc.*, 1995, 142: 2890

[39] J. Kua, W. A. Goddard III. *J. Am. Chem. Soc.*, 1999, 121: 10928-10941

[40] I. Honma, T. Toda. *J. Electrochem. Soc.*, 2003, 150: A1689-1692

[41] P. Waszczuk, G.-Q. Lu, A. Wieckowski, C. Lu, C. Rice, R. I. Masel. *Electrochim. Acta*, 2002, 47: 3637

[42] Y. Liu, X. Qiu, Y. Huang, W. Zhu. *J.Power Sources*, 2002, 111: 160

[43] K. Y. Chen, Z. Sun, A. C. C. Tseung. *Electrochem. Solid State Lett.*, 2000, 3: 10

[44] M. Kanhafar, M.Sc. Thesis, Memorial University of Newfoundland, St. John's, Newfoundland, Canada. 2003.

[45] B. Gurau, R. Viswanathan, T. J. Lafrenz, R. Liu, K. L. Ley, E. S. Smotkin, E. Reddington, A. Sapienza, B. C. Chan, T. E. Mallouk, S. Sarangapani. *J. Phys. Chem. B.*, 1998, 102: 9997-10003.

[46] Y. H. Chu, Y. G. Shul, W. C. Choi, S. I. Woo, H. S. Han. *J. Power Sources*, 2003, 118: 334.

[47] N. Wakabayashi, H. Uchida, M. Watanabe, *Electrochem. Solid-State Lett.*, 2002, 5: E62

[48] J. Y. Kim, Z. G. Yang, C. Chang, T. I. Valdez, S. R. Narayanan, P. N. Kumta. *J. Electrochem. Soc.*, 2003, 150: A1421-A1431

[49] W. D. King, J. D. Corn, O. J. Murphy, D. L. Boxall, E. A. Kenik, K. C. Kwiatkowski, S. R. Stock, C. M. Lukehart. *J. Phys. Chem. B.*, 2003, 107: 5467-5474.

[50] Y. Takasu, T. Fujiwara, Y. Murakami, K. Sakaki, M. Oguri, T. Asaki, W. Sugimoto. *J. Electrochem. Soc.*, 2000, 147: 4421

[51] J. W. Long, R. M. Stroud, K. E. Swider-Lyons, D. R. Rolison. *J. Phys. Chem. B*, 2000, 104: 9772-9776

[52] H. Hoster, T. Iwasita, H. Baumgärtner, W. Vielstich. *Phys. Chem. Chem. Phys.*, 2001, 3: 337-346

[53] F. Vigier, C. Coutanceau, F. Hahn, E.M. Belgsir, C. Lamy. *J. Electroanal. Chem.*, 2004, 563: 81-89,9

[54] T. R. Ralph, M. P. Hogarth. *Platinum Metals Rev.*, 2002, 46: 117–135

[55] O. A. Khazova, A. A. Mikhailova, A. M. Skundin, E. K. Tuseeva, A. Havránek, K. Wippermann. *Fuel Cells*, 2002, 2: 99-108

[56] J. Nordland, A. Roessler, G. Lindbergh. *J. Appl. Electrochem.*, 2002, 35: 259-265.

[57] W. H. Lizcano-Valbuena, V. A. Paganin, E. R. Gonzalez. *Electrochim. Acta*, 2002, 47: 3715

[58] H. N. Dinh, X. Ren, F. H. Garzon, P. Zelenay, S. Gottesfeld. *J. Electroanal. Chem.*, 2000, 491: 222-233

[59] H. A. Gasteiger, M. Markovic, P. N. Ross, E. J. Cairns. *J. Electrochem Soc.* 1994, 141: 1795

[60] C. Lamy, A. Lima, V. Lerhun, F. Delime, C. Coutanceau, J. M. Leger, *J. Power Sources*, 2002, 105: 283

[61] D. R. Rolison, P. L. Hagans, K. E. Swider, J. W. Long. *Langmuir*, 1999, 15: 774-779

[62] A. Pozio, R. F. Silva, M. D. Francesco, F. Cardellini, L. Giorgi. *Electrochim. Acta*, 2002, 48: 255

[63] R. A. Lampitt, L. P. L. Carrette, M. P. Hogarth, A. E. Russell. *J. Electroanal. Chem.*, 1999, 460: 80

[64] T. R. Ralph, M. P. Hogarth. *Platinum Metals Rev.*, 2002, 46: 3-14

[65] T. Abe, M. Kaneko. *Prog. Polym. Sci.*, 2003, 28: 1441-1488

[66] E. Yeager. *Electrochim. Acta,* 1984, 29: 1527

[67] F. Meier, S. Denz, A. Weller, G. Eigenberger. *Fuel Cells*, 2003, 3: 161-168

[68] Z. Qi, M. Hollett, C. He, A. Attia, A. Kaufman. *Electrochem. Solid-State Lett.*, 2003, 6: A27-A29

[69] X. Ren, S. Gottesfeld. *J. Electrochem. Soc.*, 2001, 148: A87-A93

[70] X. Ren, W. Henderson, S. Gottesfeld. *J. Electrochem. Soc.*, 1997, 144: L267-L270

[71] M. M. Mench, C. Y. Wang. *J. Electrochem. Soc.*, 2003, 150: A79-A85

[72] M. Neergat, D. Leveratto, U. Stimming. *Fuel Cells*, 2002, 2: 25-30

[73] W. Li, W. Zhou, H. Li. *Electrochim Acta*, 2004, 49: 1045-1055

[74] H. Tributsch, M. Bron, M. Hilgendorff, H. Schulenburg, I. Dorbandt, V. Eyert, P. Bogdanoff, S. Fiechter. *J. Appl. Electrochem.* 2001, 31: 739-748.

[75] T. J. Schmidt, U. A. Paulus, H. A. Gasteiger. *J. Electrochem. Soc.*, 2000, 147: 2620

[76] R. Jiang, D. Chu. *J. Electrochem. Soc.*, 2000, 147: 4605

[77] S. C. Thomas, X. Ren, S. Gottesfeld, P. Zelenay. *Electrochim. Acta*, 2002, 47: 3741-3748

[78] G. Li, P. G. Pickup. *J. Electrochem. Soc.*, 2003, 150: C745-C752

[79] E. B. Easton, Z. Qi, A. Kaufman, P. G. Pickup. *Electrochemical and Solid-State Letters*, 2001, 4: A59-A61

[80] E. Bradley Easton. Ph.D. Thesis. Memorial University of Newfoundland, St. John's, Newfoundland, Canada. 2002

[81] Q. Li, R. He, J. O. Jenson, N. J. Bjerrum. *Chem. Mater.*, 2003, 15: 4896-4915

[82] B. Baradie, J. P. Dodelet, D. Guay. *J. Electroanal. Chem.*, 2000, 489: 101-105

[83] D. I. Ostrovskii, A. M. Brodin, L. M. Torell. *Solid State Ionics*, 1996, 85: 323

[84] A.Z. Weber, J. Newman. *J. Electrochem. Soc.*, 2003, 150: A1008-A1015

[85] V. Barbi, S. S. Funari, R. Gehrke, N. Scharnagl, N. Stribeck. *Polymer*, 2003, 44: 4853-4861

[86] F. P. Orfino, S. Holdcroft. *J. New Mater. Electrochem. Systems*, 2000, 3: 285-290

[87] F. N. Buchi, G. G. Scherer, *J. Electrochem. Soc.*, 2001, 148: A183

[88] H. Haubold, Th. Vad, H. Jungbluth, P. Hiller. *Electrochim. Acta*, 2001, 46: 1559-1563

[89] A. Eisenberg. *Macromolecules*, 1970, 3: 147

[90] A. Eisenberg, B. Hird, R. B. Moore. *Macromolecules*, 1990, 23: 4098

[91] T. D. Gierke, G. E. Munn, F. C. Wilson. *J. Polym. Sci. Polym. Phys. Ed.*, 1981, 19: 1687

[92] W. Y. Hsu, T. D. Gierke. *J. Membr. Sci.*, 1983, 13: 307

[93] H. L. Yeager, A. Steck. *J. Electrochem. Soc.* 1981, 128: 1880-1884

[94] A. Heinzel, V. M. Barragán. *J. Power Sources*, 1999, 84: 70-74

[95] L. J. Hobson, H. Ozu, M. Yamaguchi, S. Hayase. *J. Electrochem. Soc.*, 2001, 148: A1185-A1190

[96] Z. Shao, I. Hsing. *Electrochem. Solid-State Lett.*, 2002, 5: A185-A187

[97] L. J. Hobson, Y. Nakano, H. Ozu, S. Hayase. *J. Power Sources*, 2002, 104: 79

[98] B. Kumar, J. P. Fellner. *J. Power Sources*, 2003, 123: 132-136

[99] K. A. Mauritz, I. D. Stefanithis, S.V. Davis, R. W. Scheetz, R. K. Rope, G. L. Wilkes, H. Huang. *J. Appl. Polym. Sci.*, 1995, 55: 181-190

[100] M. Wantanabe, H. Uchida, Y. Seki, M. Mori. *J. Electrochem. Soc.*, 1996, 143: 3847-3852

[101] P. L. Antonucci, A. S. Arico, P. Creti, E. Ramunni, V. Antonucci, *Solid State Ionics*, 1999, 125: 431-437

[102] N. Miyake, J. S. Wainright, R. F. Savinell. *J. Electrochem. Soc.*, 2001, 148: A905-A909

[103] H. Uchida, Y. Ueno, H. Hagihara, W. Wantanabe. *J. Electrochem. Soc.*, 2003, 150: A57-A62

[104] N. Jia, M. C. Lefebvre, J. Halfyard, Z. Qi, P. G. Pickup, *Electrochem. Solid-State Lett.*, 2000, 3: 529-531

[105] P. G. Pickup, Z. Qi. *Canadian Patent Application No. 2,310,310,* PCT/CA 01/00767 2000

[106] B. L. Langsdorf, B. J. Maclean, J. E. Halfyard, J. A. Hughes, P. G. Pickup. *J. Phys. Chem. B*, 2003, 107: 2480-2484

[107] B. L. Langsdorf, J. Sultan, P. G. Pickup. *J. Phys. Chem. B*, 2003, 107: 8412-8415

[108] E. B. Easton, B. L. Langsdorf, J. A. Hughes, J. Sultan, Z. Qi, A. Kaufman, P. G. Pickup, *J. Electrochem. Soc.*, 2003, 150: C735-C739

[109] J. Won, H.H. Park, Y. J. Kim, S. W. Choi, H. Y. Ha, I. Oh, H. S. Kim, Y. S. Kang, K. J. Ihn. *Macromolecules*, 2003, 36: 3228-3234

[110] J. Ding, C. Chuy, S. Holdcroft. *Macromolecules*, 2002, 35: 1348-1355

[111] J. Ding, C. Chuy, S. Holdcroft. *Chem. Mater.*, 2001, 13: 2231-2233

[112] B. Yang, A. Manthriam. *Electrochemistry Communications*, 2004, 6: 231-236

[113] B. Yang, A. Manthriam. *Electrochem. Solid-State Lett.*, 2003, 6: A229

[114] S. P. Nunes, B. Ruffmann, E. Rikowski, S. Vetter, K. Richau. *J. Membr. Sci.*, 2002, 203: 215

[115] K. D. Kreuer, *Solid State Ionics*, 1997, 97: 1

[116] K. D. Kreuer. *J. Membr. Sci.*, 2001, 185: 29-39

[117] B. Yang, A. Manthiram. *Electrochem. Solid-State Lett.*, 2003, 6: A229-A231

[118] L. Li, J. Zhang, Y. Wang. *J. Membr. Sci.*, 2003, 226: 159-167

[119] S. Hietala, M. Koel, E. Skou, M. Elomaa, F. Sundholm. *J. Mater. Chem.*, 1998, 8: 1127

[120] D. Mecerreyes, H. Grande, O. Miguel, E. Ochoteco, R. Marcilla, I. Cantero. *Chem. Mater.*, 2004, 16: 604-607.

[121] Y.-L. Ma, J. S. Wainright, M. H. Litt, R. F. Savinell. *J. Electrochem. Soc.*, 2004, 151: A8-A16

[122] D. J. Jones, J. Roziére. *J. Membr. Sci.*, 2001, 185: 41

[123] M. Kawahara, J. Morita, M. Rikukawa, K. Sanui, N. Ogata, *Electrochim. Acta,* 2000, 45: 1395

[124] J-T. Wang, J. S. Wainright , R. F. Savinell, M. Litt. *J. Appl. Electrochem.,* 1996, 26: 751-756

[125] S. R. Samms, S. Wasmus, R. F. Savinell, *J. Electrochem. Soc.,* 1996, 143: 1225

[126] J. Wang, R. F. Savinell, J. S. Wainright , M. Litt, H. Yu. *Electrochim. Acta,* 1996, 41: 193-197

[127] C. Hasiotis, Q. Li, V. Deimede, J. K. Kallitsis, C. G. Kontoyannis, N. J. Bjerrum. *J. Electrochem. Soc.*, 2001, 148: A513-A519

[128] P. Staiti. *J. New. Mat. Electrochem. Systems*, 2001, 4: 181-186

[129] V. Deimede, G. A. Voyiatzis, J. K. Kallitsis, Q. Li, N. J. Bjerrum. *Macromolecules*, 2000, 33: 7609-7617

[130] J. Kerres, W. Zhang, L. Jörissen, V. Gogel. *J. New. Mat. Electrochem. Systems,* 2002, 5: 97-107

[131] J. Kerres, W. Zhang, A. Ullrich, C.-M. Tang, M. Hein, V. Gogel, T. Frey, L. Jörissen. *Desalination,* 2002,147: 173–178

[132] G. Murgia, L. Pisani, A. K. Shukla, K. Scott. *J. Electrochem. Soc.*, 2003, 150: A1231-A1245

[133] X. Ren, T. E. springer, S. Gottesfeld. *J. Electrochem. Soc.*, 2000, 147: 92-98

[134] G. Li, P. G. Pickup. *J. Electrochem. Soc.*, 2003, 150: C745-C752

[135] M. Ciureanu, R. Roberge. *J. Phys. Chem. B*, 2001, 105: 3531-3539

[136] M. C. Lefebvre, R. B. Martin, P. G. Pickup. *Electrochem. Solid-State Lett.*, 1999, 2: 259

[137] J. Diard, N. Glandut, P. Landaud, B. L. Gorrec, C. Montella. *Electrochim. Acta*, 2003, 48: 555-562

[138] J. T. Müller, P. M. Urban, W. F. Hölderich. *J. Power Sources*, 1999, 84: 157-160

[139] J. T. Müller, P. M. Urban. *J. Power Sources*, 1998, 75: 139-143

Chapter 2

Chemicals and Instruments

Unless stated otherwise, all commercial chemicals and solvents were used as received without purification. Nanopure water was used to prepare all aqueous solutions and for washing membranes.

2.1. Electrochemical Instruments

Electrochemical experiments were performed using the following two instruments:

Solartron 1286/1250

A Solartron 1286 electrochemical interface (Schlumberger) and 1250-frequency response analyzer controlled by custom software. Electrochemical Impedance Spectra (EIS) were acquired using Z-plot software (Scribner Associates, Inc).

EG&G PAR 273A Potentiostat/Galvanostat/ 5210 Lock-in Amplifier

A EG&G PAR 273A Potentiostat/Galvanostat (Princeton Applied Research), equipped with a 5210 lock-in amplifier, was controlled by EG&G/PAR M270 electrochemical software. EIS data was collected with PAR Powersuite software.

2.2 Membrane Electrode Assembly Preparation

2.2.1 Materials

Nafion membranes were cleaned in 80 °C 15% H_2O_2(aq.) for one hour to remove organic residues in the membranes (until the membranes became colourless), washed with deionized water then soaked in 80 °C 1 M nitric acid and 1 M sulphuric acid for one hour,

respectively, to remove inorganic residues. The membranes were then washed with a large volume of deionized water several times. The clean Nafion membranes were stored in deionized water.

The PtRu anodes were prepared by Dr. Brad Easton.[1] They were composed of *ca.* 4 mg/cm^2 Pt/Ru black alloy (50% Pt and 50% Ru) with 10-20 % Nafion binder apply onto a 6 mil Toray carbon fiber paper (CFP, T090) impregnated with 10-15% Nafion. The Pt black cathodes were provided by Ballard Power System, which consisted of a total Pt loading of 4 mg/cm^2 on CFP (T090) bound with 11 % PTFE.

2.2.2 MEA Preparation

Two sizes of MEAs, 1 cm^2 and 5 cm^2, were prepared. All MEAs were assembled by hot-pressing a Nafion membrane (or modified membrane) between two electrodes at 130 °C at a pressure of 100-200 pound/cm^2 for 180s. A 1 cm^2 die and a 5 cm^2 die were used to align the electrodes.

2.3 Fuel Cell Testing

MEAs were tested in 1 or 5 cm^2 cells. The in-house made 1 cm^2 cell was constructed from Plexiglass with an open current collector ring on each side and was sealed by two O-rings on each side of the MEA. Gas/liquid flow could pass through each electrode. The 1cm^2 fuel cell is designed for room temperature experiments.

The $5cm^2$ cell was a commercial model sold by ElectroChem. Inc. A scheme of the cell is showed in Fig. 2.1. The anode and cathode of the MEA were contacted on their rear with graphite plates with serpentine flow-fields. The channels supply methanol to the anode and oxygen (or air) to the cathode. The stainless steel end-plates functioned as current collectors. Electrical heaters were placed behind each of the stainless steel plates in order to heat the cell to the desired temperature. Silicone rubber gaskets are used to seal this cell.

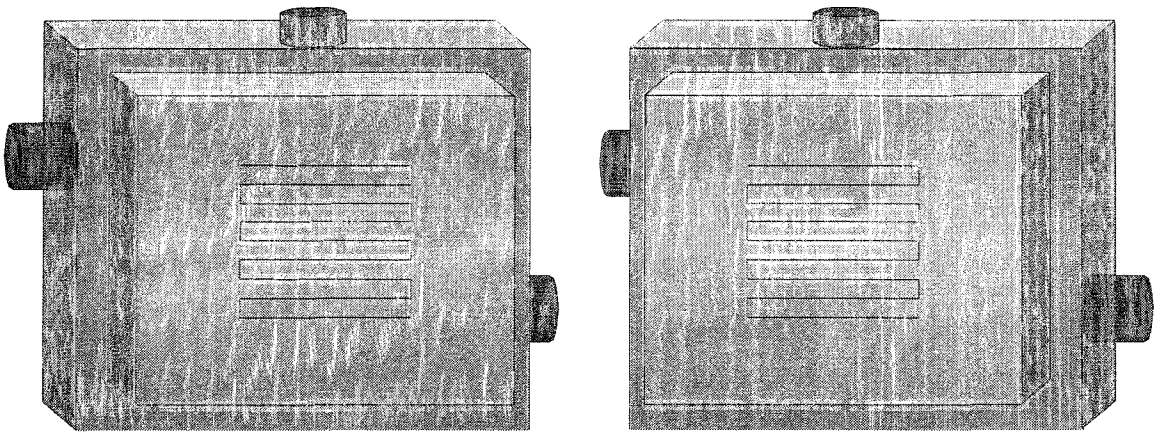

Figure 2.1. Schematic diagram of a fuel cell with serpentine flow fields

A schematic diagram of the DMFC test system is shown in Figure 2.2. The methanol solution was supplied from a 50 mL syringe using a Compact Infusion Pump (Harvard Apparatus Co. Inc., Model 975), equipped with flow rate control. Gases were supplied directly from tanks and the flow rate was controlled by flow meters (Cole-Parmer). In some experiments, humidified hydrogen gases was used instead of the methanol solution

by passing the gas flow through a water tank prior to entering the cell. For the high temperature measurements, a 50 minutes temperature stabilization time is required before every experiment.

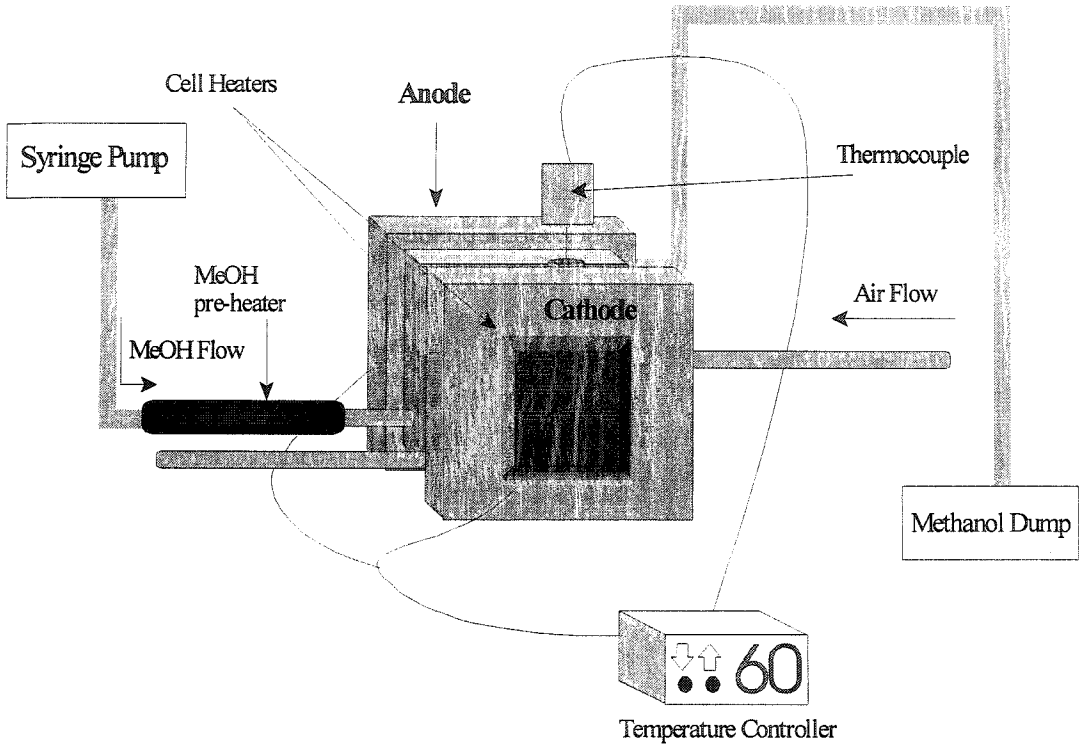

Figure 2.2. Schematic diagram of a direct methanol fuel cell testing system

The DMFC was operated with 1M methanol and air as the fuel and oxidant. The performance was tested by applying a constant current from a potentiostat. Measurements were recorded after allowing sufficient time for the reading to stabilize, typically 180 seconds.

Impedance measurements were carried out after purging the cathode compartment with N_2 and were conducted with a small perturbation amplitude of 10 mV over a frequency range of 65 KHz to 0.1 Hz. The high frequency real axis intercept is taken as the resistance of the membrane. This is not influenced by the kind of gas passed through the cathode, but the low frequency impedance is, even at open circuit potential. This is discussed in Chapter Four and Chapter Five.

Methanol crossover was measured using the voltammetric method developed by Ren *et al.*[2,3] Nitrogen was passed through the cathode compartment and the cell voltage was set at 0.8-0.9V (i.e. the fuel cell cathode was made positive relative to the anode). Under these conditions, crossover methanol on the cathode side is oxidized to carbon dioxide completely and H_2 is evolved at the anode side. Then the limiting crossover current was recorded and served as a measure of the membrane's permeability.

2.4 Attenuated Total Reflectance Fourier Transform Infrared Spectra

Attenuated Total Reflectance Fourier Transform Infrared (ATR-FTIR) spectra were obtained by a Bruker Tensor 27 infrared spectrometer equipped with a MIRacle ATR accessory.

2.5 Nuclear Magnetic Resonance Spectra

Nuclear Magnetic Resonance spectra were acquired on a Bruker AVANCE

Chapter 3

Preparation of Polypyrrole/Nafion Composite Membranes

3.1 Introduction

Direct Methanol Fuel Cells (DMFC) are currently being developed by many companies as promising candidates for portable and stationary power sources. DMFCs have attracted much attention since 1990 with the introduction of Nafion proton exchange membranes into fuel cells.[1] Due to its excellent chemical, thermal, and mechanical properties, Nafion is prevalently used as the PEM. Though DMFCs have safety advantages over H_2 fuel cells, methanol crossover through the Nafion membrane from the anode to the cathode creates very challenging problems.[2,3,4,5] Methanol crossover strongly affects DMFC performance since the presence of methanol in the cathode not only lowers the fuel utilization efficiency but also causes a mixed potential on the cathode side.[6,7] As shown in section 1.4.3, crossover methanol will be oxidized on the Pt cathode forming CO species which poison the catalyst for oxygen reduction.

3.1.1 Methanol Crossover Measurement Methods

Methanol permeation is such an important factors affecting DMFC's performance that a reliable and convenient method to determine methanol crossover is needed.

The most conventional method is by monitoring the CO_2 flux from the cathode effluent gas using an optical infrared CO_2 sensor.[8,9,10] The CO_2 can also be monitored by gas chromatographic analysis[11,12] or mass spectrometry.[13] These methods are based on the assumption that the crossover methanol is completely oxidized to CO_2 at the cathode

and that there is no CO_2 permeation from the anode to the cathode. However, in a practical DMFC, CO_2 can diffuse through the Nafion PEM, which results an underestimated crossover effect at low current density and overestimated crossover effect at high current density in DMFC.[14] In addition, these methods need complex and expensive equipment. Chu and Jiang et al. simplified this approach by applying the more accurate gravimetric method of determination $BaCO_3$ to analyze the amount of CO_2 produced at the cathode, and corrected for the CO_2 permeation effect by also monitoring the CO_2 flow at the anode.[15] The equivalent current for methanol crossover can be calculated from the discharge current of the fuel cell and the sum of dry $BaCO_3$ precipitate collected at the anode and the cathode exhausts. The method developed by Chu et al is a reliable method to measure methanol crossover during operation of the cell, but not a convenient technique due to the complexity of the DMFC system, the long times for the CO_2 collection, precipitate collection and desiccation, and so on.

Ren and coworkers developed a reliable and convenient voltammetric method to measure the methanol crossover.[16, 17] It is a very useful tool for membrane characterization and was adopted in this research. Fig. 3.1 outlines the transport and electrode reactions involved in the measurement. A methanol solution and inert N_2 were fed to the left side and right side, respectively. Methanol will crossover from the left side to the right side. By applying a positive external voltage on the right side (0.8-0.9V), the crossover methanol will be oxidized to CO_2 with hydrogen evolution as the counter

electrode process on the left side (as a dynamic hydrogen electrode, DHE).

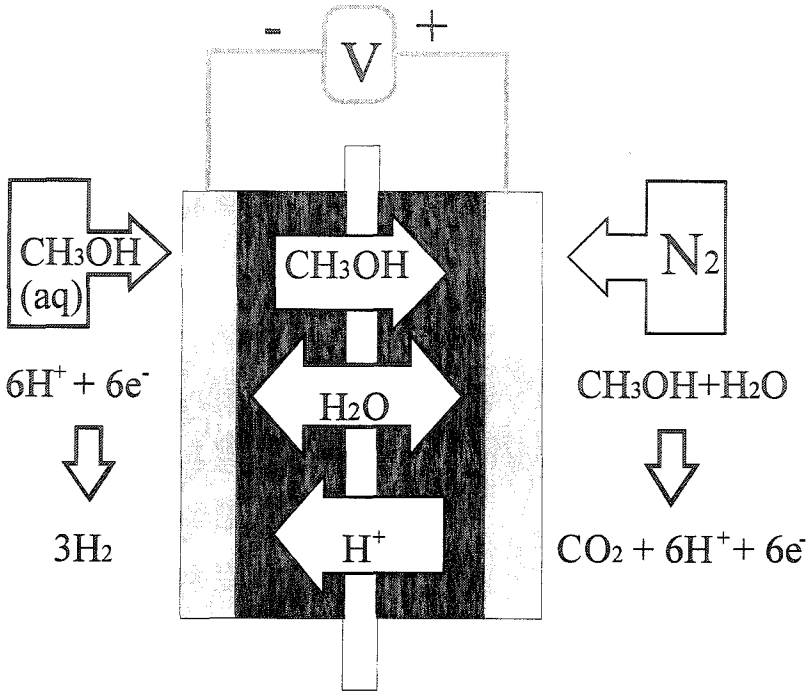

Fig. 3.1. Schematic diagram of the measurement of methanol crossover in a direct methanol fuel cell. Electrode reactions are also shown in the diagram.

The methanol permeation parameters can be determined from the steady-state limiting current density (J_{lim}) resulting from complete electro-oxidization of the crossover methanol to CO_2 at the Pt fuel cell cathode:

$$J_{\lim} = k_{dl} \frac{6FD_m C_m}{d} \qquad (3.1)$$

where D_m is the diffusion coefficient, C_m is the methanol concentration within the membrane, k_{dl} is the drag coefficient, d is the thickness of the Nafion membrane, and F is the Faraday constant.

When methanol crossover is only determined by diffusion, k_{dl} is unity. However, the elctro-osmotic drag due to the proton movement, results in $k_{dl}<1$. At open circuit potential, the effective methanol crossover current density ($J_{crossover}$) is higher than the measured limiting current density.

$$\frac{J_{crossover}}{J_{\lim}} = \frac{6\xi \cdot x_0}{\ln(1+6\xi \cdot x_0)} \qquad (3.2)$$

where ξ is the elctro-osmotic drag coefficient and x_0 is the molar fraction of methanol in the feed methanol solution. For simplicity, J_{lim} is used in this thesis as a relative measure of crossover and used directly to compare the methanol crossover properties of different membranes.

3.1.2 Conducting Polymer/Nafion Composite Membranes

Composites are an important class of materials that can take advantages of desired properties of different components. To reduce methanol crossover through Nafion membranes, significant research efforts have focused on the preparation of Nafion based hybrid composite membranes (e.g. SiO_2/Nafion, TiO_2/Nafion, PVA/Nafion, et al).[18,19,20,21,22,23] However, the decreased methanol crossover of these modified membranes is always accompanied by low proton conductivities.

The polymerization of aromatic compounds within Nafion membranes has shown to be a good potential for the preparation of composite membranes for DMFCs.

Poly(1-methylpyrrole)/Nafion composite membranes have displayed a 40% reduction of methanol permeation without a significant increase in resistance.[24,25]

In this work, pyrrole was selected over 1-methylpyrrole as the monomer due to its higher water solubility, which simplifies the polymerization process. Pyrrole can be easily loaded into the acid form of Nafion and polymerized by water-soluble oxidants. Moreover, polypyrrole is insoluble in water and is not washed out of the membrane during fuel cell operation.[26] In addition, preliminary results in our group have shown that the polypyrrole modified Nafion membranes have better performance than poly(1-methylpyrrole) modified ones.[26]

Polypyrrole/Nafion membranes have been prepared and studied in DMFCs in our lab.[27,28] However, systematic work was required to elucidate the factors that influence the rate, and extent of polypyrrole incorporation into Nafion membranes.

In this chapter, the factors that determine the production of polypyrrole in Nafion membranes are examined. A reproducible and optimized preparation procedure is established.

3.2 Experimental

3.2.1 Materials

Nafion membranes (Dupont; donated by H Power Corp.) were cleaned following section 2.2.1. Pyrrole (Aldrich) was distilled under N_2. Every pyrrole solution used in the

experiments was freshly prepared. Nanopure DI water was used to prepare all aqueous solutions and for washing membranes. All other chemicals were used as received.

All electrodes used in the work in this chapter are Pt black cathodes provided by Ballard Power Systems, which consisted of a total Pt loading of 4 mg/cm^2 on CFP (T090) bonded with 11% PTFE.

3.2.2 Preparation of Polypyrrole/Nafion Composite Membranes

Polypyrrole/Nafion membranes were prepared according to the three steps shown in Fig. 3.2. Nafion 115 was immersed in a pyrrole solution to load the monomer; then transferred to an oxidizing reagent solution (such as Fe^{3+}, or H_2O_2) to polymerize the pyrrole; and finally removed from the oxidizing solution and rinsed with water to stop the polymerization. The composite membranes were then washed with 1M HNO_3 and 1M H_2SO_4 until the acid wash remained colorless. The membranes were washed with DI water after every step. The polypyrrole/Nafion membranes were then stored in a large volume of DI water before use.

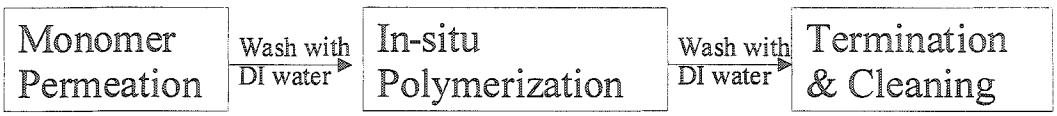

Fig. 3.2. Schematic of the procedure for modification of Nafion with polypyrrole

3.2.3 Fuel Cell Experiments

Methanol crossover was measured in the $1cm^2$ fuel cell. The cell was fed with 1M methanol solution and N_2 gas with a methanol pumping rate of 0.153 ml/min and a N_2 flow rate of 12.3 ml/min. A two-step chronoamperometry experiment was applied. The fuel cell was conditioned at 0.7 V for 50 seconds prior to measurements to oxidize the methanol accumulated on the cathode side. The potential was then stepped to 0.9 V for 100 seconds, and then stepped to 0.8 V for 100 seconds. Fig. 3.3 shows a typical chronoamperometric current density vs. time diagram for Nafion 115. After a sharply decaying charging current at the beginning of the potential step from 0.7 V to 0.9 V, the crossover current stabilized after *ca.* 30 seconds. On the second step, the charging current sharply decreased at the beginning of the potential step from 0.9 V to 0.8 V and then stabilized at a constant value. The crossover current of Nafion 115 was determined from the average of the last 20 seconds of the two potential steps (0.9 V and 0.8 V). Table 3.1 summarizes the methanol crossover currents collected by the same method for different composite membranes.

Ionic resistances were measured by impedance spectroscopy on fully hydrated membranes sandwiched (pressure contact) between two 1 cm^2 Ballard cathodes. Fig.3.4 shows a Nyquist plot for Nafion 115. The membrane resistance is determined by the average of the two intercepts on the real resistance axis as shown in the inserted figure in Fig. 3.4. The resistances of the membranes are collected and recorded in Table 3.1.

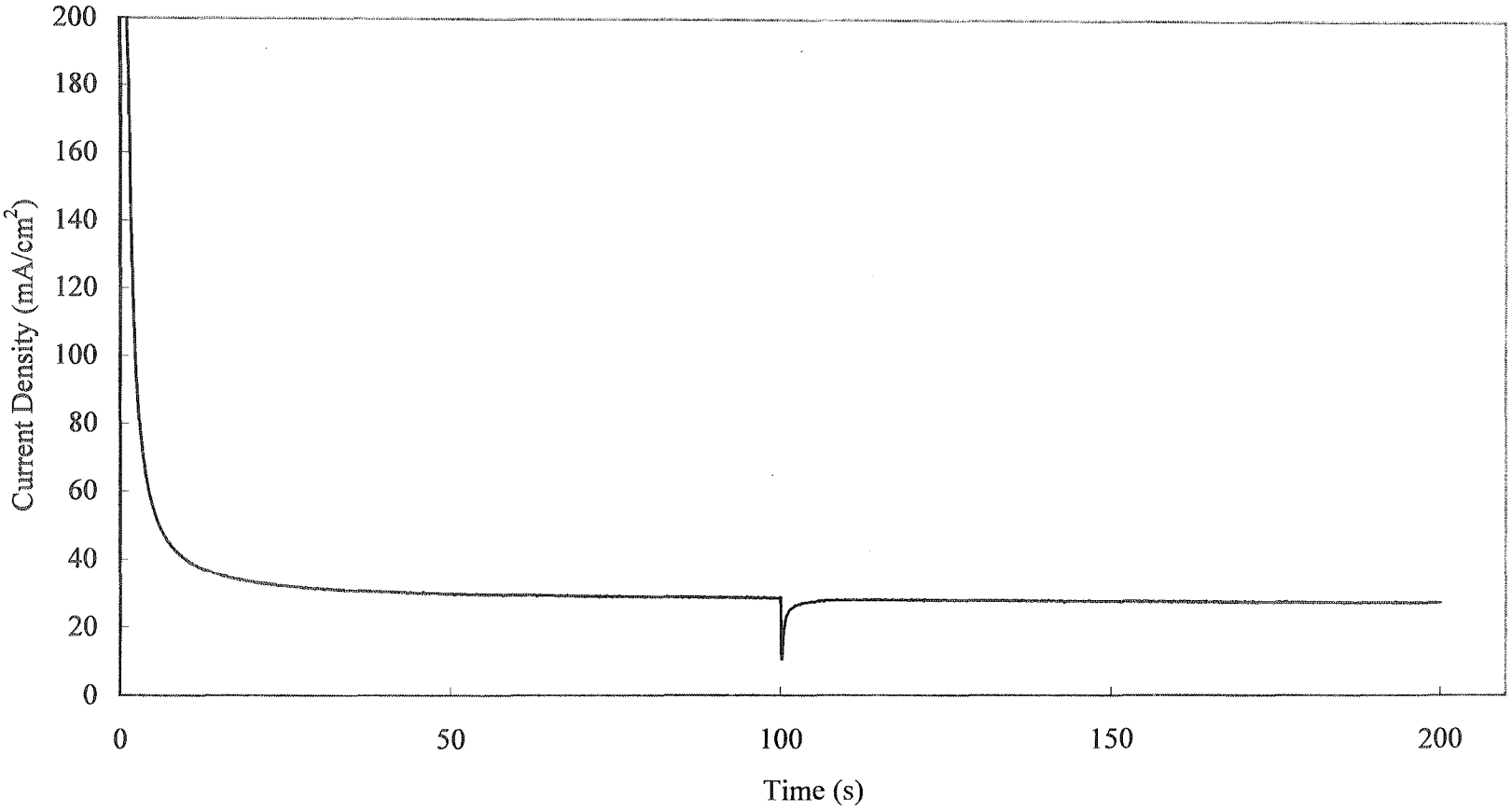

Fig. 3.3. Two-step chronoamperometric current density vs. time diagram for Nafion 115.

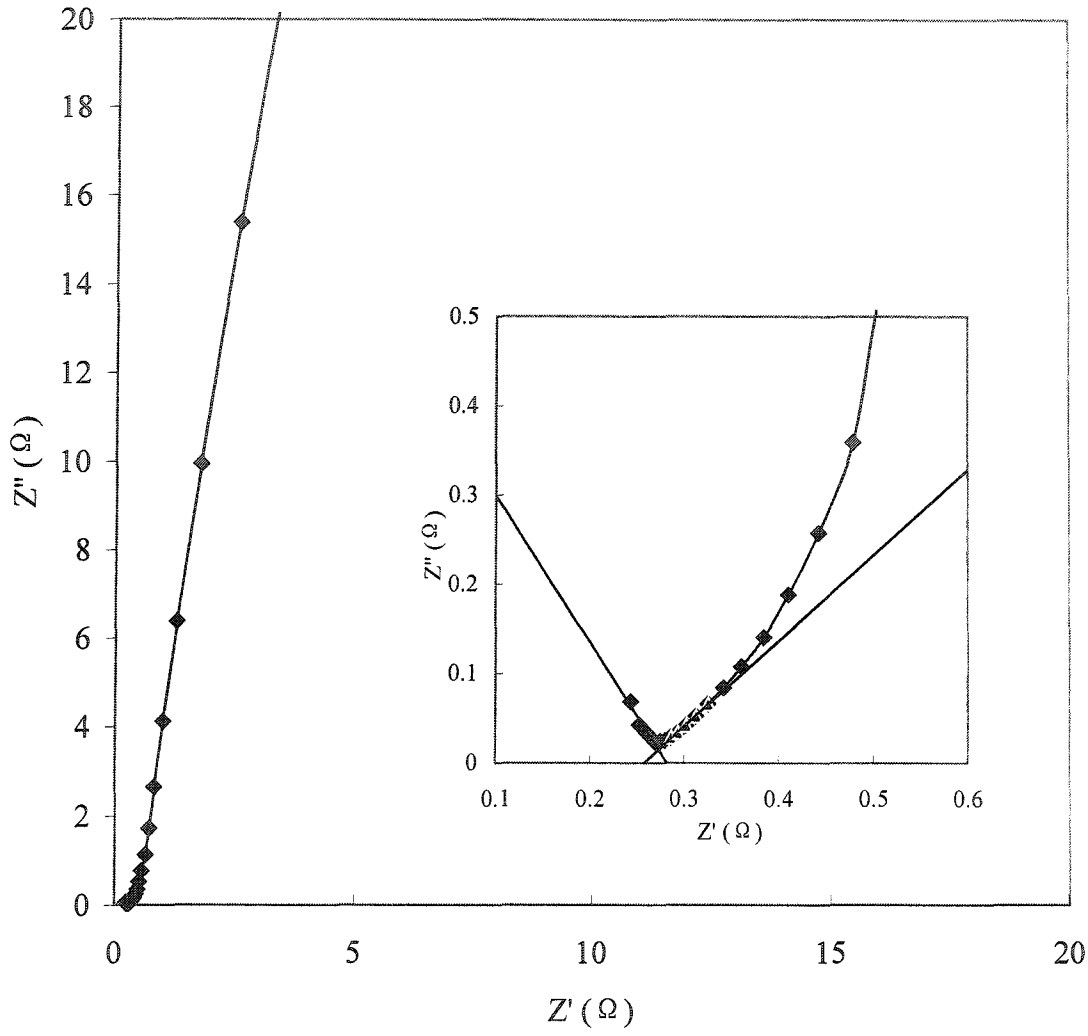

Fig. 3.4. Nyquist impedance spectra for a 1 cm^2 DMFC at the open circuit potential. Inset shows an expansion of the high frequency region of the plot. The cell was operated at ambient temperature (22 ± 3 °C) with 0.153 mL/min 1 M methanol solution and 24.6 mL/min N_2.

All electrochemical data in this chapter were collected with an EG&G PAR 273A Potentiostat/Galvanostat/5210 Lock-in Amplifier electrochemical analysis system at ambient temperature (22 ± 3°C).

3.3 Results and Discussion

Nafion membranes are composed of three distinct regions as showed in Fig. 3.5 (A): the hydrophilic anion clusters, the hydrophobic PTFE backbone and an interfacial region between the two. Pyrrole monomer can easily partition into the strongly acidic hydrophilic anion clusters in Nafion membranes (showed in Fig. 3.5 (B)), and this is followed by protonation and polymerization. The presence of polypyrrole in the hydrophilic region effectively blocks methanol permeation.

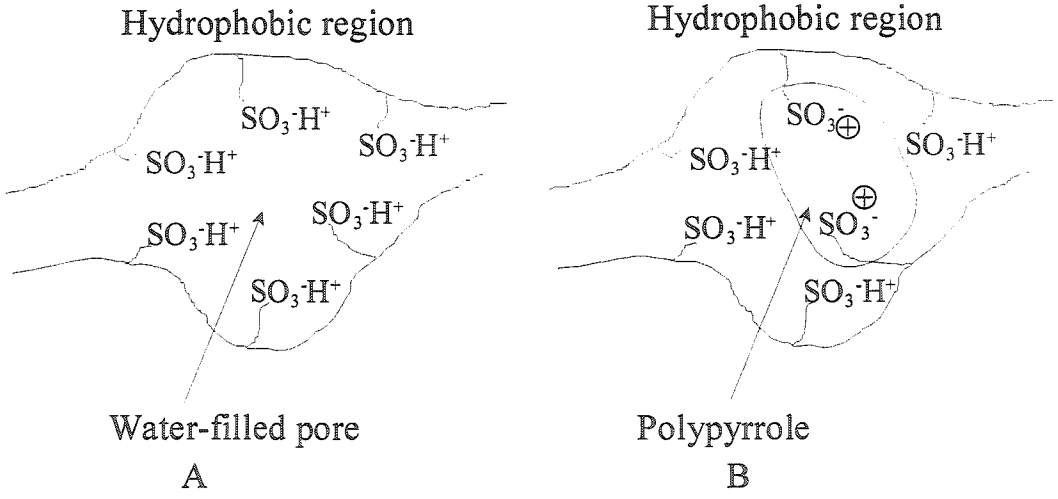

Fig.3.5. Schematic structure of fully hydrated membranes before (A. Nafion) and after modification (B. polypyrrole/Nafion composites)

Many factors could affect the polymerization of polypyrrole in Nafion membranes, and thus influence the permeation properties and ionic conductivities of the composite membranes. One of the most important is the choice of oxidizing agent. H_2O_2 is chosen as the oxidizing agent instead of Fe^{3+} in all the experiments for two reasons: 1) Fe^{3+} can promote the formation of polypyrrole at the outer surface of the membrane;[29,30] and 2) a small amount of Fe^{3+} residue can remarkably influence the O_2 reduction kinetics at a Pt cathode.[31] H_2O_2 can drive the polymerization of pyrrole in an acid environment and introduces no impurities into the Nafion membranes; $H_2O_2 + 2H^+ + 2e^- \rightarrow 2H_2O$. The modification process could be easily controlled by varying the concentration of the pyrrole solution, loading time, and the polymerization time.

The conditions used for Nafion modification are listed in Table 3.1, together with methanol crossover currents measured in a 1 cm^2 cell and resistance measured by impedance in a sandwich cell. All modification conditions have been repeated at least once and the electrochemical measurement results have shown excellent reproducibility. The crossover limiting current density and impedance data shown in this table are averaged for MEAs made from different modification experiments. Their standard deviations were less than 5%. The polypyrrole modified Nafion membranes all exhibited excellent reduction of methanol crossover. However, their impedances were higher than the pristine membrane.

Different pyrrole concentration solutions, from 0.1 M to 0.5 M, were used to load

Table 3.1. Methanol crossover currents and resistances of polypyrrole/Nafion composite membranes

Membrane code	Resistance (Ω cm^2)[a]	Methanol Crossover (mA/cm^2)[a]	J_{115}/J_m	Polymerization Conditions: Pyrrole Loading Concentration, Time	Polymerization Conditions: Time in 5% H_2O_2
Nafion 115	0.27	28.3	1		
A	0.44	12.0	2.35	0.1 M, 20 min	1 h
B	0.42	10.6	2.66	0.1 M, 20 min	2 h
C	0.42	14.6	1.93	0.1 M, 20 min	6 h
D	0.41	14.4	1.96	0.1 M, 20 min	12 h
E	0.36	16.4	1.72	0.1 M, 20 min	18 h
F	0.43	11.5	2.46	0.1 M, 40 min	12 h
G	0.59	5.9	4.79	0.1 M, 60 min	12 h
H	1.03	3.2	8.88	0.1 M, 120 min	12 h
I	0.78	11.4	2.48	0.2 M, 20 min	12 h
J	3.02	0.1	353	0.5 M, 20 min	12 h

[a] Measured at room temperature.

the monomer. With increasing monomer concentration, more monomer could be loaded into the Nafion membranes under same loading time. However, polypyrrole is an electronic conducting polymer. With increase of the polypyrrole content, the composite membranes' properties can change from flexible and ionic conducting to stiff and electronic conducting. Relatively low polypyrrole loading (1-5 wt.%) is required for the composite membranes to decrease the methanol crossover but maintain high proton conductivity.[24]

To study other aspects of the modification process, 0.1 M pyrrole solution was used in all the other modifications.

3.3.1 Influence of Polymerization Time in H_2O_2

Pieces of Nafion membranes were immersed in 0.1M aqueous pyrrole solutions for 20 mintues, and then the pyrrole was polymerized in 5% H_2O_2 solutions for 1 to 18 hours. The crossover limiting currents and impedance are showed in Table 3.1.

Fig. 3.6 shows the methanol crossover current as a function of polymerization time. Methanol crossover sharply dropped during the first 1-2 hours of polymerization. With longer H_2O_2 treatment times, methanol crossover increased a little and then remained nearly constant from 6-12 hours. These results show that pyrrole is rapidly polymerized in Nafion by 5% H_2O_2 and that the degradation of the resulting polymer by excess H_2O_2 is very slow. Even after oxidization with 5% H_2O_2 for weeks (>2 weeks), a large amount of

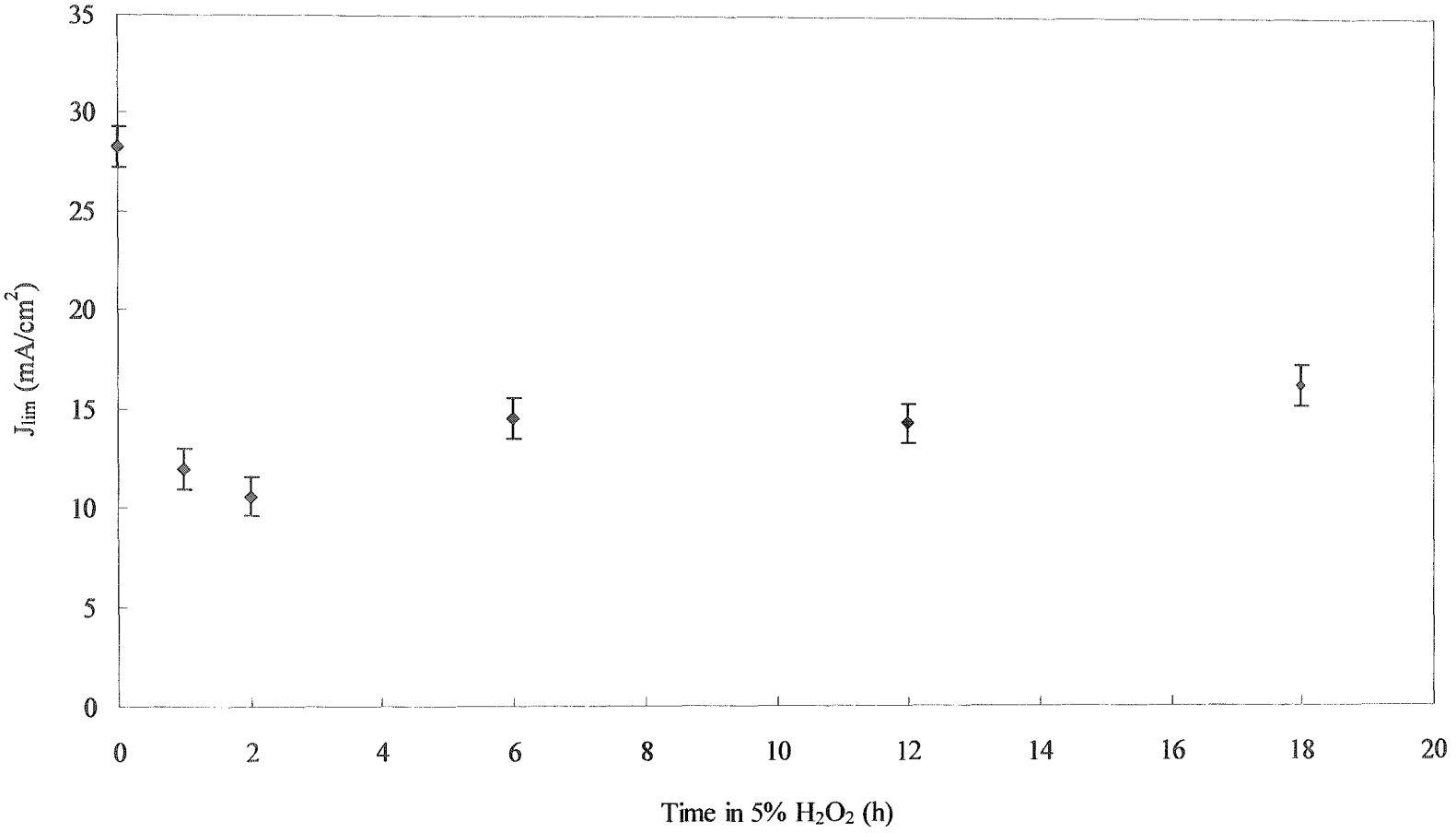

Fig. 3.6. Methanol crossover through polypyrrole/Nafion modified membranes at different polymerization times

polypyrrole remained in composite membranes. However, when 30% H_2O_2 was used, rapid polymerization was followed by fast degradation of the polypyrrole. Hot 30% H_2O_2 can be used to return the membranes to a clear colourless unmodified state in minutes. A 5% H_2O_2 solution was used here in all modifications because it is effective for the polymerization of pyrrole in Nafion and its relatively low oxidation activity is useful for removal of polypyrrole from the membrane's surface but it does not induce severe degradation.

Methanol transport through the membrane is accomplished by diffusion through the ion cluster pores and the connecting ion channels. From equation 3.1, three variables, k_{dl}, D_m and C_m control the crossover limiting current. At low pyrrole loadings, polypyrrole maybe formed mainly in the ionic pores and so may not significantly interrupt the transport properties of Nafion membranes. k_{dl} and D_m are almost the same as for unmodified Nafion membranes. However, the presence of polypyrrole in Nafion will decrease the ionic pore size and thus reduce the concentration of methanol in the membrane (C_m in equation 3.1). Ren *et al.*[16] and Skou *et al.*[32] have reported that the methanol concentration within Nafion pores is the same as that of the feed methanol solution (C_0). Hence, C_m is determined by the membrane porosity, ε.

$$C_m = \varepsilon C_0 \qquad (3.3)$$

For composite membranes, their porosity (ε_m) is given by equation 3.4:

$$\varepsilon_m = \varepsilon_{Nafion} - \frac{V_{polypyrrole}}{V_{membrane}} \qquad (3.4)$$

where ε_{Nafion} is the porosity of pure Nafion membrane, $V_{polypyrrole}$ and $V_{membrane}$ are the volume of polypyrrole inside the membrane and the volume of the membrane, respectively.

The reduction of methanol crossover is thus expected to be proportional to the content of polypyrrole in the modified membranes. Lower methanol crossover current is assumed to mean higher polypyrrole content. The partitioning of pyrrole into Nafion membranes has been studied by a gravimetric method by Yepez and Pickup.[33] The reduction of the methanol crossover current was approximately proportional to the amount of polypyrrole in the modified membranes at relatively low pyrrole loadings (1-20 wt.%).

In the above discussion, it was assumed that k_{dl} and D_m do not change by modification of the membrane. However, as the ionic pores size decreases, the bulk-like water content decreases and the proton transfer mechanism could be affected significantly.[34] The mechanism of proton transport through PEMs is still debated.[35] In general, a decrease of the membrane's porosity always results in lower proton conductivity. The gravimetric results also showed that the resistances for composite membranes increased with the increasing of polypyrrole content.[33] Fig. 3.7 shows the resistances of modified membranes plotted against the polymerization time. These data

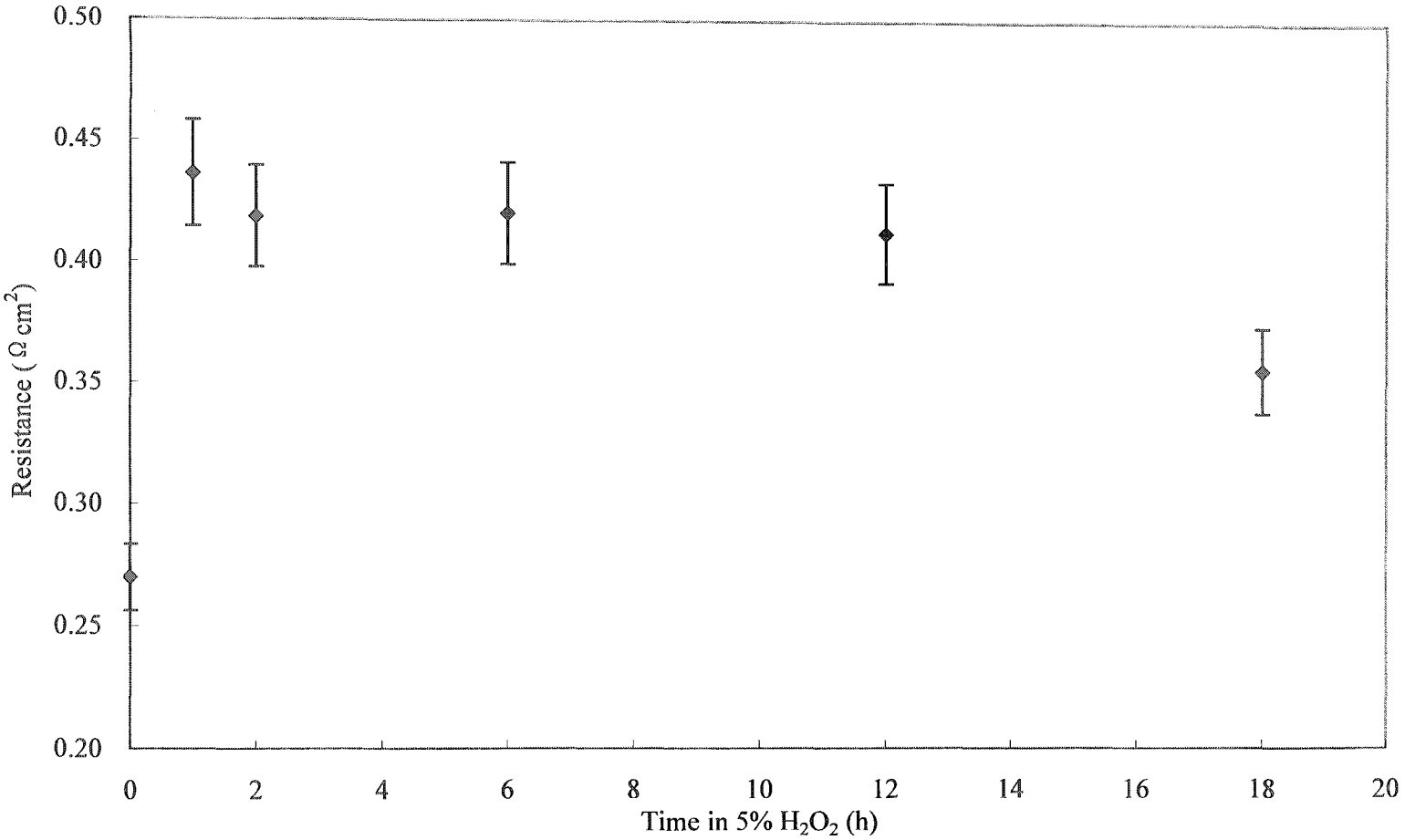

Fig. 3.7. Resistance of polypyrrole/Nafion modified membranes at different polymerization times

support the above conclusions that rapid polymerization is followed by slow degradation of the resulting polypyrrole. The highest resistance was reached after polymerization for 1 hour. A slow decrease in resistance was observed at longer times.

3.3.2 Influence of Pyrrole Loading Time

Nafion membranes were soaked in 0.1M pyrrole solutions for various times and then immersed in 5% H_2O_2 for 12 hours to complete the polymerization. The monomer loading times and crossover limiting currents and resistance of each membrane are shown in Table 3.1.

As described in section 3.3.1, the methanol crossover and the conductivity of the polypyrrole/Nafion composite membranes, which are directly related to the membrane's porosity, have a linear relationship with their polypyrrole content. The uptake of pyrrole could be estimated from the crossover current of the composites membranes by assuming that the same percentage of pyrrole monomer loaded into the Nafion is polymerized in each experiment.

Fig. 3.8 shows the methanol crossover current plotted against the square root of the pyrrole partition time. The crossover limiting current was found to decrease linearly with the square root of pyrrole loading time ($t^{1/2}$), indicating a diffusion-controlled process. This affirms our previous UV results.[26]

Fig. 3.9 shows membrane conductivity against the square root of pyrrole partition

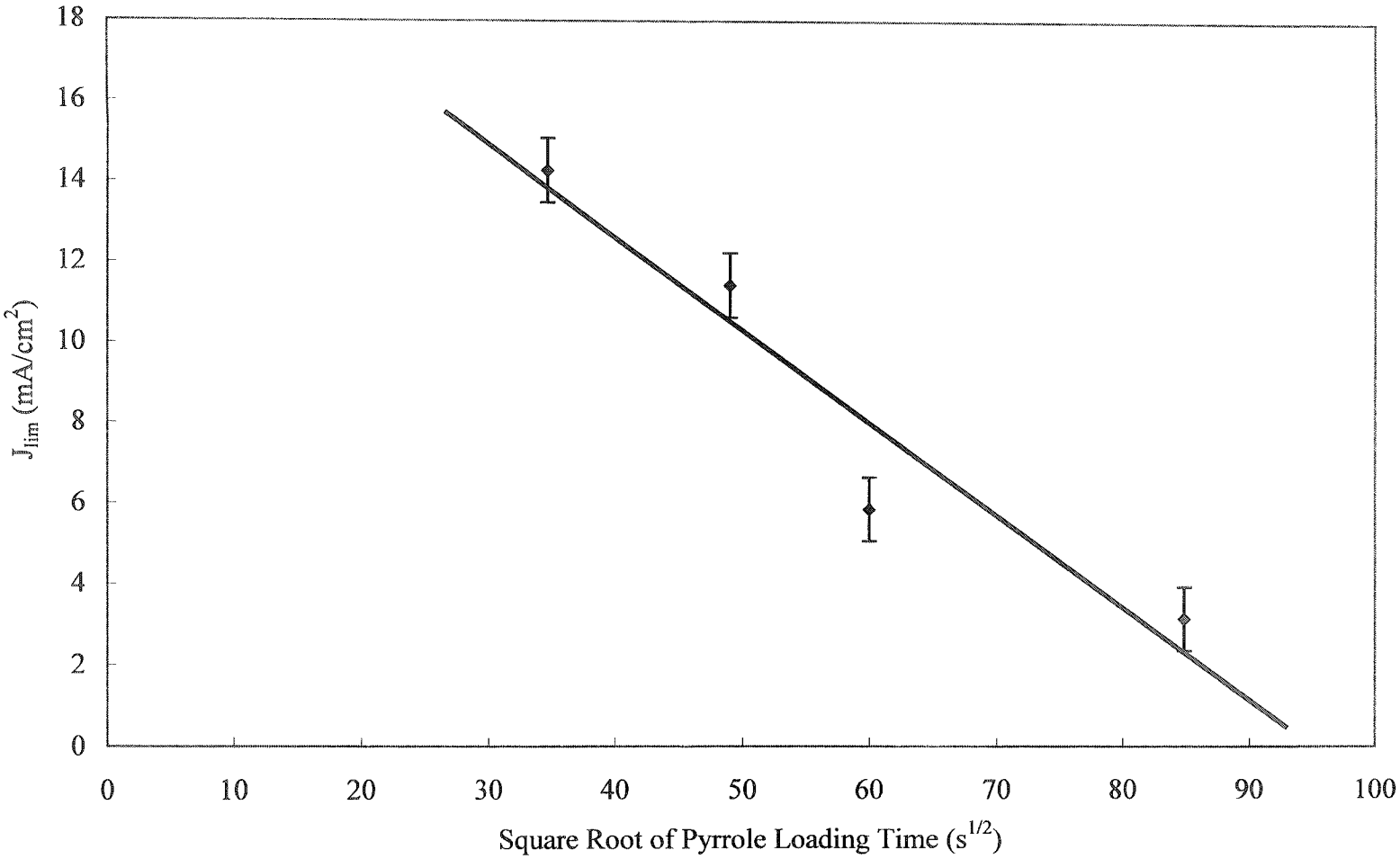

Fig. 3.8. Methanol crossover through polypyrrole/Nafion modified membranes as a function of the square root of the pyrrole loading time.

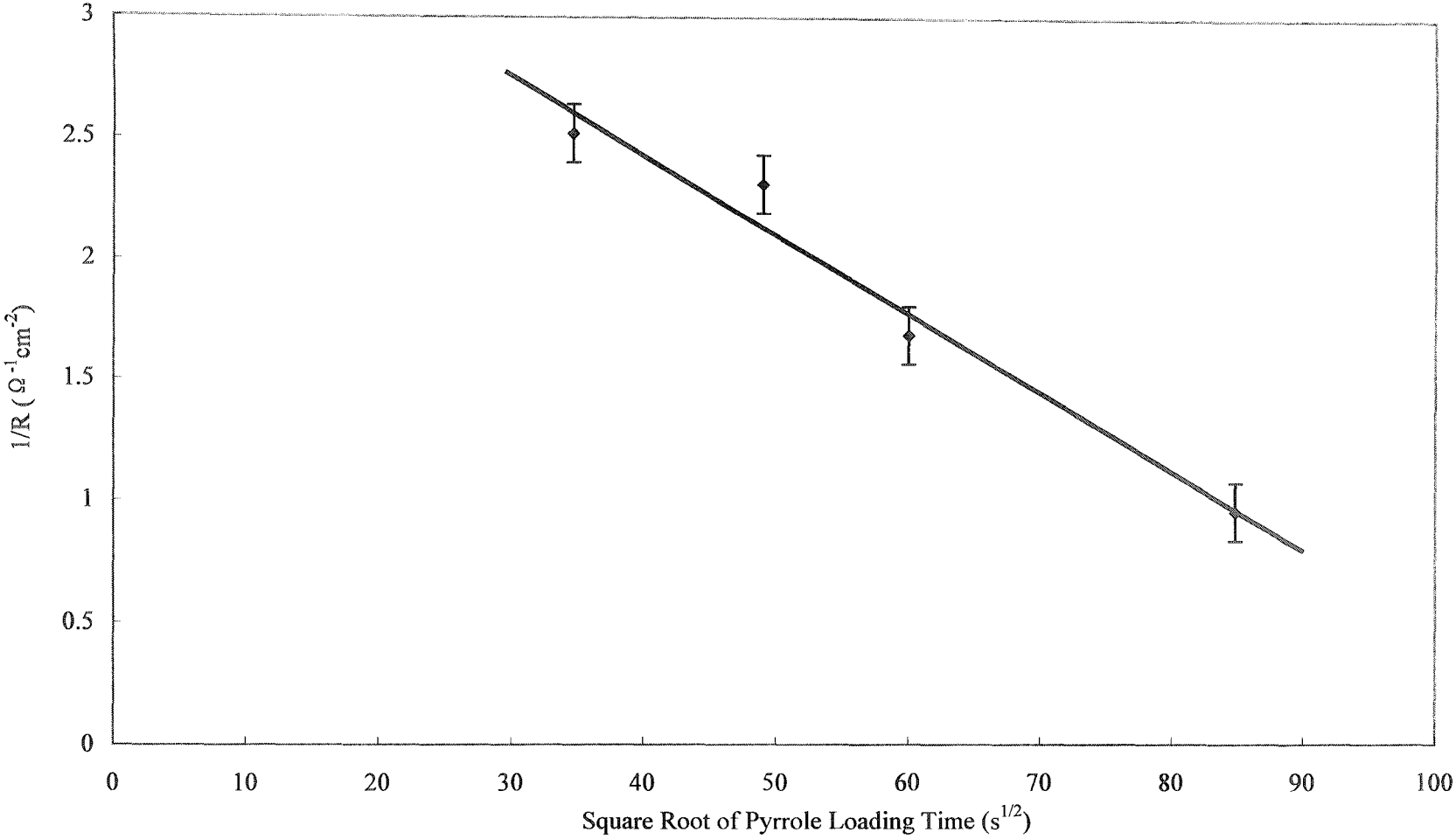

Fig. 3.9. Conductivity of polypyrrole/Nafion modified membranes vs. the square root of the pyrrole loading time

time. The conductivity of the modified membranes decreased linearly with the square root of pyrrole loading time, again indicating diffusion control of the pyrrole loading process.

This provides strong evidence that the extent of the polymerization of loaded pyrrole is not influenced in every experiment.

3.3.3 Selectivity of Polypyrrole/Nafion Composite Membranes

It is clear that the composite membranes prepared in this work can effectively reduce methanol crossover but this is accompanied by significantly higher resistances than for the unmodified membrane. It is a challenge to prepare a composite membrane with high methanol blocking ability and relatively low resistance. Selectivity for blocking methanol vs. proton transport can be assessed as follows.

A crossover reduction factor is proposed and defined as the ratio of Nafion 115's crossover current to that of the modified membrane (J_{115}/J_m). According to equation 3.1, methanol crossover can be depressed by increasing the thickness of the membrane.[36] The membrane's resistance is controlled by Ohm's Law:

$$R = \rho\frac{d}{A} \qquad (3.5)$$

where ρ is the resistivity of the membrane and A is its area.

For a series of different thickness Nafion membranes with the same equivalent weight of 1100 (Nafion), J_{115}/J_m has a linear relationship with resistance (shown in Fig. 3.10 as the unmodified membrane tendency line). Any membranes that have a higher

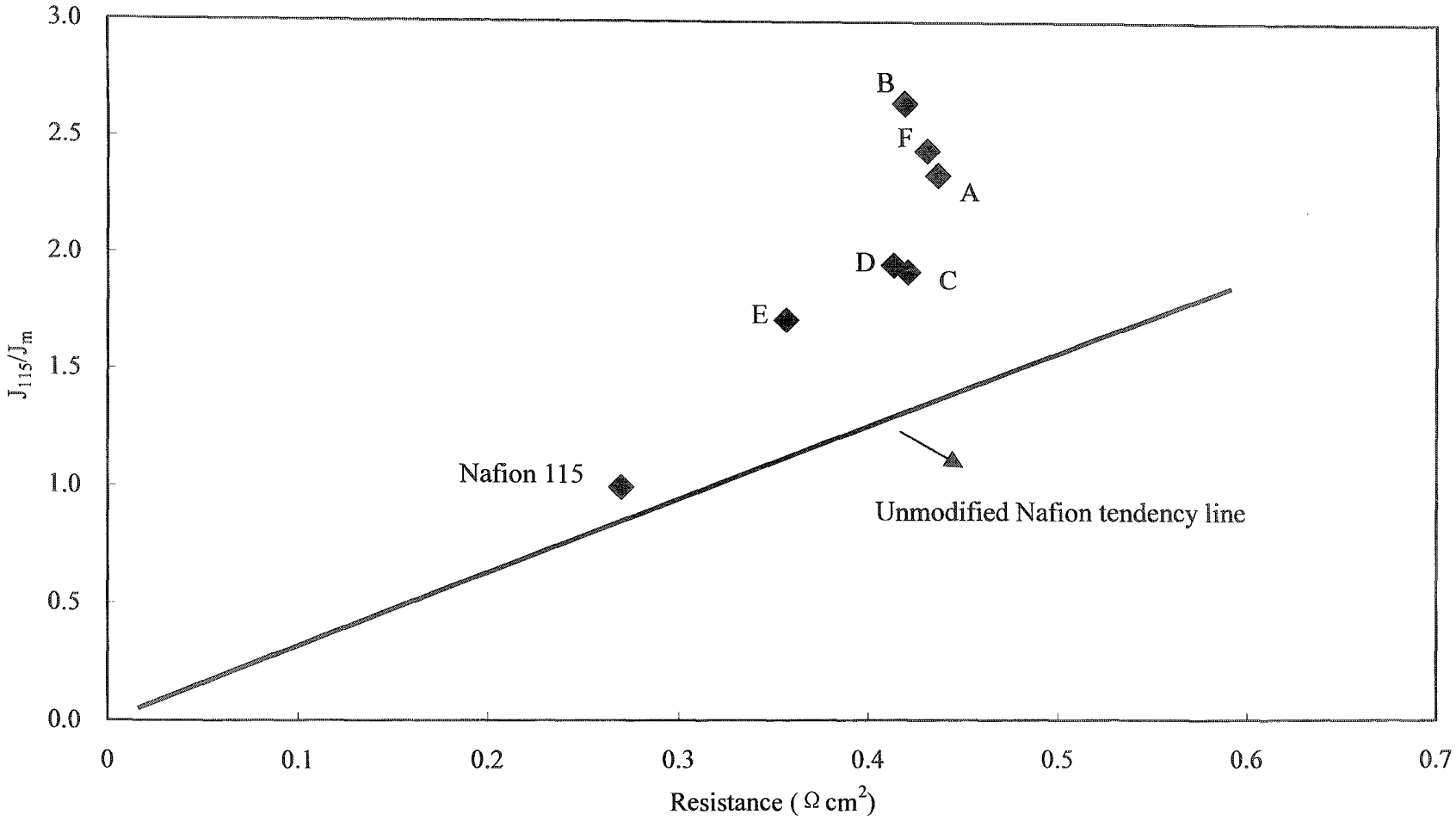

Fig. 3.10. Selectivity of polypyrrole/Nafion modified membranes. J_{115} and J_m are the limiting crossover current of Nafion 115 and composite membranes, respectively.

crossover selective factor but lower impedance are promising candidate for DMFCs. In a straightforward way, the higher the data point above the unmodified tendency line, the better membrane performance is expected.

The composite membranes' crossover reduction factors are plotted in Fig. 3.10. Membranes G, H, I and J are not shown in this figure because of their extremely high resistances compared with the other modified membranes. Membrane B showed the highest crossover reduction factor (about 2.7) and an acceptable resistance (0.42 $\Omega \cdot cm^2$ compared with 0.27 $\Omega \cdot cm^2$ for Nafion 115).

3.4 Conclusions

Polypyrrole/Nafion composite membranes have been prepared and their methanol crossover currents and resistances have been measured, respectively, by two-step chronoamperometry using a 1 cm^2 DMFC and EIS using a sandwich cell. The following conclusions summarize the results presented here.

1. H_2O_2 can polymerize pyrrole and overoxidize polypyrrole at the same time. In the first hours, the polymerization reaction is dominated and polypyrrole is quickly formed. When the monomer has been consumed, further oxidation by H_2O_2 leads to overoxidation of the polypyrrole. Use of 5% H_2O_2 does not cause severe degradation of polypyrrole.

2. Methanol crossover limiting current and the conductivity of the composite membranes decrease linearly with the square root of the pyrrole loading time, indicating

that the pyrrole loading process is diffusion-controlled.

3. Compared with unmodified Nafion membranes, the composite membranes have lower methanol crossover but higher resistance. However, the modified membranes do not follow the unmodified Nafion membrane tendency line. Membrane B shows excellent potential for DMFC applications because of its high crossover reduction factor of J_{lim}/J_m=2.7 and an acceptable resistance (only 50% higher than Nafion 115).

References

[1] T. E. Springer, T. A. Zawodzinski, S. Gottesfeld. *J. Electrochem. Soc.*, 1999, 138: 2334

[2] X. Ren, S. Gottesfeld. *J. Electrochem. Soc.*, 2001, 148: A87-A93

[3] Z. Qi, M. Hollett, C. He, A. Attia, A. Kaufman. *Electrochem. Solid-State Lett.*, 2003, 6: A27-A29

[4] J. Kallo, W. Lehnert, R. V. Helmolt. *J. Electrochem. Soc.*, 2003, 150: A765-A769

[5] A. Heinzel, V. M. Barragán. *J. Power Sources*, 1999, 84: 70-74

[6] L. J. Hobson, H. Ozu, M. Yamaguchi, S. Hayase. *J. Electrochem. Soc.*, 2001, 148: A1185-A1190

[7] Z. Shao, I-M. Hsing. *Electrochem. Solid-State Lett.*, 2002, 5: A185-A187

[8] S. C. Thomas, X. Ren, S. Gottesfeld, P. Zelenay. *Electrochim. Acta*, 2002, 47: 3741-3748

[9] A. S. Aricò, S. Srinivasan, V. Antonucci. *Fuel Cells*, 2001, 1: 133-161

[10] L. Carrette, K. A. Friedrich U. Stimming. *ChemPhysChem*, 2000, 1, 162-193

[11] P. Dimitrova, K. A. Friedrich, A. Vogt, U. Stimming. *J. Electrianal. Chem.*, 2002, 532: 75

[12] M. Walker, K. M. Baumgartner, M. Kaiser, J. Kerres, A. Ullrich, E. Rauchle. *J. Appl. Polym. Sci.*, 1999, 74:67-73

[13] J. T. Wang, Wasmus, R. F. Savinell. *J. Electrochem. Soc.*, 1996, 143: 1233

[14] R. Jiang, and D. Chu. *Electrochem. Solid-State Lett.*, 2002, 5: A156-A159

[15] R. Jiang, and D. Chu. *J. Electrochem. Soc.*, 2004, 151: A69-A76

[16] X. Ren, T. E. Springer, S. Gottesfeld. *J. Electrochem. Soc.*, 2000, 147: 92-98

[17] X. Ren, T. E. Springer, T. A. Zawodzinski, S. Gottesfeld. *J. Electrochem. Soc.*, 2000, 147: 466-474

[18] Z. Shao, I. Hsing. *Electrochem. Solid-State Lett.*, 2002, 5: A185-A187

[19] L. J. Hobson, Y. Nakano, H. Ozu, S. Hayase. *J. Power Sources*, 2002, 104: 79

[20] B. Kumar, J. P. Fellner. *J. Power Sources*, 2003, 123: 132-136

[21] H. Uchida, Y. Ueno, H. Hagihara, W. Wantanabe, *J. Electrochem. Soc.*, 2003, 150: A57-A62

[22] N. Miyake, J. S. Wainright, R. F. Savinell. *J. Electrochem. Soc.*, 2001, 148: A905-A909

[23] P. L. Antonucci, A. S. Arico, P. Creti, E. Ramunni, V. Antonucci, *Solid State Ionics*, 1999, 125: 431-437

[24] N. Jia, M. C. Lefebvre, J. Halfyard, Z. Qi, P. G. Pickup, *Electrochem. Solid-State Lett.*, 2000, 3: 529-531

[25] P. G. Pickup, Z. Qi. *Canadian Patent Application No. 2,310,310,* PCT/CA 01/00767 2000

[26] E. B. Easton, B. L. Langsdorf, J. A. Hughes, J. Sultan, Z. Qi, A. Kaufman, P. G. Pickup, *J. Electrochem. Soc.*, 2003, 150: C735-C739

[27] B. L. Langsdorf, B. J. Maclean, J. E. Halfyard, J. A. Hughes, P. G. Pickup. *J. Phys. Chem. B*, 2003, 107: 2480-2484

[28] B. L. Langsdorf, J. Sultan, P. G. Pickup. *J. Phys. Chem. B*, 2003, 107: 8412-8415

[29] T. Sata. *Chem. Mater.* 1991, 3: 838-843

[30] T. Sata, T. Funakoshi, K. Akai. *Macromolecules*, 1996, 29: 4029-4035

[31] T. Abe, M. Kaneko. *Prog. Polym. Sci.*, 2003, 28: 1441-1488

[32] E. Skou, P. Kauranen, J. Hentschel. *Solid State Ionics*, 1997, 97: 333

[33] O. Yepez, P. G. Pickup. Unpublished work

[34] A. Z. Weber, J. Newman. *J. Electrochem. Soc.*, 2003, 150: A1008-A1015

[35] S. J. Paddison. *Annu. Rev. Mater. Res.*, 2003, 33: 289-319

[36] E. B. Easton. Ph.D. thesis. Memorial University of Newfoundland, St. John's, NF, Canada. 2002

Chapter 4

Characterization of Polypyrrole/Nafion Modified Membranes in Direct Methanol Fuel Cells

4.1 Introduction

Polypyrrole/Nafion is not a new material and has been exploited in many applications.[1] Sata *et al.* have prepared polypyrrole/Nafion ion exchange membranes that remarkably decrease the permeation of alkali earth metal cations relative to sodium ions and neutral molecules.[2] Moreover, research in the Pickup group has shown that polypyrrole/Nafion composite membranes have reduced methanol permeability that makes them very attractive for direct methanol fuel cells (DMFCs).

The preparation of polypyrrole/Nafion composite membranes is described in Chapter Three. These membranes showed less methanol crossover and therefore significantly decrease the energy efficiency losses due to methanol crossover in a DMFC. The steps that compose the modification process were studied by electrochemical methods, and an optimized modification procedure was developed. In this chapter, the properties of polypyrrole/Nafion composite membranes are characterized in an operational DMFC. Methanol crossover and DMFC performances were evaluated and are compared with those of unmodified Nafion 115 membranes.

Because polypyrrole is a positively charged conducting polymer when doped, it can interacted with the sulfonate groups in the ion pores and ion channels of the Nafion, and thus reduced the membrane's proton conductivity. Two approaches were therefore applied to decrease the resistance of the composite membranes: the provision of negatively charged counter ions during the polymerization and the use of a pyrrole solfonate

monomer. Preliminary results are presented at the end of this chapter.

4.2 Experiment

4.2.1 MEA Preparation

Polypyrrole/Nafion composite membranes were prepared according to section 3.2.2 using the same modification conditions as membrane B. All further modification are applied to this kind of membrane and coded as B-X (e.g. B-4).

Anodes used in this chapter were PtRu anodes prepared by Dr. Brad Easton (Pt/Ru loading 4 mg/cm^2, described in section 2.2.1). Pt cathodes were provided by Ballard Power Systems (Pt loading 4 mg/cm^2, described in section 2.2.1). MEAs were prepared by hot pressing at 130 °C under 100 pound/cm^2 pressure for 180s.

4.2.2 Fuel Cell Experiments

Membranes were evaluated at 60 °C in a commercial 5 cm^2 active area fuel cell (ElectroChem. Inc.) as previously described (section 2.3). Electrochemical data in this chapter were collected by a Solartron 1286/1250 electrochemical analysis system (Schlumberger).

In DMFC polarization measurements, the fuel cell was fed with 1 M methanol solution at 0.153 mL/min and air at a fixed flow rate of 73.1 mL/min, corresponding to a stoichiometry of 3.7 mol O_2 /4 mol electrons at 200 mA/cm^2. The cell was conditioned at

0.5V (or 100 mA/cm^2) before polarization measurements until a steady-state current density (or voltage) was reached. Polarization data were recorded by applying a constant current from the potentiostat. The voltage at each current was recorded after stabilization for 3 min. Cell resistances were measured by impedance spectroscopy.

Anode polarization curves were obtained by passing H_2, instead of air, through the cathode compartment of the fuel cell at a flow rate of 25.6 mL/min. A positive potential was applied to the anode. Under these conditions, the cathode evolves H_2 and behaves as a dynamic hydrogen electrode (DHE).

Methanol crossover was measured by a two-step chronoamperometry method developed by Ren et al.[3] (described in section 3.2.3). 1 M methanol solution was fed at 2.25 mL/min and N_2 was flushed through the cathode side at 23 mL/min. For the purpose of relative comparisons, the correction for electro-osmotic drag was not applied.

4.3 Characterization of Polypyrrole/Nafion Composite Membranes

MEAs were evaluated in a commercial $5cm^2$ fuel cell for all of the work in this chapter. Because the mass-transport characteristics of the $5cm^2$ cell are different from that of the $1cm^2$ cell (used in the work in chapter 3) and the two cells were run at different temperatures, the crossover current results are not directly comparable.

Membranes prepared according to procedure B exhibited excellent blockage of methanol crossover. Table 4.1 summarizes the crossover currents, membrane resistances

and open circuit potentials obtained with the composite membranes. Due to the low methanol crossover rate, modified membranes yield higher open circuit potentials (OCPs) than unmodified Nafion 115.

Table 4.1. Methanol crossover, resistance and open circuit potential (OCP) of polypyrrole/Nafion composite membranes

Membrane Code	MeOH crossover (mA/cm^2)	Cell resistance (Ω)	OCP (mV)
Unmodified 115	126.5	0.037	768.7
B-1[a]	73.4	0.066	779.3
B-3[b]	110.2	0.041	778.6
B-4[c]	75.0	0.065	827.3
B-7[c]	76.8	0.065	836.5

a. no further washing step; b. Washing with hot H_2O_2 for 30 seconds after modification; c. Washing with hot H_2O_2 for 10 seconds after modification.

B-1 was modified strictly following procedure B. A more than 40 % reduction of crossover current was achieved. Fig. 4.1 showed the performance improvement of B-1 with time. Surprisingly, its peak performance in the DMFC was very poor even after full hydration (Fig.4.1). The poor performance of the B-1 membrane might be due to the

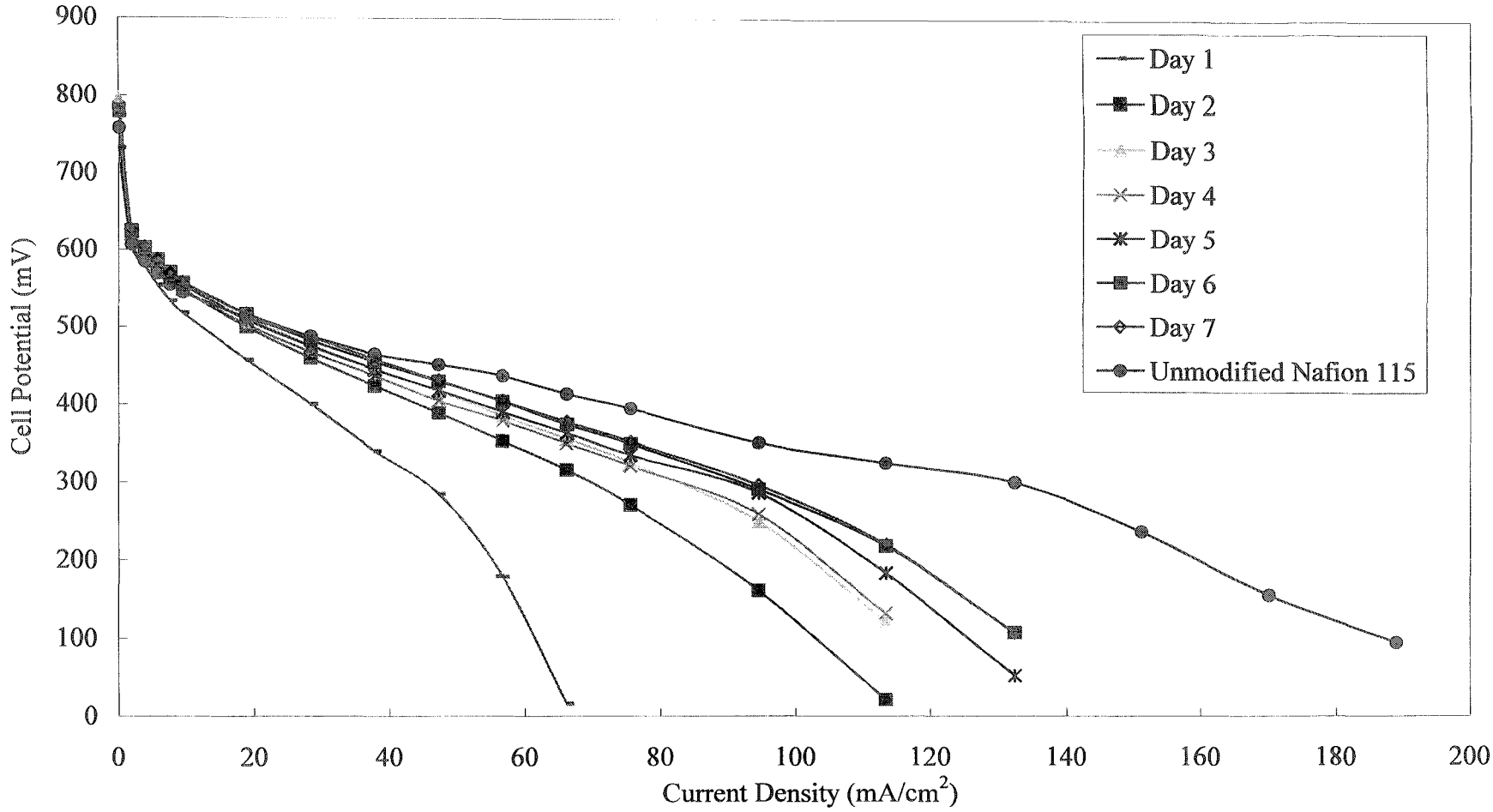

Fig. 4.1 DMFC Performance curves for B-1 and unmodified Nafion 115. The cell was operated at 60 °C, with a 73 mL/min air flow rate (3.7 air stoichiometry at 200 mA/cm^{-2}), and with 1 M methanol solution 0.153 mL/min.

presence of polypyrrole on its surface. The surface properties of the Nafion membrane would be changed and this could cause poor bonding with the electrodes, which would result in low catalyst utilization.

4.3.1 Surface Cleaning to Improve the Composite Membrane/electrode Interface

Nafion solution has been widely used to prepare fuel cell catalyst layer to improve their proton conduction properties and bonding to Nafion membranes.[4] Dipping these composite membranes in Nafion solution have been shown as an effective method for the improvement of membranes bonding with electrodes.[5] To improve the Nafion character of the composite membranes, a surface-cleaning step was developed.

The surface functionality of composite membranes was characterized by attenuated total reflectance Fourier transform infrared (ATR-FTIR, Bruker Tensor 27 with a MIRacle ATR accessory) and the spectra obtained are shown in Fig. 4.2. B-7 was prepared by modification Nafion 115 according to procedure B followed by a washing step with a hot (80 °C) 30% H_2O_2 solution for 10 seconds. Washing for a longer period in hot H_2O_2 (e.g. 30 seconds for B-3 membrane) caused severe polypyrrole degradation (indicated by the high methanol crossover of B-3 in Table 4.1). Membrane F was prepared as described in chapter 3 with a higher polypyrrole content than B series membranes.

Nafion 115 has a broad adsorption peak at 3000-3600 cm^{-1}, which is due to adsorbed water. It is clear that B-7 membrane has more Nafion-like surface characteristics

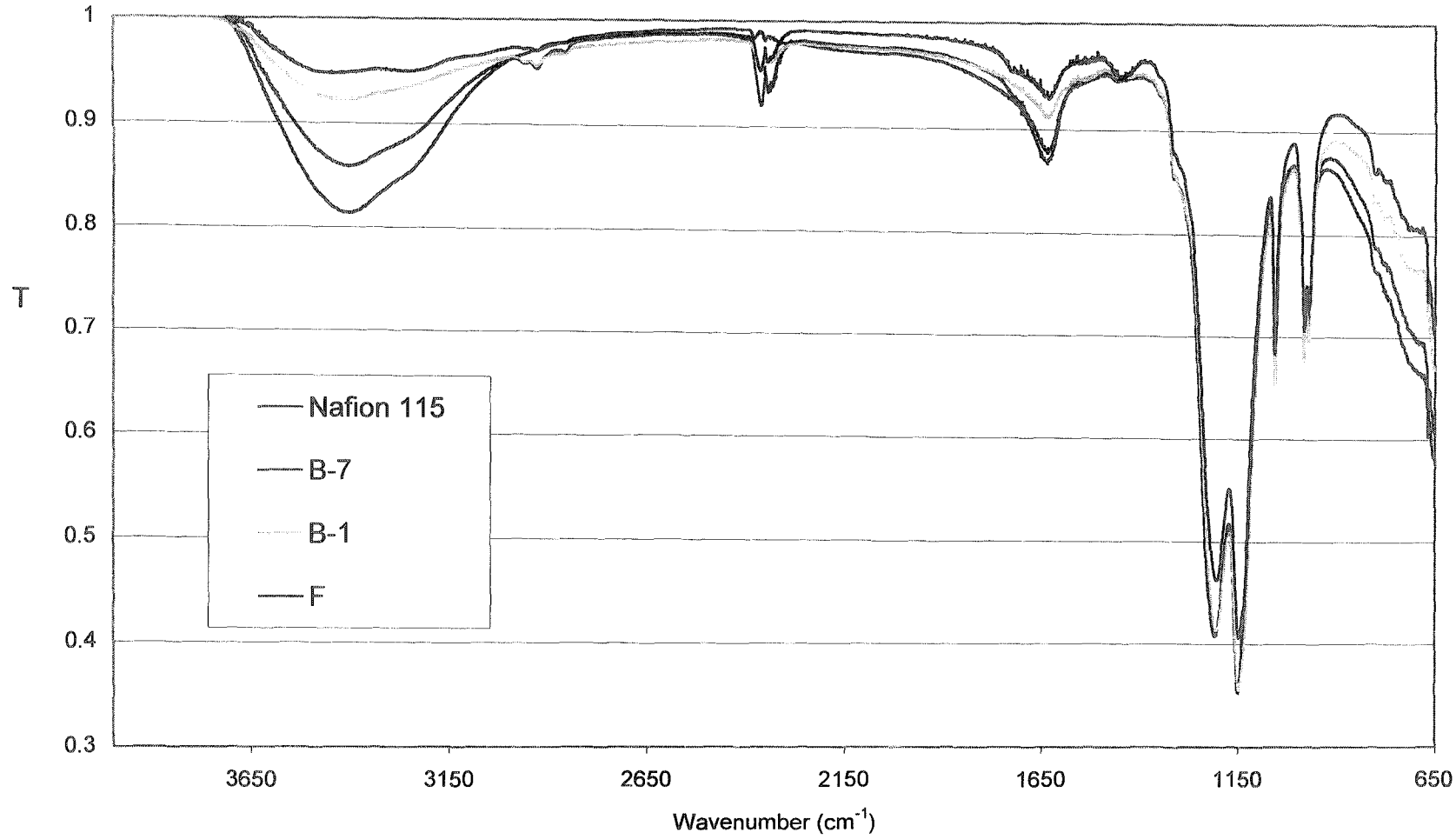

Fig. 4.2. ATR-FTIR spectra of composite membranes and unmodified Nafion 115. Every membrane was fully hydrated by immersion in water. B-7 membrane was washed with hot 30% H_2O_2 for 10 seconds after modification. F was prepared as described in Chapter 3.

than B-1 and F (this can also be seen from the peak at 1620 cm^{-1} and the fingerprint region of 650-950 cm^{-1}). The increased hydrophobic polypyrrole content on membrane surface would decrease the hydrophilic properties of the Nafion surface and thus leads to a poor electrode/membrane interface. This can also explain an observed increase in the water/composite membrane's contact angles with increased polypyrrole loading.

It can be seen from Table 4.1 that short time surface washing with H_2O_2 only oxidizes the polypyrrole on the membrane surface and does not significantly interrupt the polypyrrole within these membranes. Moreover, the short time washing step has very good reproducibility. B-4 and B-7 were prepared and washed in the same way. After washing, their methanol crossover limiting currents (75-76.8 mA/cm^2) and resistances ($0.065\,\Omega$) were almost the same as for the unwashed B-1 form (73.4 mA/cm^2, $0.066\,\Omega$). As described above, longer washing times cause severe degradation of polypyrrole inside the membrane and result in high crossover currents, e.g. 110.2 mA/cm^2 for B-3 and lower resistance ($0.041\,\Omega$ for B-3).

4.3.2 Performance of Polypyrrole/Nafion Composite Membranes

The performances of composite membranes in a DMFC are shown in Fig. 4.3. Excellent DMFC performances are achieved after surface washing. The cell potential significantly increased from 299.2 mV (B-1) to 370.5 mV (B-4 or B-7) at 100 mA/cm^2.

At low current densities, all composite membranes gave higher performances than

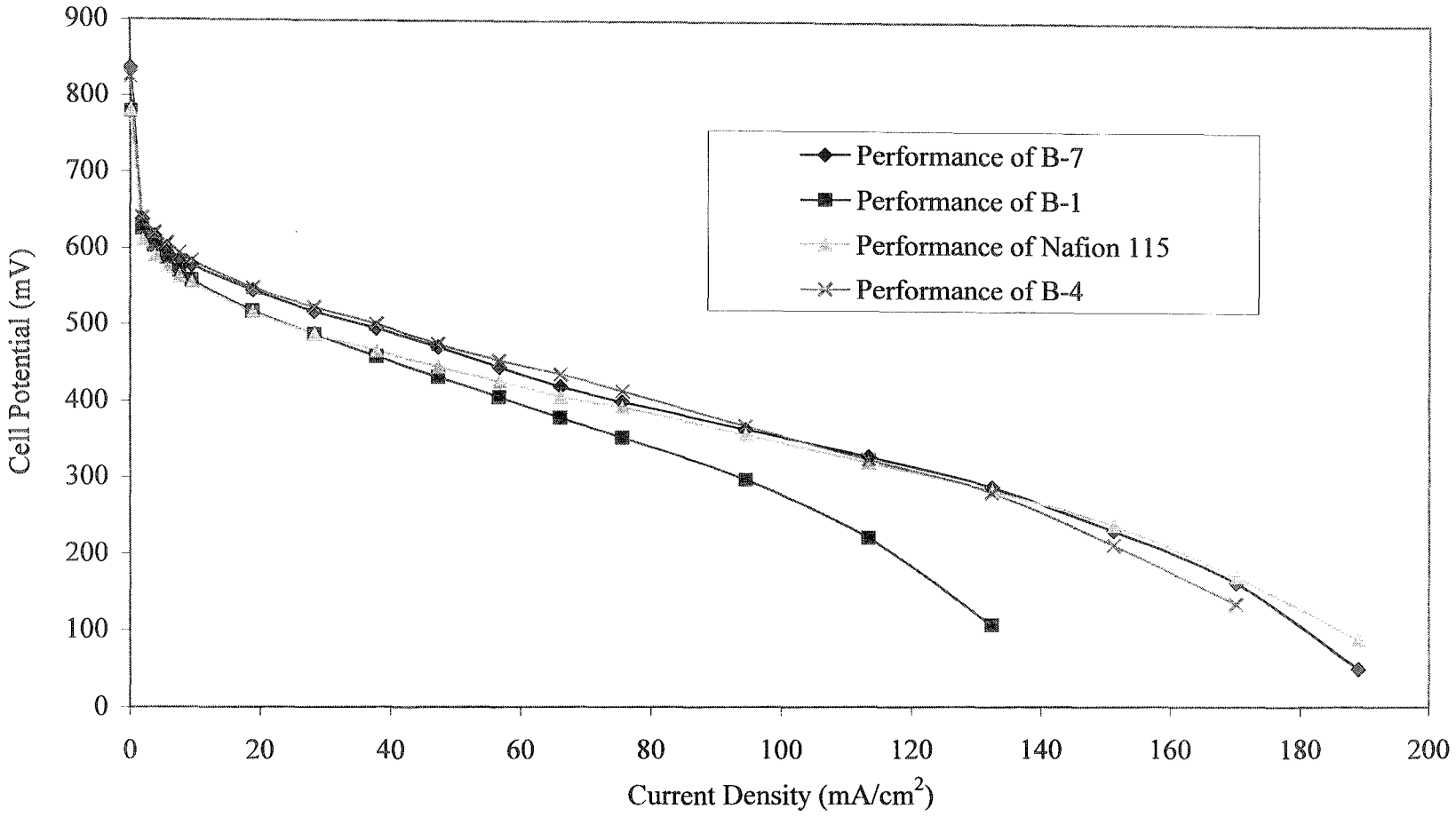

Fig. 4.3. DMFC Performance curves for polypyrrole/Nafion composite membranes and unmodified Nafion 115 (60 °C, 73 mL/min air, 0.153 mL/min 1 M methanol solution)

Nafion 115 as a result of their lower methanol crossover. In the Ohmic loss region and mass transport region, B-1 showed the worst performance due to the low catalyst utilization (shown in section 4.3.1) and high resistance. B-4 and B-7 outperformed Nafion 115 in the kinetic region and ohmic loss region, but had poorer performance than Nafion 115 at high current density. After compensation for the IR loss in Fig. 4.4, the B-4 and B-7 outperformed Nafion 115 in all three regions. This verified that the lower performance of surface cleaned composite membranes at higher current density is due to their high resistance.

From Fig. 4.4, one can also find that the effects of reduced methanol crossover become less prominent at high current density: the performance difference between B-4 (or B-7) and Nafion 115 decreases at high current density. This agrees with the results of Chu et al. that methanol crossover decreased significantly with increasing discharging current.[6,7] Therefore the effect of methanol crossover is small at high current density and results in similar performances for composite membranes and Nafion 115. Researchers have proposed to run DMFCs at higher current density to eliminate the methanol crossover problem.[8] However, increasing the discharge current density will result in a low fuel cell voltage, leading to low efficiency of energy conversion. Decreasing methanol crossover is still an important issue for direct methanol fuel cells.

The improved DMFC performances attained with the modified membranes can be explained directly by the higher cathode activity resulting from their reduced methanol

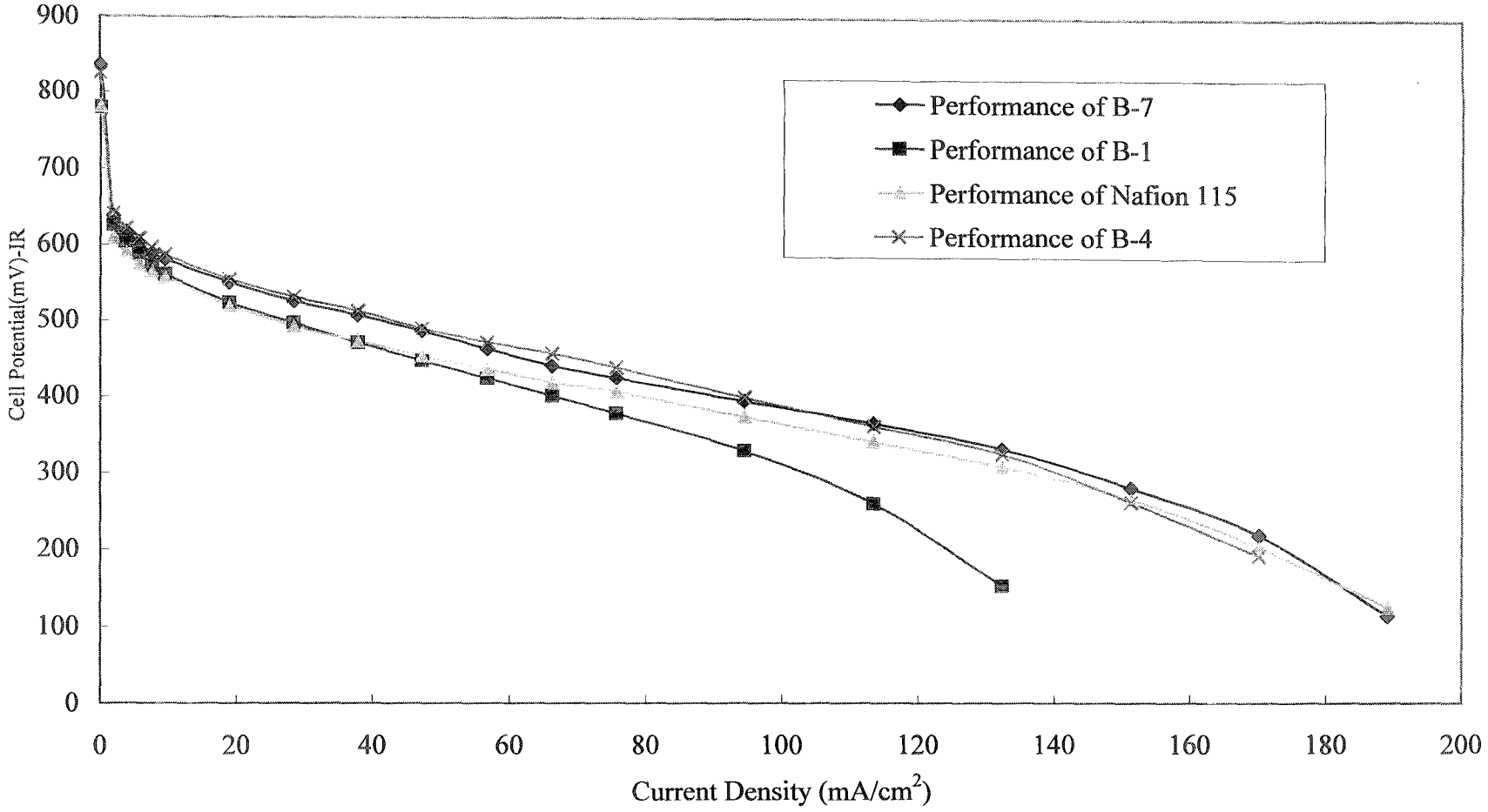

Fig .4.4. Performance curves for Polypyrrole/Nafion composite membranes and unmodified Nafion 115 after compensation for IR loss. (60 °C, 73 mL/min air , 0.153 mL/min 1M methanol solution)

crossover. Fig. 4.5 compares anode polarization curves for the composite membranes and Nafion 115. Membrane B-1 has the worst anode performance because of its poor catalyst/membrane interface. The anode polarization curves for B-4 and B-7 were almost the same as for Nafion 115. The cathode polarization curves were calculated from the cell performance minus the anode performance and were also shown in Fig. 4.5. The improved cathode performances of the composite membranes than that of unmodified Nafion 115 (B-4 and B-7) were due to their low methanol crossover. Again, the influence of methanol crossover is small at high current densities and results in similar cathode polarizations for composite membranes and Nafion 115. Due to membrane B-1's poor electrodes bonding but high methanol reduction rate, its cathode polarization outperformed Nafion 115 at low current densities and poor performed than Nafion 115 at high current densities.

4.3.3 Impedance Spectroscopy of DMFCs with Polypyrrole/Nafion Composite Membranes

Electrochemical Impedance Spectrometry (EIS) is a powerful technique for fuel cell study. However, most research has focused on H_2/O_2 PEMFCs.[9,10,11] The reactions, charge transfer, and mass transfer processes at both the cathode and anode of the DMFC are so complicated and so hard to separate that only 4 papers on the EIS of DMFCs have been published.[12,13,14,15]

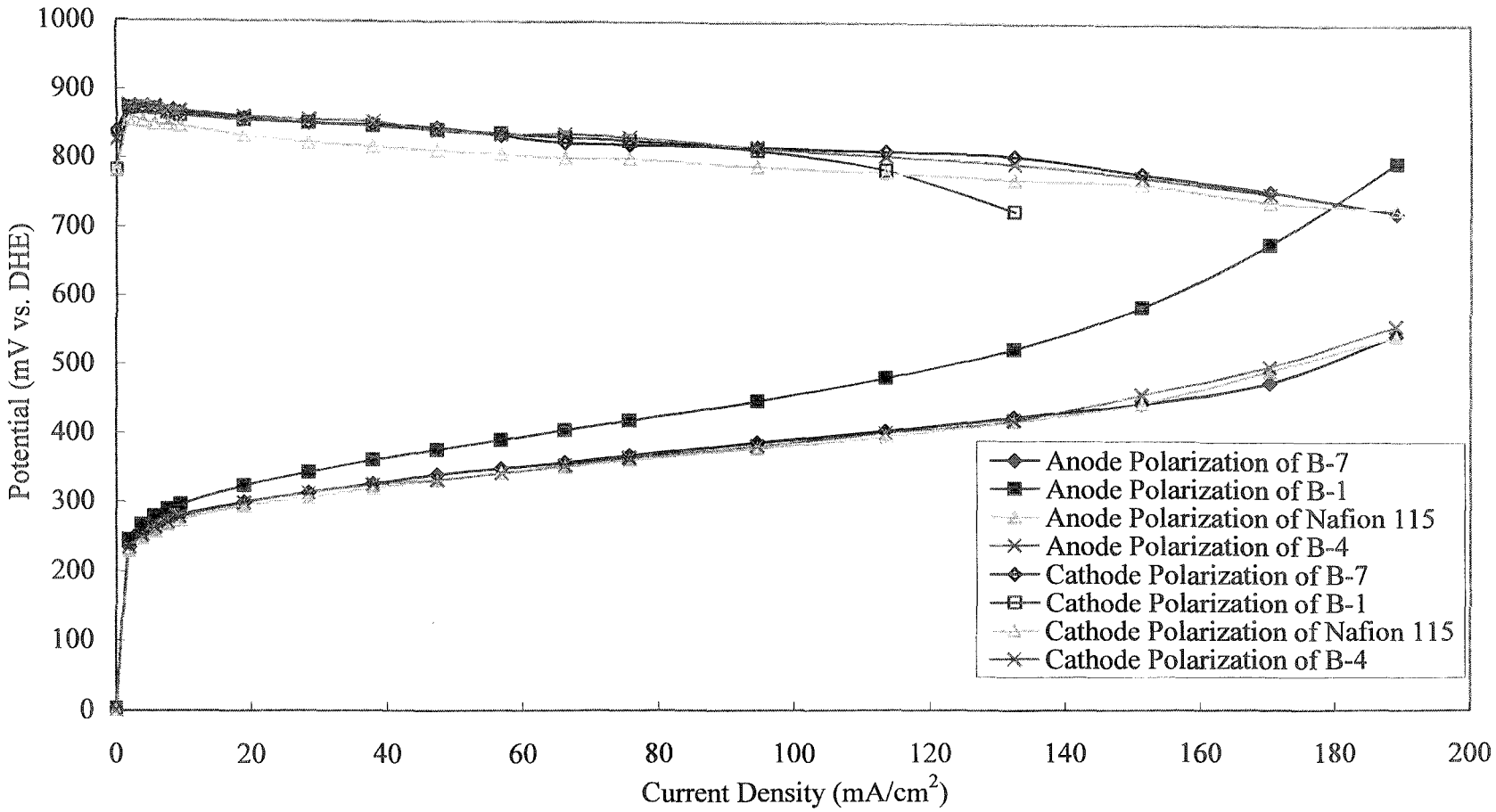

Fig. 4.5. Anode and cathode polarization curves for polypyrrole/Nafion composite membranes and unmodified Nafion 115 at 60 °C, with 25.6 mL/min H_2 and 0.153 mL/min 1 M methanol solution flowing through cathode and anode, respectively.

The impedance of an MEA can be physically separated into three parts: the membrane impedance, anode impedance and cathode impedance. The membrane impedance can be determined from the real intercept of the impedance at high frequency. Müller et al. have proposed a standard procedure by replacing air with H_2 at the cathode to separate the anode impedance and cathode impedance.[12,13] When the cathode is supplied with H_2, protons are reduced to H_2 and the cathode will behave as a DHE. Then the contribution of the cathode to the impedance can be neglected due to the fast electrode reaction. Hence, the impedance spectra measured between anode and the DHE in a complete cell can be taken as approximately equal to the sum of membrane resistance and the anode impedance. Normal cell impedance spectra are then recorded by flowing air through the cathode. The cathode impedance spectra can then be determined by subtracting the anode impedance and membrane resistance from the normal impedance spectra. Impedance spectra measured at different electrode overpotentials can provide more diagnostic information. However, the spectra are more difficult to explain. More work is needed to appropriately design EIS experiments to separate every factor that influences DMFC performance. Because EIS is not the main focus of this thesis, only spectra measured at open circuit are discussed here.

Fig. 4.6 shows the Nyquist plots for DMFC with B-1, B-7 and unmodified Nafion 115. Spectra were obtained at the open circuit potential under DMFC operation conditions. The intercept of the high frequency 45° region with the real impedance axis (Z' axis) is

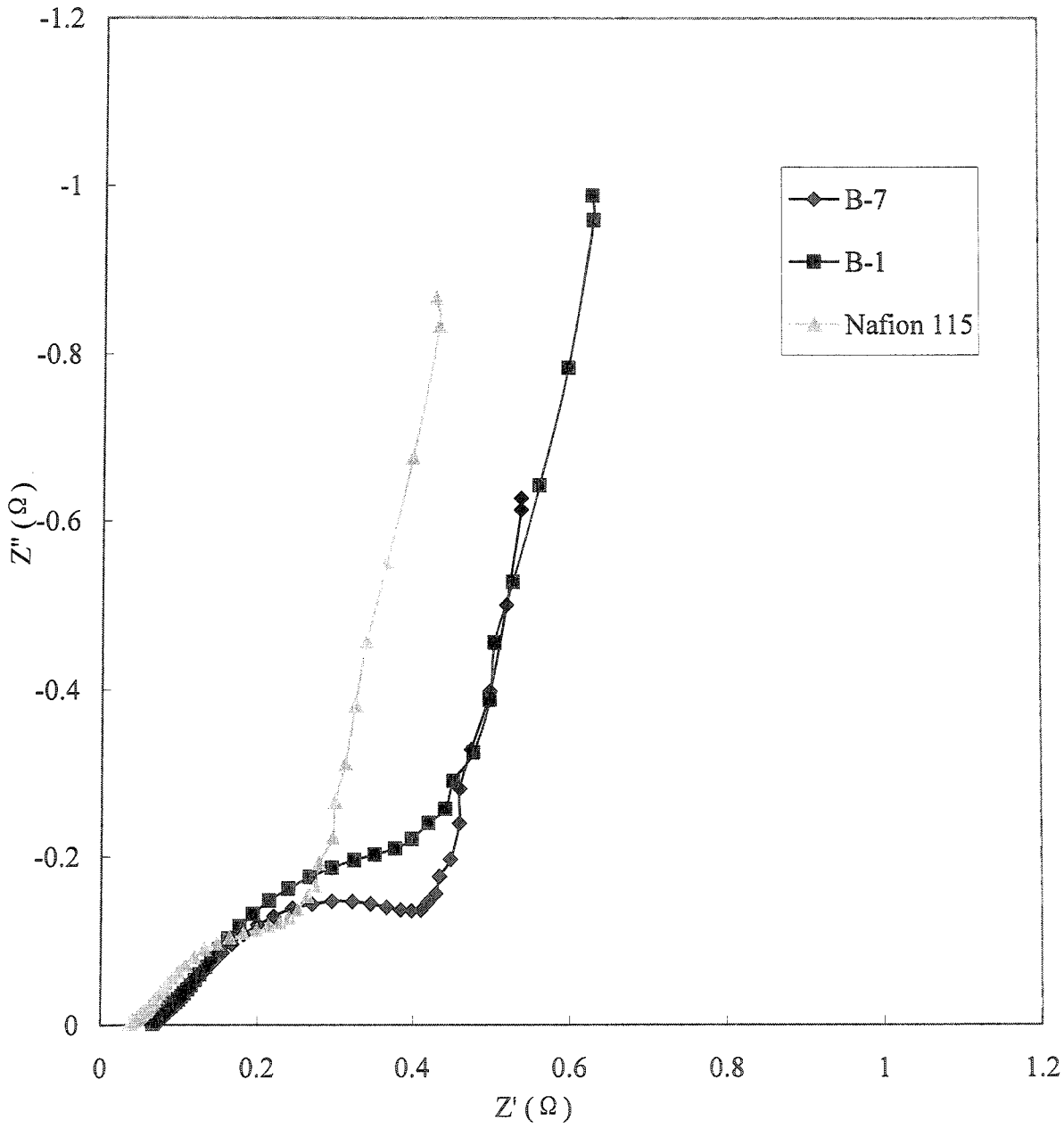

Fig. 4.6. Nyquist plots of DMFC impedance spectra. (60 °C, 73 mL/min air, 0.153 mL/min 1 M methanol solution)

the membrane resistance and is recorded in Table 4.1. In general, a DMFC impedance spectrum is composed of three regions: a high frequency region determined by membrane ionic resistance and catalyst layer resistance and capacitance; a medium frequency region controlled by the charge transfer resistance; and a low frequency region attributed to mass transfer resistance.

Replacing air with a continuous stream of H_2, produced the impedance spectra shown in Fig. 4.7. At high frequency, the first semicircle (flattened in the case of the unmodified membrane) intercepts to the Z' axis at a point corresponding to the membrane resistance. The intercept values were identical to the membrane resistance values listed in Table 4.1. Subtracting the membrane ionic resistance, anode impedance spectra are obtained as shown in Fig. 4.8. The first semicircle in the high-medium frequency region in Fig 4.8 is due to methanol electro-oxidization kinetics. The much larger semicircle at the low frequencies is dominated by electrode capacitance and does not show in this figure. The poor interface between B-1 and the anode leads to low catalyst utilization and results in poor charge transfer properties as indicated by the larger high frequency semicircle. Good bonding of B-7 to the anode resulted in nearly the same charge transfer properties as Nafion 115.

Nyquist plots of DMFC cathode impedance spectra are shown in Fig. 4.9. These were obtained by subtracting anode impedance spectra and membrane resistances from the full cell impedance spectra. The first semicircle in Fig. 4.9 is due to the charge

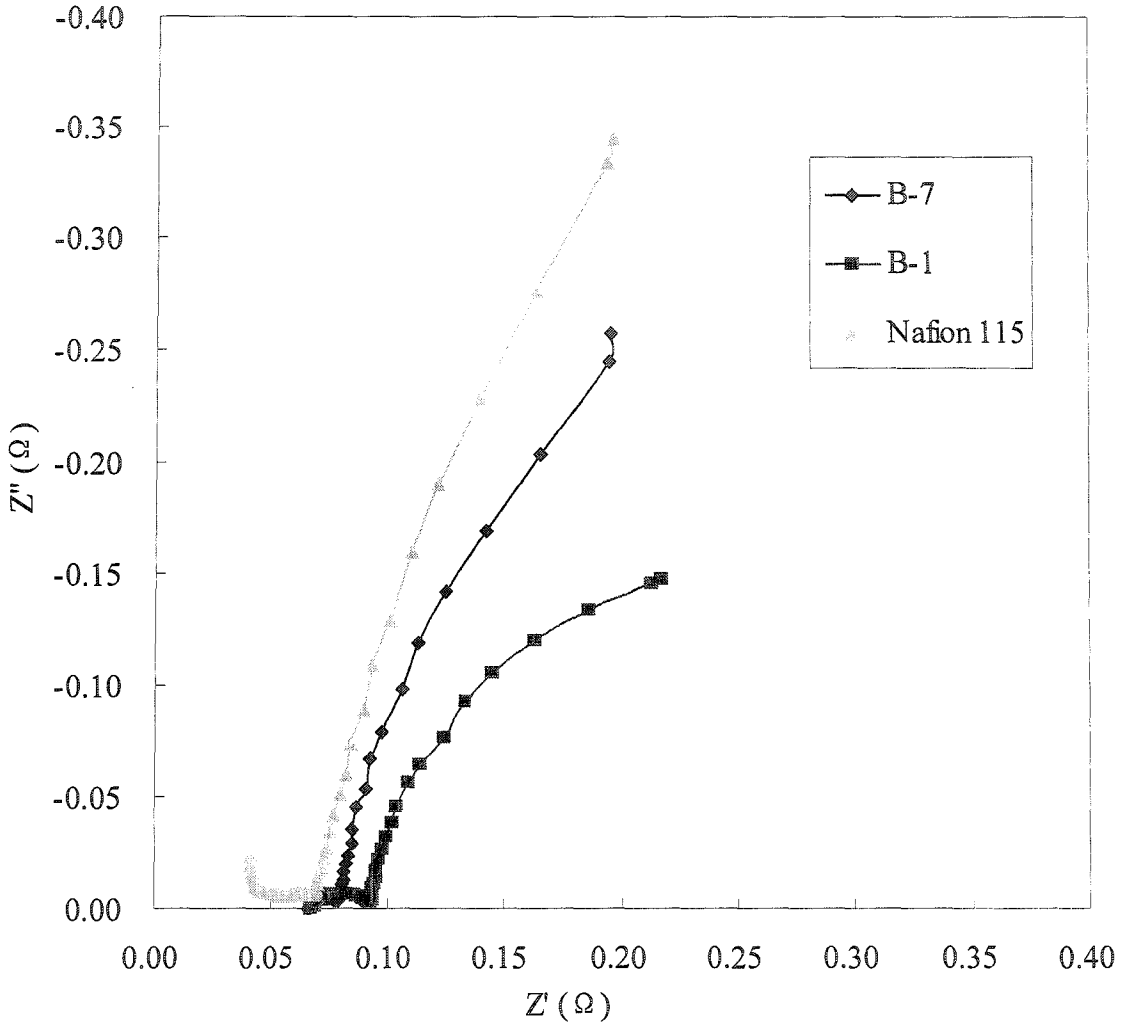

Fig. 4.7. Nyquist plots of DMFC impedance spectra measured between anode and DHE. (60 °C, 25.6 mL/min H_2, 0.153 mL/min 1 M methanol solution)

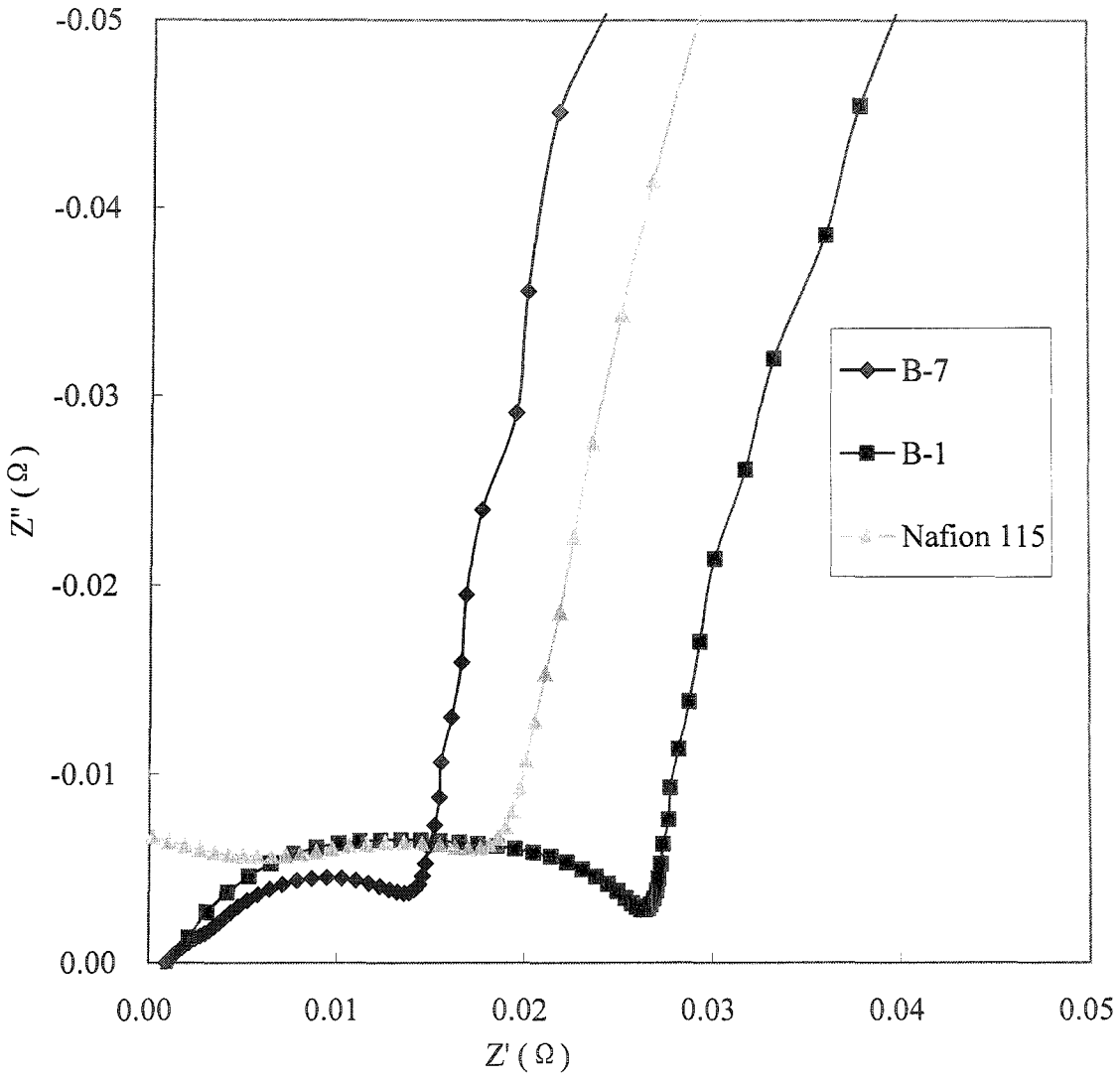

Fig. 4.8. Nyquist plots of DMFC anode impedance spectra. (60 °C, 25.6 mL/min H_2, 0.153 mL/min 1 M methanol solution)

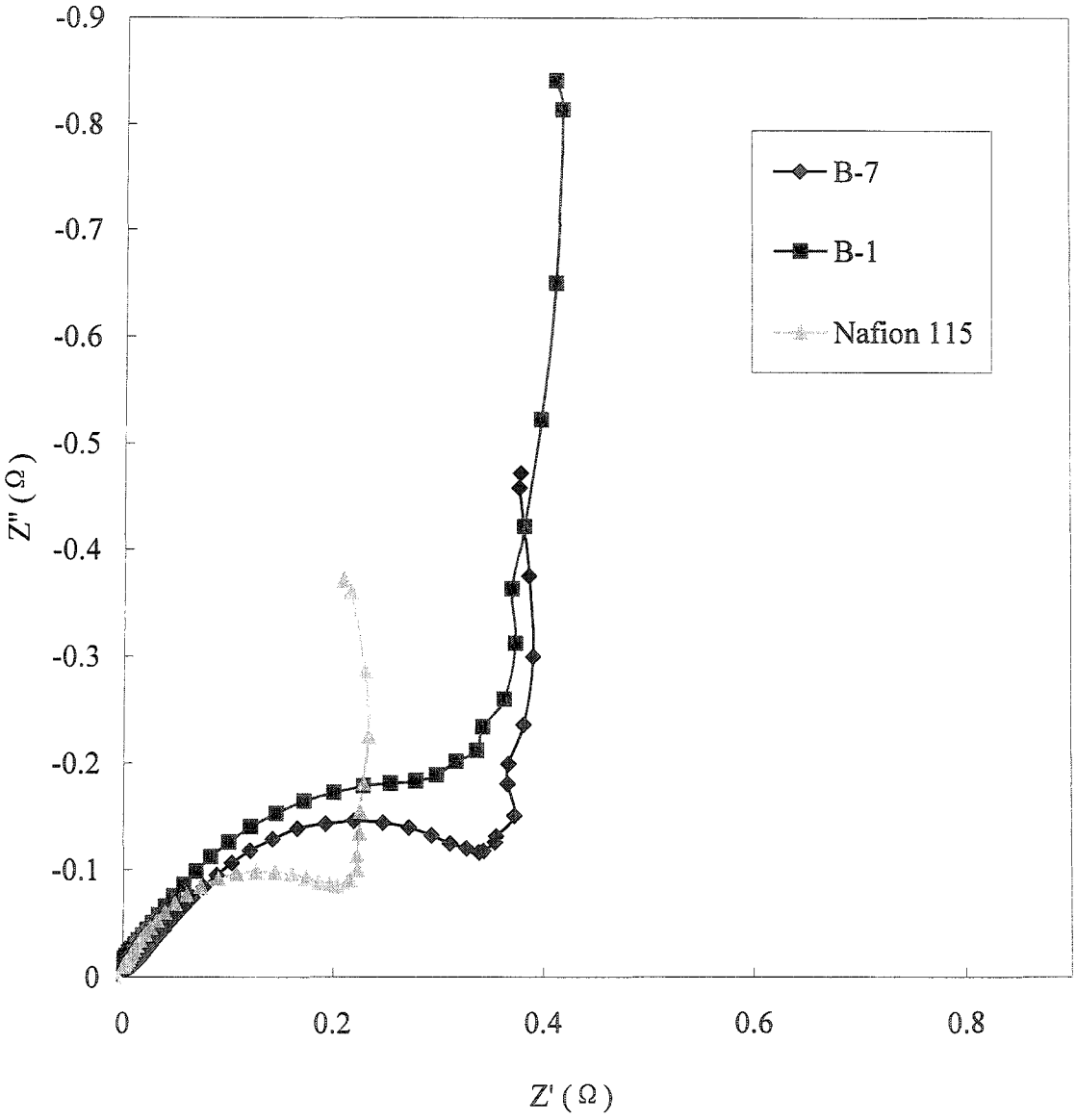

Fig. 4.9. Nyquist plots of DMFC cathode impedance spectra. Obtained by subtracting anode impedance spectra and membrane resistance from full cell impedance spectra.

transfer resistance for the oxygen reduction reaction. Müller et al. reported that when pure oxygen is used, the mass transfer semicircle is avoided.[12] In our measurement, air was flushed through the cathode side. The presence of the second semicircle is strongly related to oxygen mass transfer. It is verified again that B-1 has the poorest surface bonding within these three MEAs. Unexpectedly, B-7 also showed poorer charge transfer properties than Nafion 115. This is may be a possible reason that the performance of B-7 did not improve more significantly over Nafion 115 even with a 40% methanol crossover reduction.

As seen from Fig. 4.8 and Fig. 4.9, it is clear that the anode charge transfer resistance and mass transfer resistance are in the same frequency region as the cathode charge transfer region at the open circuit potential. Measuring impedance spectra at different overpotentials, it becomes more complicated to separate each factor. Charge-transfer on the cathode side involves three phases (gas, catalyst, electrolyte) and thus has a much bigger charge transfer resistance than that of the anode. The Pt cathodes used in this research were using PTFE as a catalyst binder and showed strong hydrophobic properties. The strong hydrophobic properties of the cathode have a tremendous advantage to prohibit cathode flooding by water. However, it also reduces the proton transfer rate from the membrane surface to the catalyst surface. Adding Nafion into the catalyst layer has been proved to be an effective way to improve an electrode's proton conductivity.[5,16]

In performance measurements, MEAs made from polypyrrole/Nafion composite

membranes typically reach peak DMFC performance after about three days (e.g., Fig. 4.10 for B-7), compared to less than one day for unmodified Nafion 115. It has been speculated that the longer activation time is due to the formation of polypyrrole in Nafion connecting channels.[17] A long "break in" time is needed for the full hydration of modified membranes. Obviously, the blocking of such channels results in higher membrane resistance, as seen in Table 4.1. The resistance of B-7 decreases from 0.100 Ω to 0.065 Ω in three days, shown in Fig. 4.11. However, the improvement of cell performance cannot be explained solely by that. The charge transfer and mass transfer properties of the B-7 MEA changed significantly with time and then became constant after three days.

The anode impedance spectra and cathode impedance spectra were also monitored for 4 days and are recorded in Fig. 4.12 and Fig. 4.13, respectively. The aqueous methanol solution supplied to the anode and the Nafion binder used in catalyst preparation favored the rapid hydration of the catalyst layer. Anode impedance spectra were nearly constant with time. The large charge transfer semicircle in the cathode impedance decreased significantly with time and reached a constant state after 3 days which corresponds to the slow activation process of the cathode charge transfer. In conclusion, the tardy optimum performance of B-7 was thus mainly due to a slow cathode activation process and in part to slow membrane hydration.

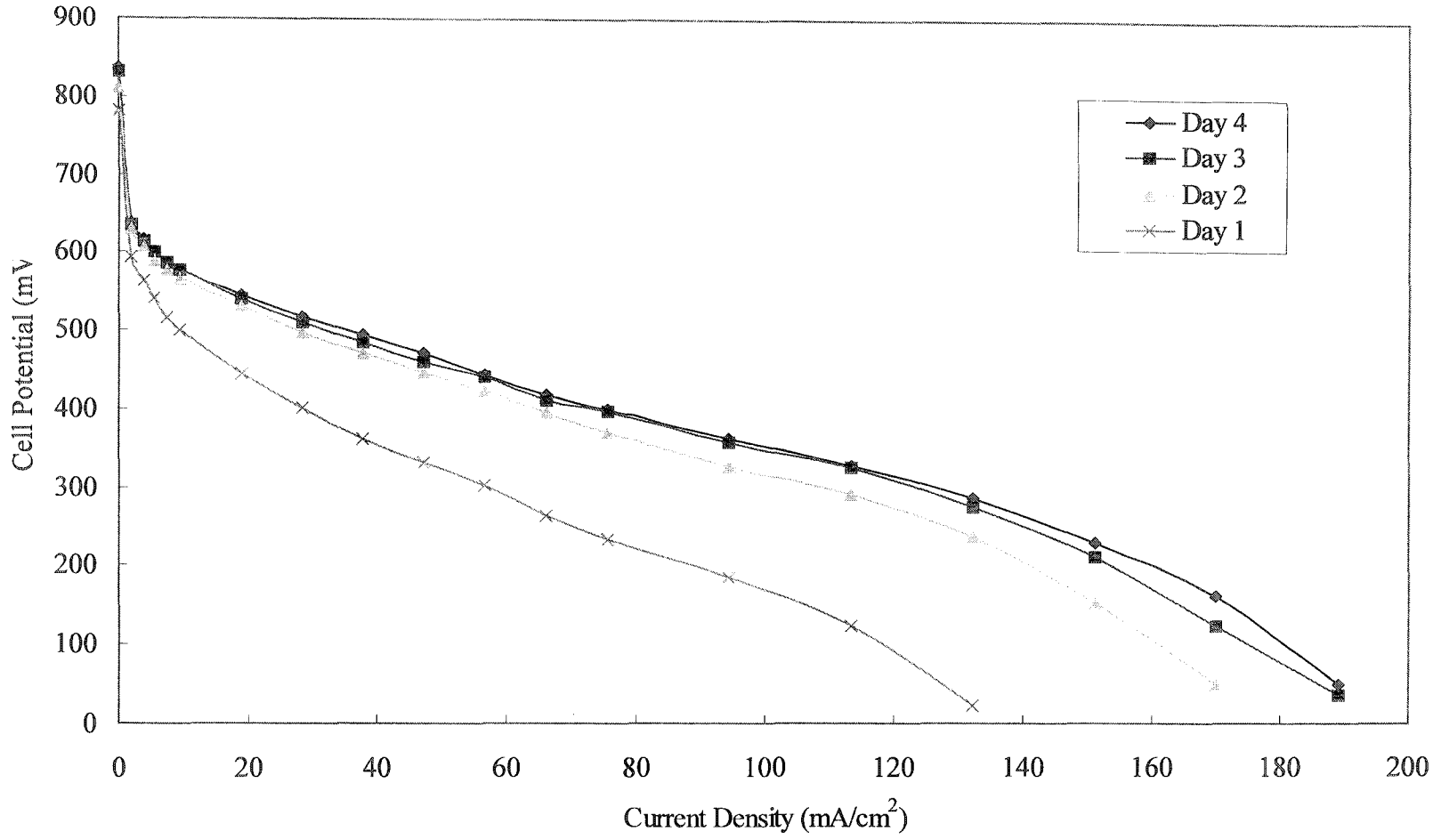

Fig. 4.10. Polarization curves for a 5cm^2 active area DMFC with membrane B-7 over 4 days. (60 °C, 73 mL/min air, 0.153 mL/min 1 M methanol solution)

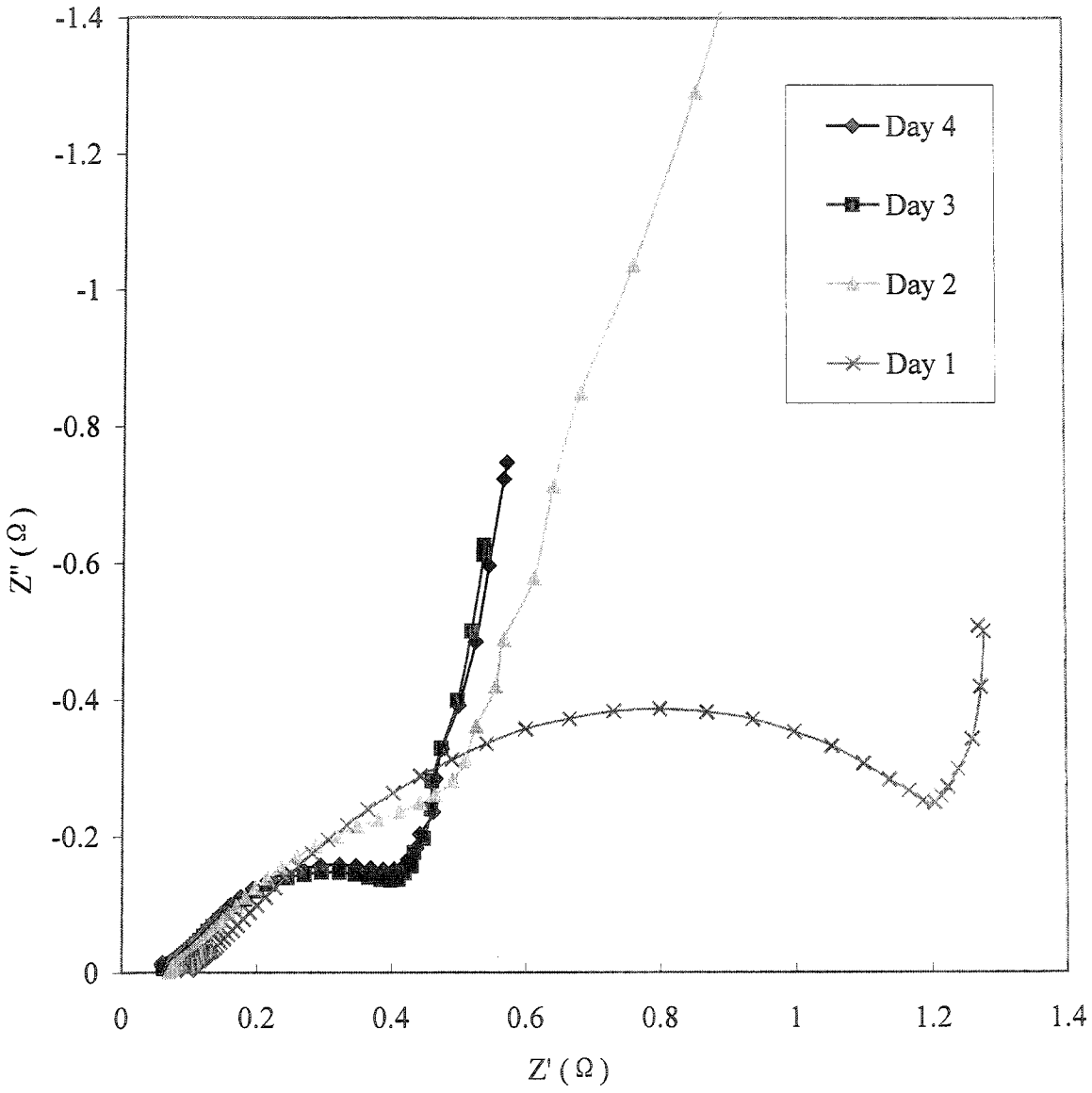

Fig. 4.11. Nyquist plots of DMFC impedance spectra of B-7 over 4 days. (60 °C, 73.1 mL/min air, 0.153 mL/min 1 M methanol solution)

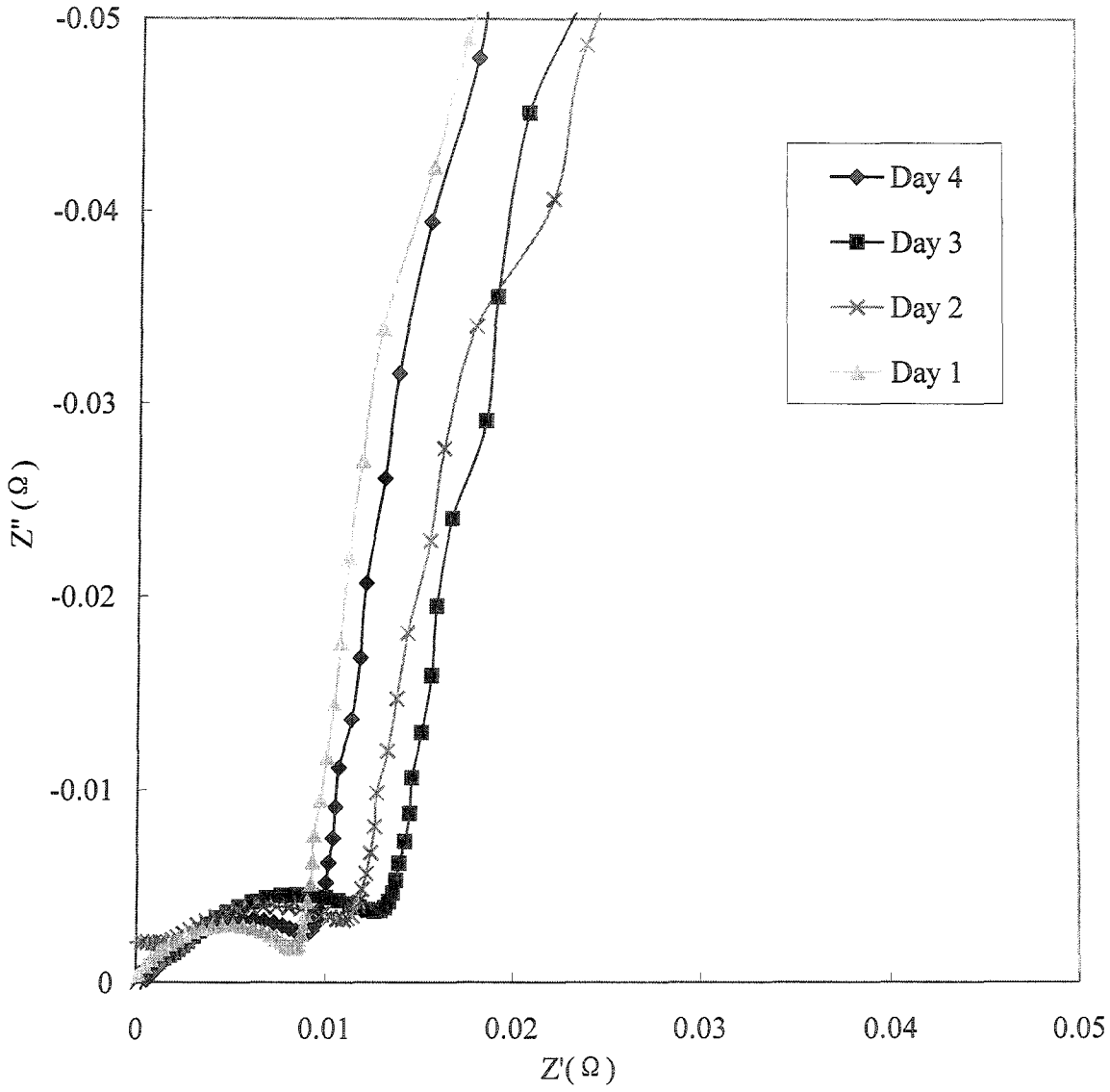

Fig. 4.12. Nyquist plots of anode impedance spectra of B-7 for 4 days. (60 °C, 25.6 mL/min H_2 , 0.153 mL/min 1 M methanol solution)

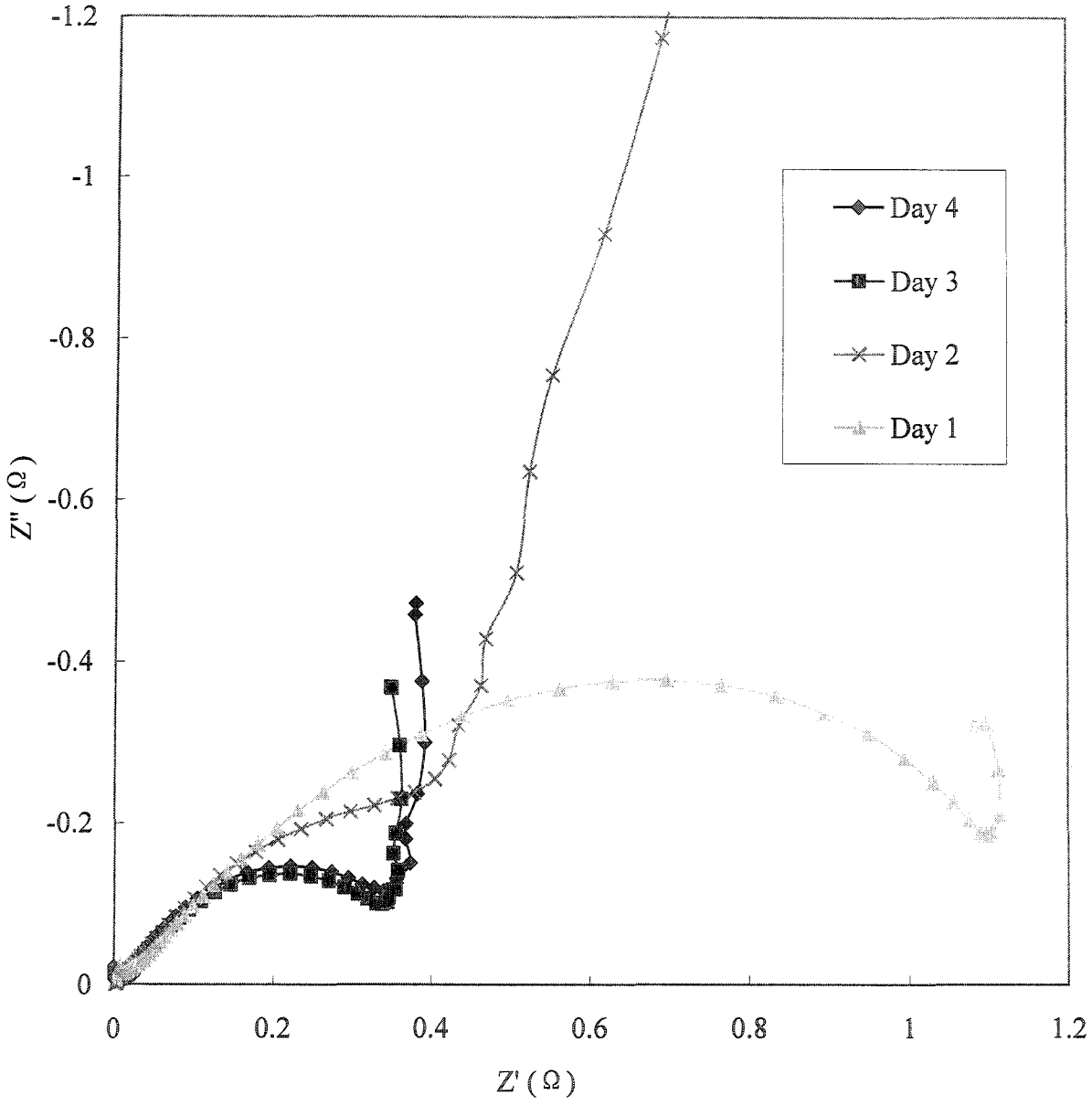

Fig. 4.13. Nyquist plots of DMFC cathode impedance spectra of B-7 for 4 days, obtained by subtracting anode impedance spectra and membrane resistance from full cell impedance spectra.

4.3.4 Cyclic Voltammetry of DMFC Cathodes

Cyclic voltammetry (CV) has long been used to measure the active area of Pt catalysts. Specifically, the coulombic charge under the hydrogen adsorption/desorption peaks is considered as a measure of the active area.[18] It is assumed that 210 $\mu C/cm^2$ is used to produce a monolayer of adsorbed H on the Pt catalyst.[19] The Pt catalyst active area is thus determined as:

$$A = \frac{\int IdE}{210\mu C/cm^2} \qquad (4.1)$$

where I is current density, dE is the differential potential. The charge is calculated by integrating the IdE from -10 mV to 340 mV.

Cathode CVs was measured by running the DMFC at 60 °C with a stream of H_2 at a 25.6 mL/min through the anode and 0.153 mL/min water flushed through the cathode. The anode is a reversible hydrogen electrode (RHE) and served as a reference electrode and counter electrode in these measurements.

Fig. 4.14 shows the cathode CVs with B-1, B-7 and unmodified Nafion 115. The two oxidization/reduction peaks in the potential region between –10 mV and 340 mV are due to the desorption/adsorption of hydrogen. The broad peaks above 600 mV are attributed to the oxidization and reduction of the Pt catalyst surface. It is clear from the CVs that the active area for B-7 and Nafion are similar while the active area is very low for B-1. This supports the hypothesis that B-1 produces a poor membrane electrode interface. This

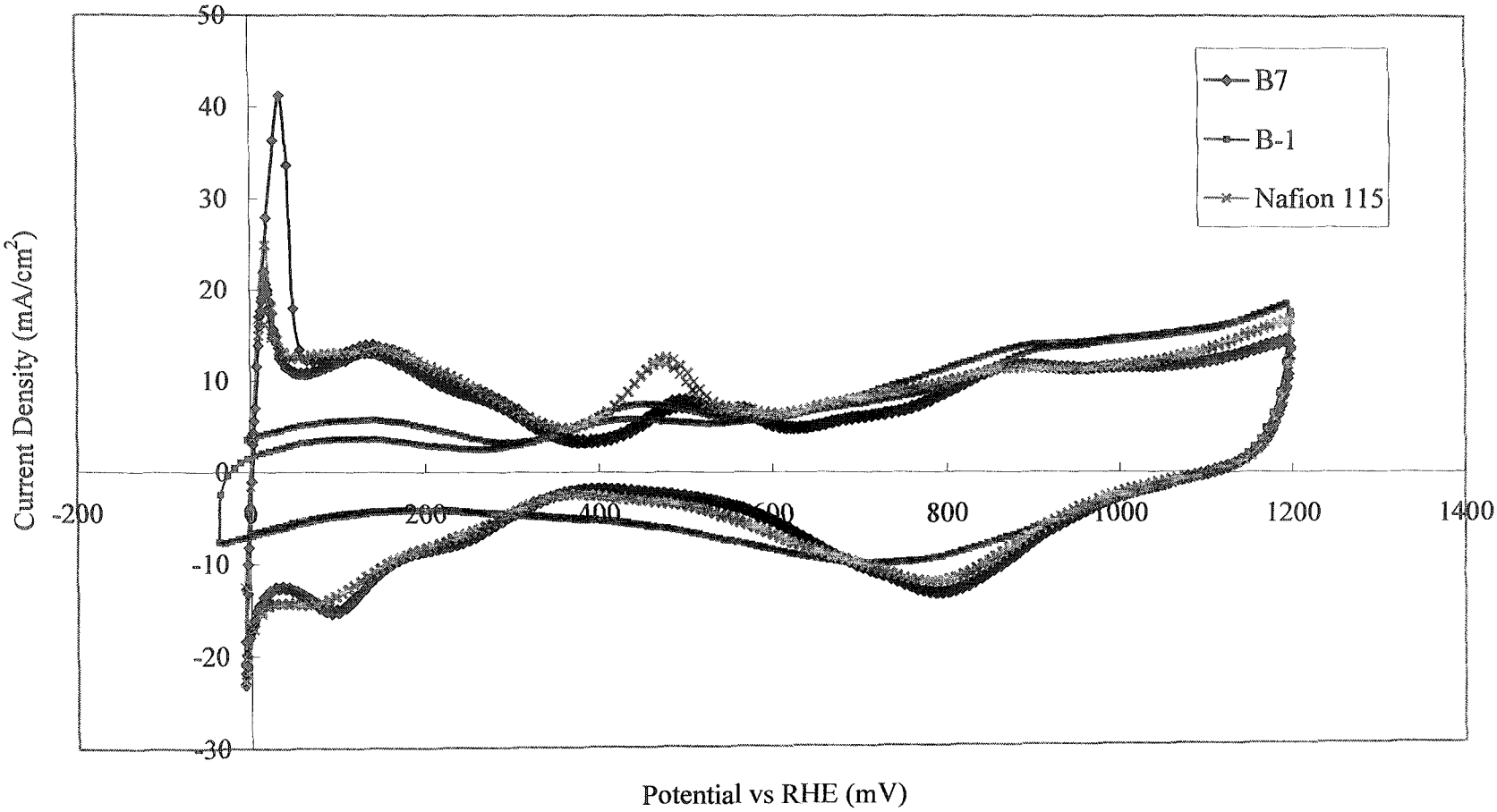

Fig. 4.14. Cathodes cyclic voltammograms of MEAs prepared with composite membranes and unmodified Nafion 115. Scan rate: 20 mV/s; Temperature: 60 °C; anode: 25.6 mL/min H_2; and cathode: 0.153 mL/min water.

explains the poor charge transfer properties and poor cell performance obtained for B-1. The interfacial properties between B-7 and the catalyst are much better, showing a great improvement with surface washing.

4.4 Increasing the Ionic Conductivity of Composite Membranes

It is clear that the composite membranes prepared in this work effectively reduce methanol crossover and leads to better DMFC overall performance. However, the increased membrane resistance offsets part of the benefits of the low methanol crossover. Polypyrrole is positively charged and easily bonds with the anionic sulfonate group inside the Nafion hydrophilic pores and channels. Sungpet has reported that the ion exchange capacity of polypyrrole/Nafion composites was over 10% less than the unmodified acid form of Nafion.[20] Providing counter anions in the polymerization step was therefore expected to weaken the polypyrrole/sulfonate group interactions. Another approach is to synthesize anionic monomers.

4.4.1 Provision of Counter Anions During Modification Process

A membrane was modified according to a modified B procedure in which 5% H_2O_2 in 2M H_2SO_4 was used to polymerize the pyrrole. The resulting membrane is coded as B-SA2M. Fig. 4.15 shows the DMFC results for this membrane. B-SA2M showed increased cell performance over Nafion in all three regions but had a slightly higher

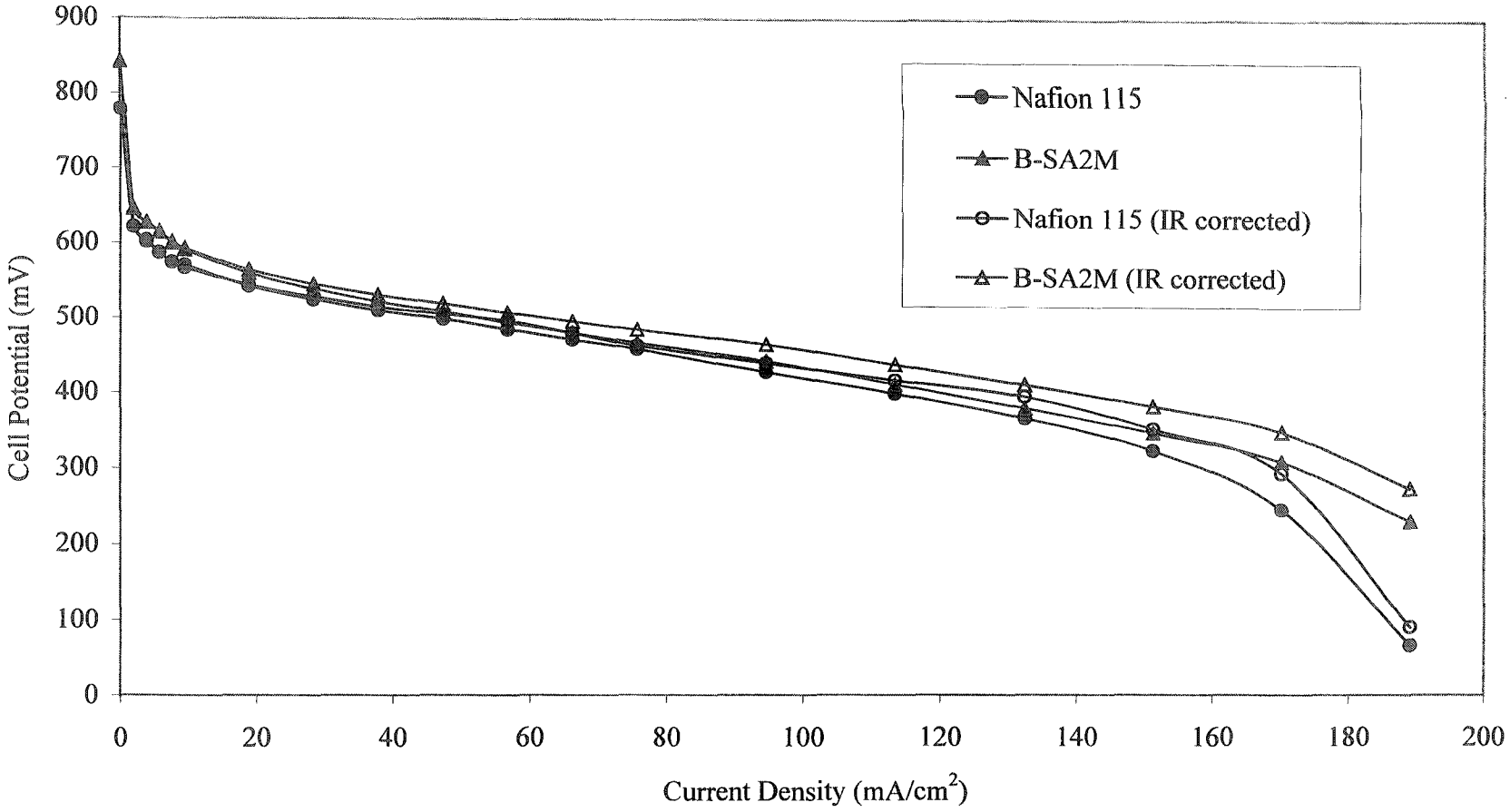

Fig .4.15. DMFC performance curves for B-SA2M and unmodified Nafion 115 (60 °C, 73 mL/min air, 0.153 mL/min 1 M methanol solution)

resistance. It reduced methanol crossover by 20%. Because of the high acid concentration outside the membrane, loaded pyrrole was easily washed out during the polymerization reaction. More work is needed to optimize this modification method and elucidate the improvement mechanism.

4.4.2 Preparation of Poly[3-(pyrrole-1-yl)propanesulfonate]/Nafion Composite Membranes

3-(pyrrole-1-yl)propanesulfonate (abbreviated as "pyrrole sulfonate", structure 1) was synthesized by substitution of the pyrrole ring with a sulfonated pendant group. After bulk polymerization or copolymerisation with pyrrole into Nafion membranes, it can provide anionic groups and moderate the polymer interaction with the sulfonate groups in Nafion.

4.4.2.1 Synthesis of Sodium 3-(pyrrole-1-yl)propanesulfonate

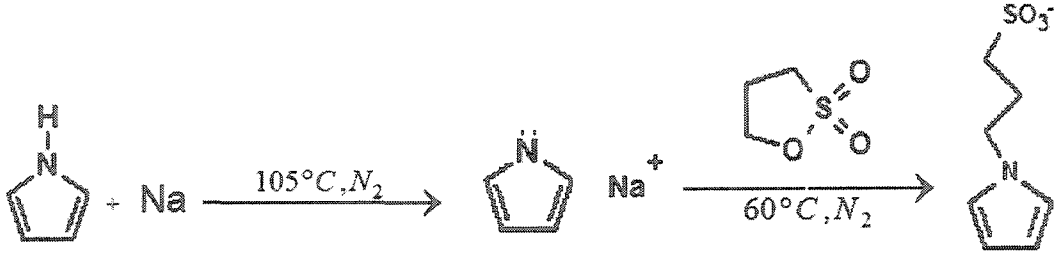

(1)

Sodium pyrrole sulfonate was synthesized following the literature.[21,22] Pyrrole sodium salt was synthesized by refluxing 10 g pyrrole with 1.6 g sodium at 105 °C for 12 hours. 6.5 g 1,3-propanesultone (Aldrich) was then added at 60°C and reacted for 12 hours. All reactions were under N_2 protection. The product was then washed with hot tetrahydrafuran (THF) to remove the unreacted propanesultone. The product was characterized by ^1H NMR (Bruker AVANCE 500MHz), as shown in Fig. 4.16.

4.4.2.2 Preparation of Poly[3-(pyrrole-1-yl)propanesulfonate]/Nafion Membranes

Poly[3-(pyrrole-1-yl)propanesulfonate]/Nafion membranes were prepared by loading pyrrole sulfonate into Nafion 115 for 20 min, then polymerizing in 5% H_2O_2 for 2 hours. The preliminary results were shown in Fig. 4.17. The poly(pyrrole sulfonate)/Nafion membranes could increase the cell performance without a significant increase in membrane resistance. However, the high concentration of sulfonate groups in the Nafion pores strongly inhibits permeation of the pyrrole sulfonate anion into the membrane, and so high loadings have not been achieved. More work needs to be done to increase the monomer loading.

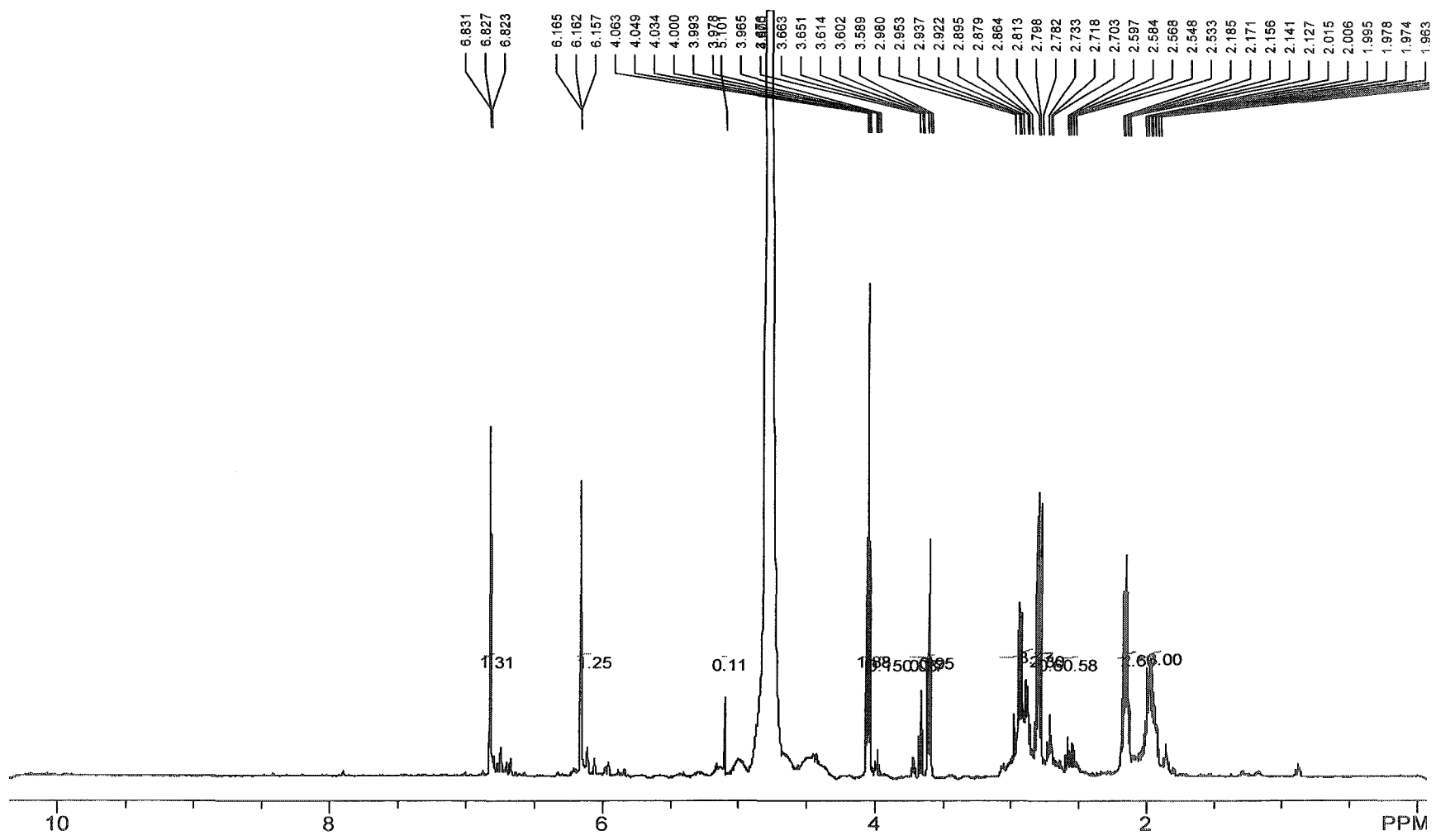

Fig. 4.16. ^{1}H NMR spectrum of 3-(pyrrole-1-yl)propanesulfonate

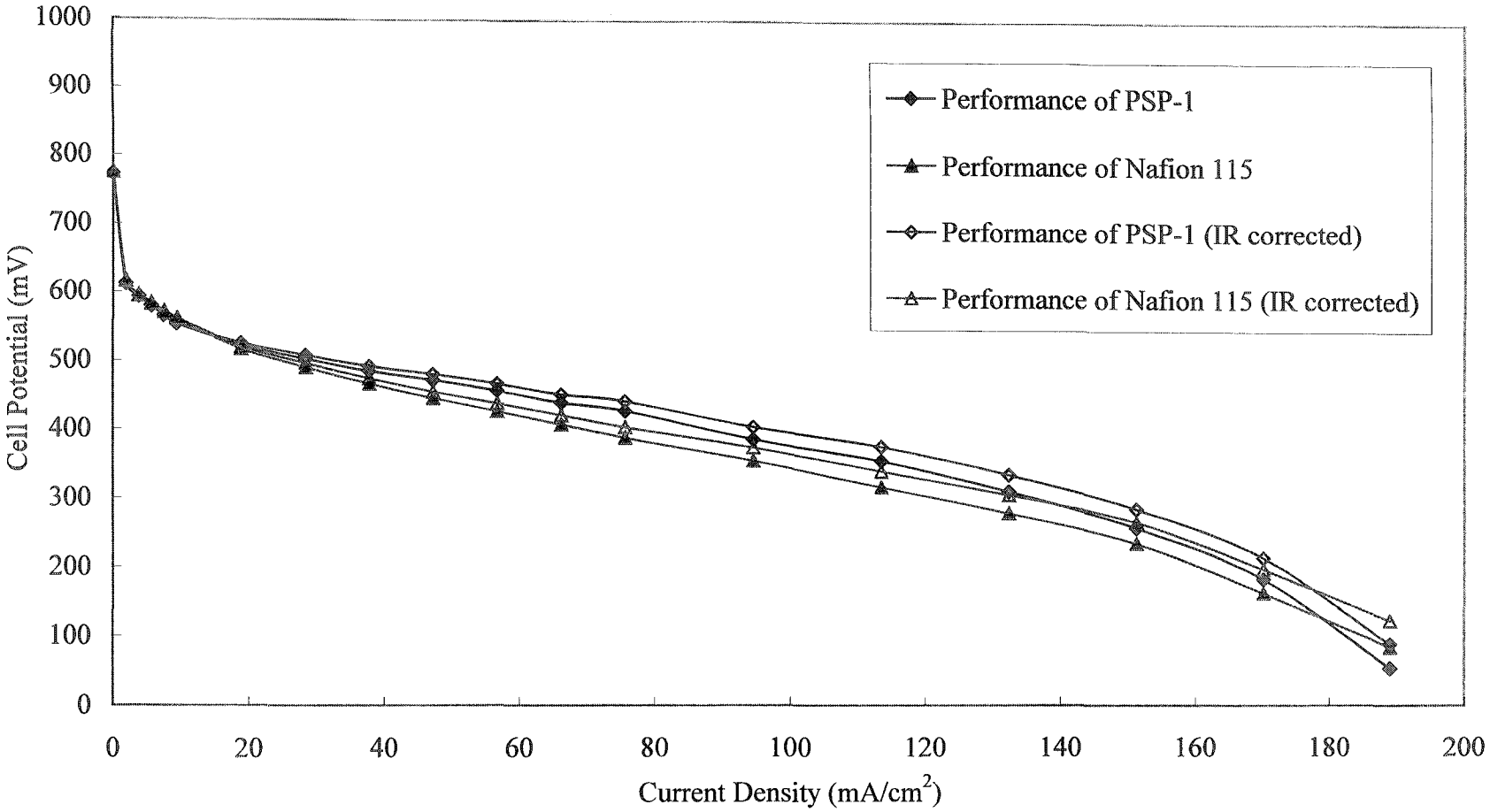

Fig .4.17. DMFC performance curves for PSP-1 and unmodified Nafion 115 (60 °C, 73 mL/min air, 0.153 mL/min 1 M methanol solution)

4.5 Conclusions

Polypyrrole/Nafion composite membranes have been characterized in DMFC in this chapter. Modified membranes have been shown to outperform Nafion 115. The improved cell performance is due to the lower methanol crossover, which leads to increased cathode performance.

Poor interfacial bonding between the electrodes and membrane results in lower catalyst utilization. Surface cleaning with H_2O_2 increases the modified membranes' Nafion surface character and improves the membrane/electrode bonding.

EIS is a powerful tool for fuel cell study and can provide diagnostic criteria to evaluate DMFC performance. Impedance spectra show that the improvement of cell performance with composite membranes with time is not only due to the slow hydration of composite membranes, also the activation of the cathode plays an important role.

To take advantage of the low methanol crossover of composite membranes but avoid the offset of their high resistance, two alternatives are proposed: providing anionic counter ions and using a new anionic monomer. The preliminary results showed that these two methods are promising and warrant further research.

In conclusion, a standard modification procedure to prepare polypyrrole/Nafion composite membranes has been developed and evaluated. The modified membranes decreases methanol crossover by 40% and outperform Nafion in a DMFC with tolerable resistances. Moreover, this procedure has very good reproducibility.

References

[1] P. G. Pickup. In *Handbook of Advanced Functional Molecules and Polymers*; H. S. Nalwa, Ed.; Gordon and Breach: Amsterdam, 2001; Vol. 3, pp155-175

[2] T. Sata, T. Funakoshi, K. Akai. *Macromolecules*, 1996, 29: 4029-4035

[3] X. Ren, T. E. Springer, T. A. Zawodzinski, S. Gottesfeld. *J. Electrochem. Soc.*, 2000, 147: 466-474

[4] G. Li, P. G. Pickup. *J. Electrochem. Soc.*, 2003, 150: C745-C752

[5] B. E. Easton. Ph.D. Thesis. Memorial University of Newfoundland. St. John's, Newfoundland, Canada. 2002

[6] R. Jiang, D. Chu. *J. Electrochem. Soc.*, 2004, 151: A69-A76

[7] R. Jiang, D. Chu. *Electrochem. Solid-State Lett.*, 2002, 5: A156-A159

[8] A. S. Aricò, S. Srinivasan, V. Antonucci. *Fuel Cell*, 2001, 1: 133-161

[9] M. Ciureanu, R. Roberge. *J. Phys. Chem. B.*, 2001, 105: 3531-3539

[10] M. C. Lefebvre, R. B. Martin, P. G. Pickup. *Electrochem. Solid-State Lett.*, 1999, 2: 259

[11] M. C. Lefebvre, Z. Qi, P. G. Pickup. *J. Electrochem. Soc.*, 1999, 146: 2054-2058

[12] J. Diard, N. Glandut, P. Landaud, B. L. Gorrec, C. Montella. *Electrochimica Acta*, 2003, 48: 555-562

[13] J. T. Müller, P. M. Urban, W. F. Hölderich. *J. Power Sources*, 1999, 84: 157-160

[14] J. T. Müller, P. M. Urban. *J. Power Sources*, 1998, 75: 139-143

[15] J. C. Amphlett, B. A. Peppley, E. Halliop, A. Sadiq. *J. Power Sources*, 2001, 96: 204

[16] S. C. Thomas, X. Ren, S. Gottesfeld. *J. Electrochem. Soc.*, 1999, 146: 4354-4359

[17] E. B. Easton, B. L. Langsdorf, J. A. Hughes, J. Sultan, Z. Qi, A. Kaufman, P. G. Pickup. *J. Electrochem. Soc.*, 2003, 150: C735-C739

[18] T. Biegler, A. J.Rand, R. Woods. *J. Electroanal. Chem.,* 1971, 29: 269-277

[19] E. A. Ticianelli, C. R. Derouin, S.Sirinivasan. *J. Electroanal. Chem.,* 1988, 251: 275

[20] A. Sungpet. *J. Membr. Sci.*, 2003, 226: 131-134

[21] N. S. Sundaresan, S. Basak, M. Pomerantz. J. R. Reynolds. *Chem. Commun.*, 1987: 621-622

[22] S. Basak, K. Rajeshwar. *Anal. Chem.*, 1990, 62: 1407-1413

Chapter 5

Characterization of a Dynamic Hydrogen Reference Electrode for Direct Methanol Fuel Cells

5.1 Introduction

While the benefits of direct methanol fuel cells as power sources for portable or mobile applications have long been demonstrated, their performances are still lower than hydrogen fuel cells and are far from commercialization.[1,2] The overall performance of a DMFC depends on many factors, such as catalyst activation on both electrodes, membrane ionic conductivity, and water management on cathode. Optimization of each component of DMFCs will lead to a significant enhancement of fuel cell performance. Therefore, a reference electrode is needed to measure and monitor both of the anode and cathode independently.[3,4]

Unfortunately, no commercial reference electrodes are available for direct methanol fuel cell studies. Unlike liquid electrolyte systems, where the working electrode potential can be obtained by placing a reference electrode in a Luggin capillary in the main current flow path close to the working electrode, the geometric restriction of thin PEMs makes it very hard to insert a reference electrode between the anode and cathode. Researchers have tried to sandwich a reference electrode between two pieces of membranes.[5,6] However, this kind of configuration causes an increase in the membrane resistance by a factor of two or more. Moreover, the presence of a reference electrode in the main current flow path may affect the current distribution in the membrane.

The anode and cathode performance can also be resolved by bonding a dynamic hydrogen electrode (DHE) on the exposed Nafion membrane as a reference electrode.[7,8]

A schematic diagram of a literature DHE is showed in Fig. 5.1. This electrode has been considered as the most reliable reference electrode. However, it is difficult to construct and use. The DMFC setup with an internal DHE reference electrode becomes very complicated and needs special design and fabrication.

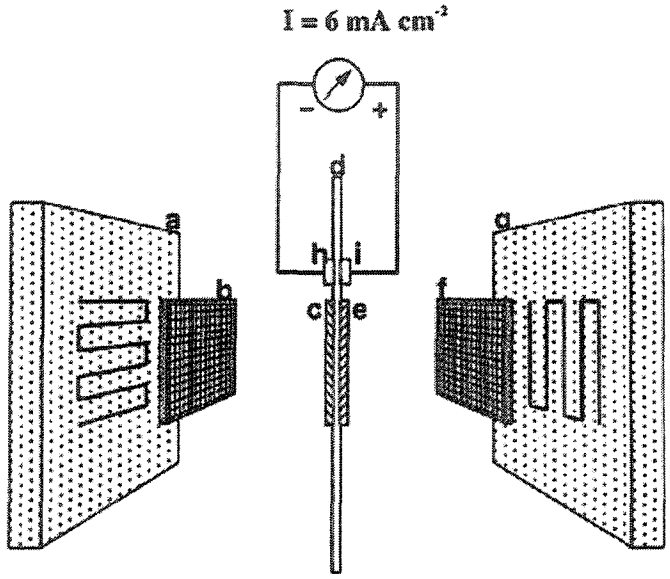

Fig. 5.1. Schematic diagram of the configuration of a DHE in a DMFC: (a) and (g) graphite blocks with cross-patterned flow field; (b) and (f) carbon cloth backings; (c) and (e) anode and cathode catalyst layers; (d) Nafion membrane; (h) DHE electrode; and (i) counter DHE electrode.

Reprinted from X. Ren, T.E. Springer, and S. Gottesfeld. *J. Electrochem. Soc.* 2000, 147: 92-98. Copyright 2000, Reproduced with the permission of the Electrochemical Society.

Another popular method, used in Chapter Four to obtain anode polarization curves,

is to pass H_2 through the cathode compartment of the cell and assume that the cathode behaves as a reversible hydrogen electrode (RHE).[9,10] The main advantage of this method is that no modification of the fuel cell setup is needed. However, the measurement is performed under different operating conditions. Therefore the anode polarization curve recorded in this way may not reflect the real anode performance of an operating DMFC.

A simple edge type DHE reference electrode configuration has been developed in the Pickup group.[11] In this chapter, this kind of reference electrode was characterized in a PEMFC and DMFC. The Pt wire reference electrode is easy to use and can provide good qualitative information for fuel cell diagnostic. However, this reference electrode suffers from potential drift when applied in DMFCs. The potential drift makes quantitative diagnosis unreliable.

5.2 Experimental

5.2.1 Configuration of the Dynamic Hydrogen Electrode (DHE) Reference Electrode

Fig. 5.2 shows a schematic diagram of the configuration of the DHE reference electrode used in this chapter. Two 0.1mm diameter Pt wires (Aldrich) were placed on the exposed Nafion membrane surface on the cathode side, and served as the DHE reference electrode and counter electrode, respectively. The distance between the Pt wires ends and the cathode edge was 0.5 cm, larger than three times of the Nafion 115 membrane thickness (125 μm) to avoid potential gradients.[12] Hydrogen is evolved on the cathodic Pt

wire, which serves as the dynamic hydrogen electrode. A current of 2-4 μA was passed through the two Pt wires to sustain hydrogen coverage on the cathodic Pt wire. Before measurements, the fuel cell was supplied with H_2 gas through the anode side and air through the cathode side. The anode side is then considered being a reversible hydrogen electrode (RHE) with a potential of zero. The DHE reference electrode potential was then adjusted to zero relative to the RHE by adjusting the current. A laboratory DC power supply (GW, model GPS-1830D) and a resistance box (General Radio Co., type 1434-G) were used to control the reference electrode potential and to maintain the current through the DHE.

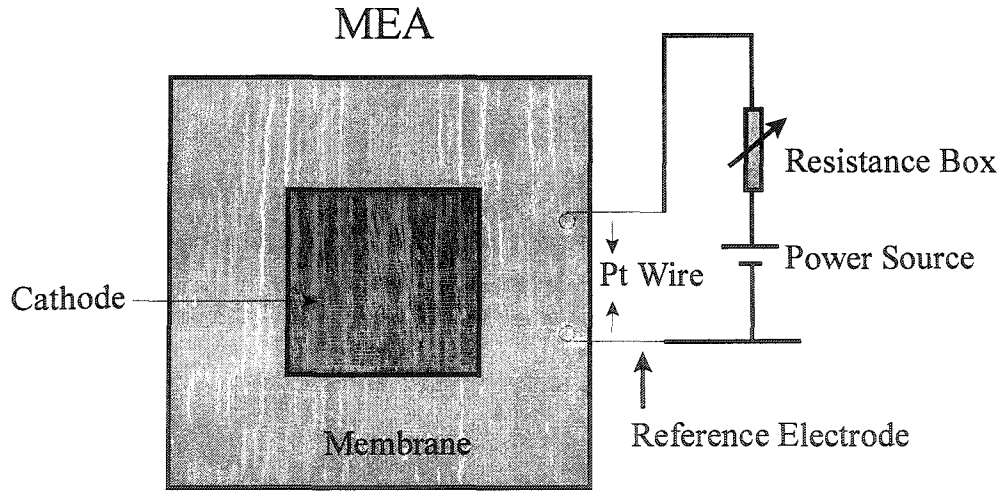

Fig. 5.2. Schematic diagram of the configuration of the DHE reference electrode.

5.2.2 Fuel Cell Measurements

Nafion 115 membranes (Dupont) were cleaned with 10% H_2O_2, 1M HNO_3, 1M

H_2SO_4 and water following the standard protocol in section 2.2.1. PtRu anodes used in this chapter consisted of 4 mg/cm^2 Pt/Ru black and 15 % Nafion on Toray carbon fiber paper (prepared by Dr. Brad Easton, described in section 2.2.1). Pt cathodes consisted of 4 mg/cm^2 Pt and 14 % PTFE on Toray carbon fiber paper (provided by Ballard Power Systems). MEAs were prepared by hot pressing at 130 °C under 100 pound/cm^2 pressure for 180s.

Electrochemical measurements were performed using a commercial 5cm^2 fuel cell (ElectroChem. Inc.) at 60 °C. Electrochemical data were recorded using a Solartron 1286/1250 electrochemical analysis system (Schlumberger).

5.3 Results and Discussion

5.3.1 Characterization of the DHE in a Hydrogen PEMFC

The electrode polarizations could be separated by measuring each electrode potential versus the reference electrode. Afterwards the fuel cell performance curve could be obtained by subtracting the anode polarization from the cathode polarization. Due to the reference electrode design, the anode and cathode versus reference electrode potential could be determined simultaneously. However, an ideal reference electrode should have certain stability over a period of time. Therefore, the cell performance, the anode polarization and cathode polarization curves were measured consecutively.

The hydrogen cell was operated with humidified H_2, by passage H_2 through a

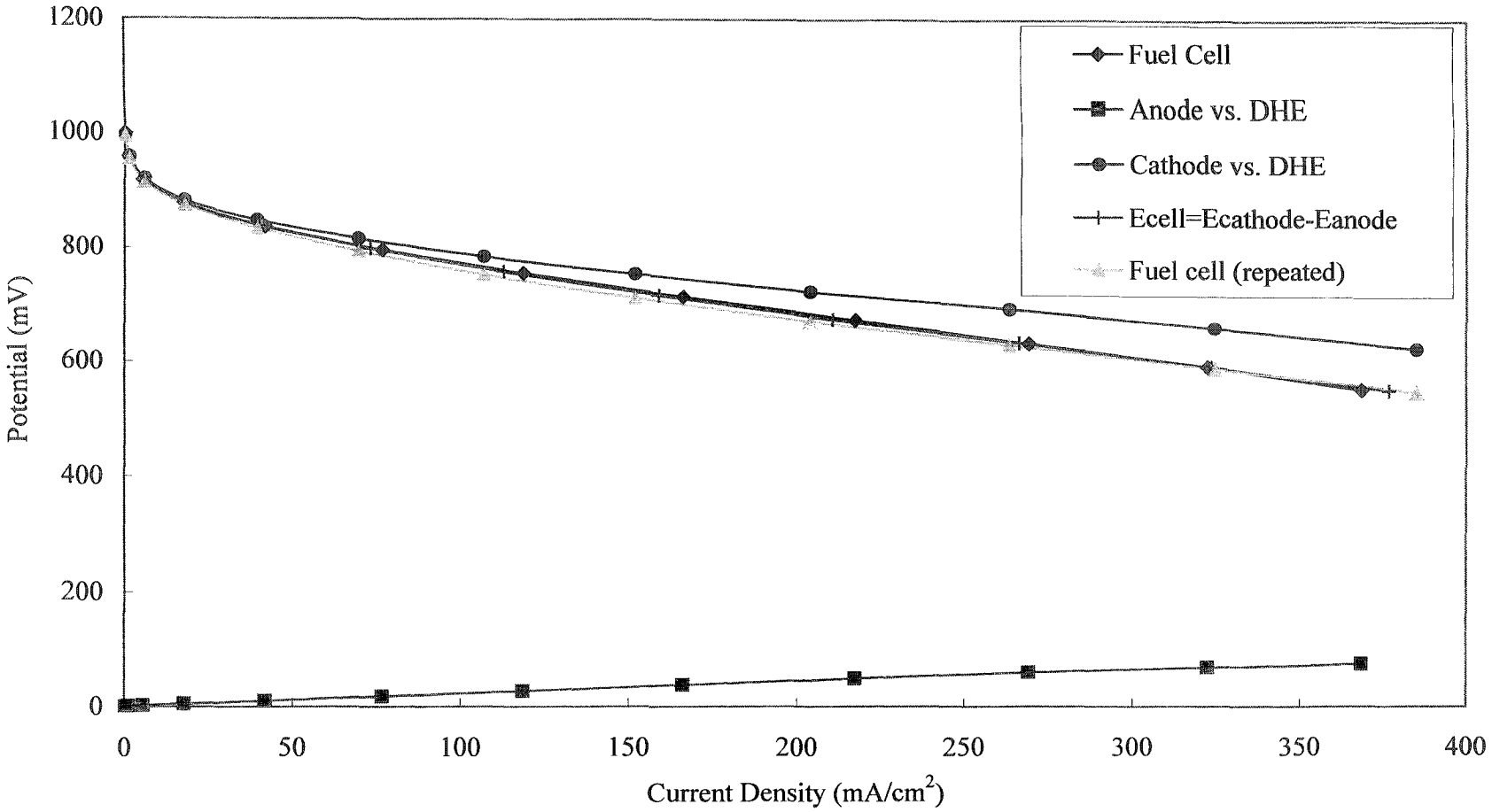

Fig. 5.3. Anode, cathode, and full cell polarization curves for a 5cm^2 fuel cell with a DHE reference electrode (RE) at 60 °C. The cell was operated with 24.6 mL/min humidified H_2 and 73.1 mL/min air.

temperature-controlled water bottle, and air at flow rate of 24.6 mL/min and 73.1 mL/min, respectively. The single electrode polarization curves and fuel cell performance curves are shown in Fig.5.3. At low current density, the cathode overpotential increases significantly with increasing current density. This reveals the slow kinetics of the oxygen reduction reaction. Then the cathode potential decreases linearly with further increase of current density. For the anode polarization, the anode can be considered as a reversible hydrogen electrode at low current density (i.e. very little overpotential). However, the anode overpotential becomes significant at high current densities. This confirms the result of Thomas *et al.*[13] A remarkable result in Fig.5.3 is that the calculated fuel cell polarization curve (E_{cell}) is almost identical to the measured ones. It can be concluded that the potential of DHE reference electrode has good stability during the hydrogen fuel cell measurements.

5.3.2 Characterization of the DHE in a DMFC

The reference electrode also characterized in a DMFC. The fuel cell was supplied with 1 M methanol solution and air at flow rates of 0.153 mL/min and 73.1 mL/min, respectively. Fig.5.4 shows the polarization curves of a $PtRu|Nafion115|Pt$ MEA. The fuel cell performance curve is nearly equal to the cathode minus the anode polarization curve. This confirms that the reference electrode showed reasonable stability during the measurements. However, it was found that the DHE potential drifted by up to 50-200mV

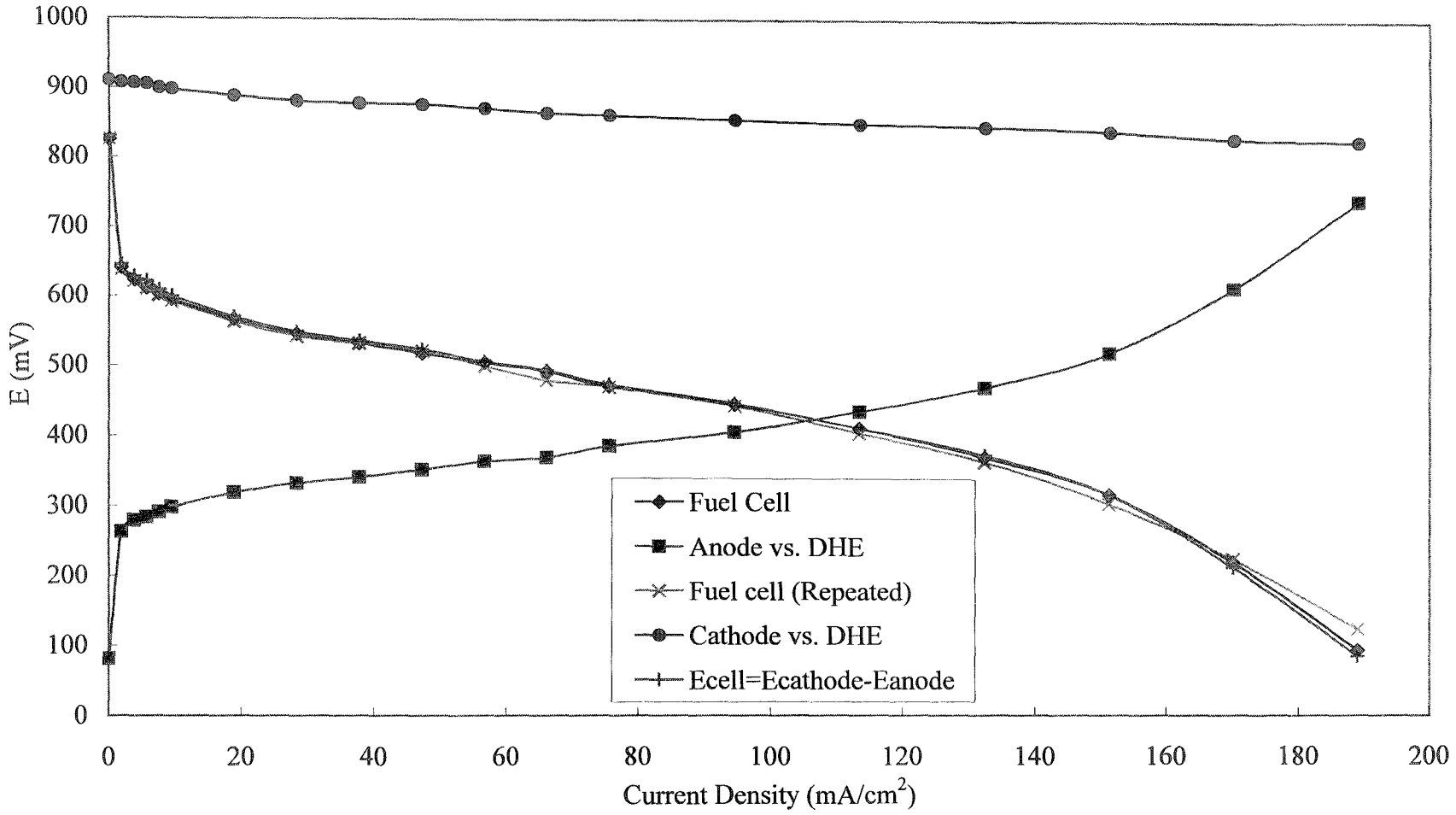

Fig. 5.4. Anode, cathode, and full cell polarization curves for a 5cm^2 DMFC with a DHE reference electrode (RE) at 60 °C. The cell was operated with 0.156 mL/min 1 M methanol solution and 73.1 mL/min air. (PtRu/Nafion 115/Pt)

when doing long-term experiments, such as the monitoring of polypyrrole/Nafion membranes. The drift is believed to be caused by poisoning of the DHE by methanol. When the reference electrode power source shut down, methanol can permeate to the Pt wire surface and adsorb. The poisoning effect could be diminished by maintaining the current through the DHE all the times. However, the RE potential drift still could not be prevented, making the long-term measurement unreliable. A methanol tolerant reference electrode is preferred to approach this problem.

Seen from Fig. 5.4, there are large overpotentials for both the PtRu anode and Pt cathode even at low current densities. This reflects the slow kinetics of methanol oxidization on anode and oxygen reduction on cathode. In this case, the cell performance is limited by the methanol mass transfer on the anode.

The electrochemical impedance spectra for the DMFC are shown in Fig. 5.5 and Fig. 5.6. Again, the agreement of the sum of the anode impedance and cathode impedance with the full cell impedance certified the validation of the DHE reference electrode. The reference electrode showed certain stability when current flow through the DMFC electrodes.

5.3.3 Comparison of Different MEAs in a DMFC

As the reference electrode shows reasonable stability, a comparison of different MEAs were done to test its usefulness. Two different MEAs were assembled using the

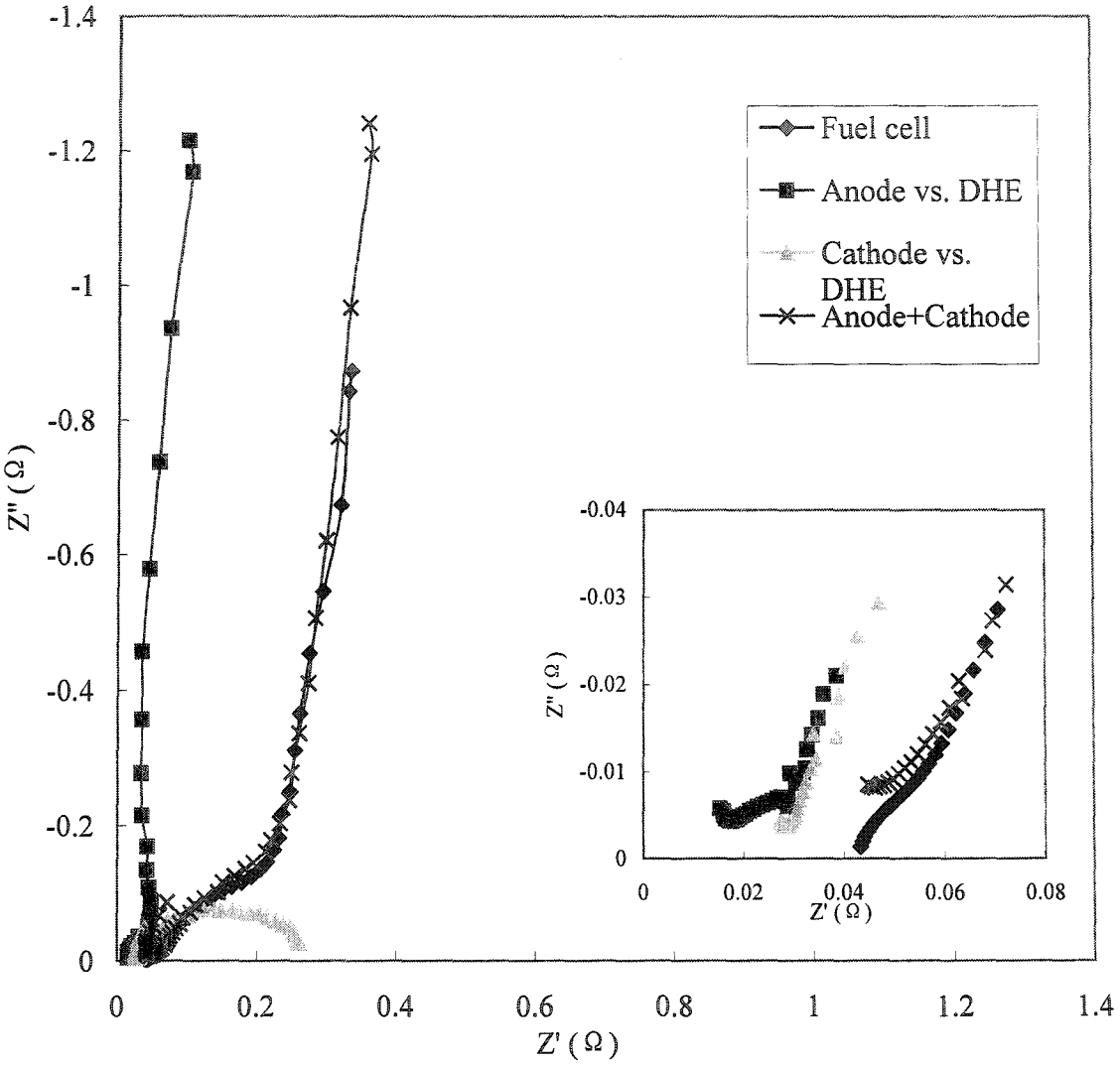

Fig. 5.5. Nyquist impedance spectra for a 5cm^2 DMFC with a DHE reference electrode at open circuit potential (65,000 to 0.82Hz). The inset shows an expansion of the high frequency region of the plots. The cell was operated at 60 °C with 0.156 mL/min 1 M methanol solution and 73.1 mL/min air.

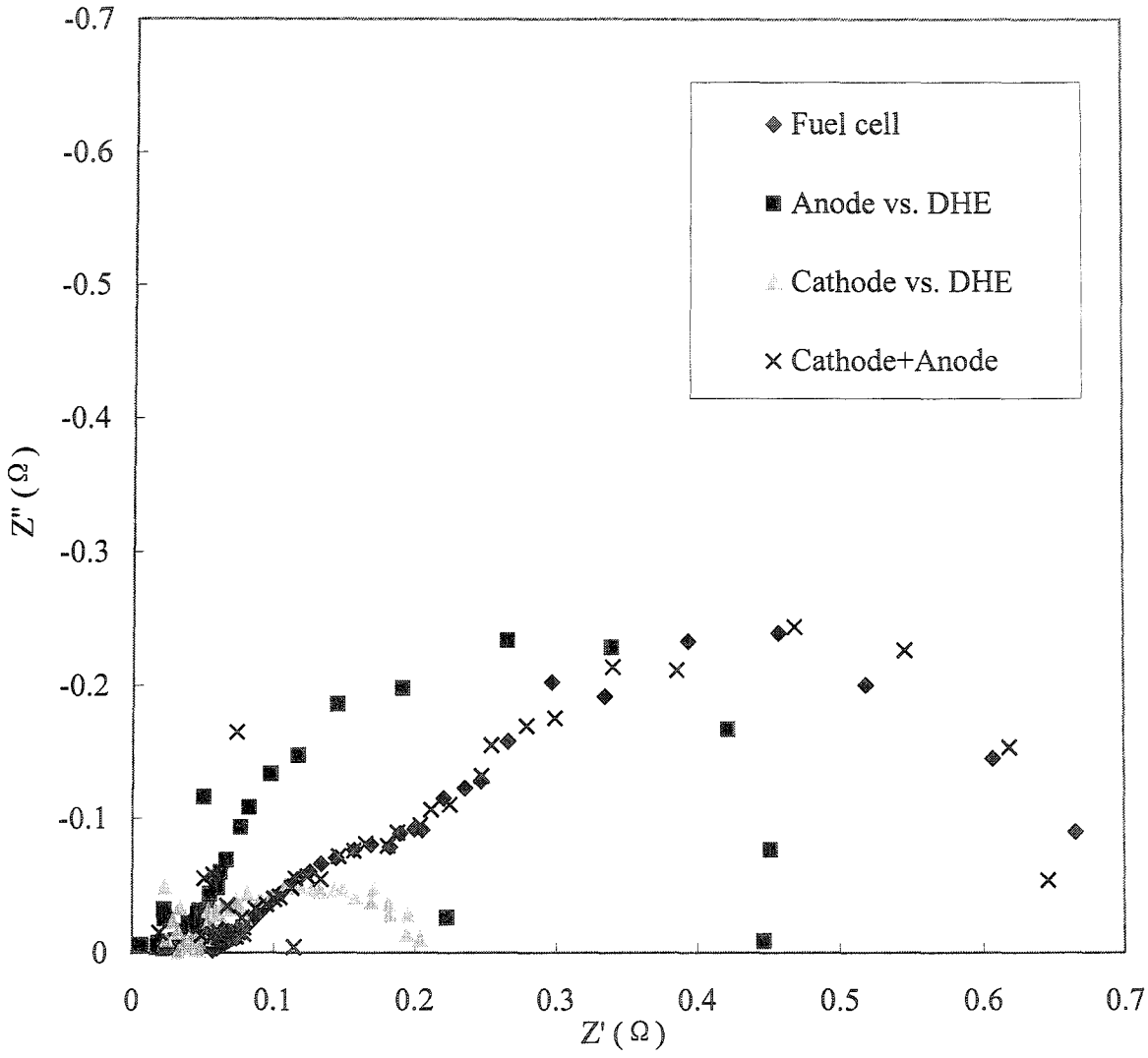

Fig. 5.6. Nyquist impedance spectra for a 5 cm^2 DMFC with a DHE reference electrode (RE) at 200 mA (65,000 to 0.82 Hz). The cell was operated at 60 °C with 0.156 mL/min 1 M methanol solution and 73.1 mL/min air.

same Pt cathode but different anodes: a) $PtRu|Nafion115|Pt$ and b) $Pt|Nafion115|Pt$.

Fig. 5.7 shows results for these two MEAs. The "anode polarization" in Fig. 5.7 was measured by the conventional method used in Chapter Four, by passing H_2 instead of air through the cathode. For each MEA, their anode vs. DHE, cathode vs. DHE and full cell data agreed very well. Unexpectedly, their cathode performances appear to differ significantly even though the cathodes were the same. One possible reason is that the RE potential was different for MEAs.

It is clear that the Pt anode needs a much higher overpotential than the PtRu anode to oxidize methanol. However, as the anode overpotential exceeds 400mV, the electrode activity improves due to the desorption of CO from the Pt surface. It is anticipated that the Pt anode will have better performance than the PtRu anode at very high current density because of more available catalyst sites. The "anode polarization curve" is also shown in Fig. 5.7. At low current density, the anode vs. DHE curve is nearly identical to the "anode polarization". However, the two polarization curves deviate from each other with increasing current density. One possible reason is that the "anode polarization" records the average potential along the electrode. For the DHE reference electrode, the measurement values may be affected by the current distribution on the electrode.[14,15] At low current density, the current is more evenly distributed on the electrodes. Thus the anode vs. DHE is close to the "anode polarization". With increasing current density, the current is less homogeneously distributed on the electrodes.

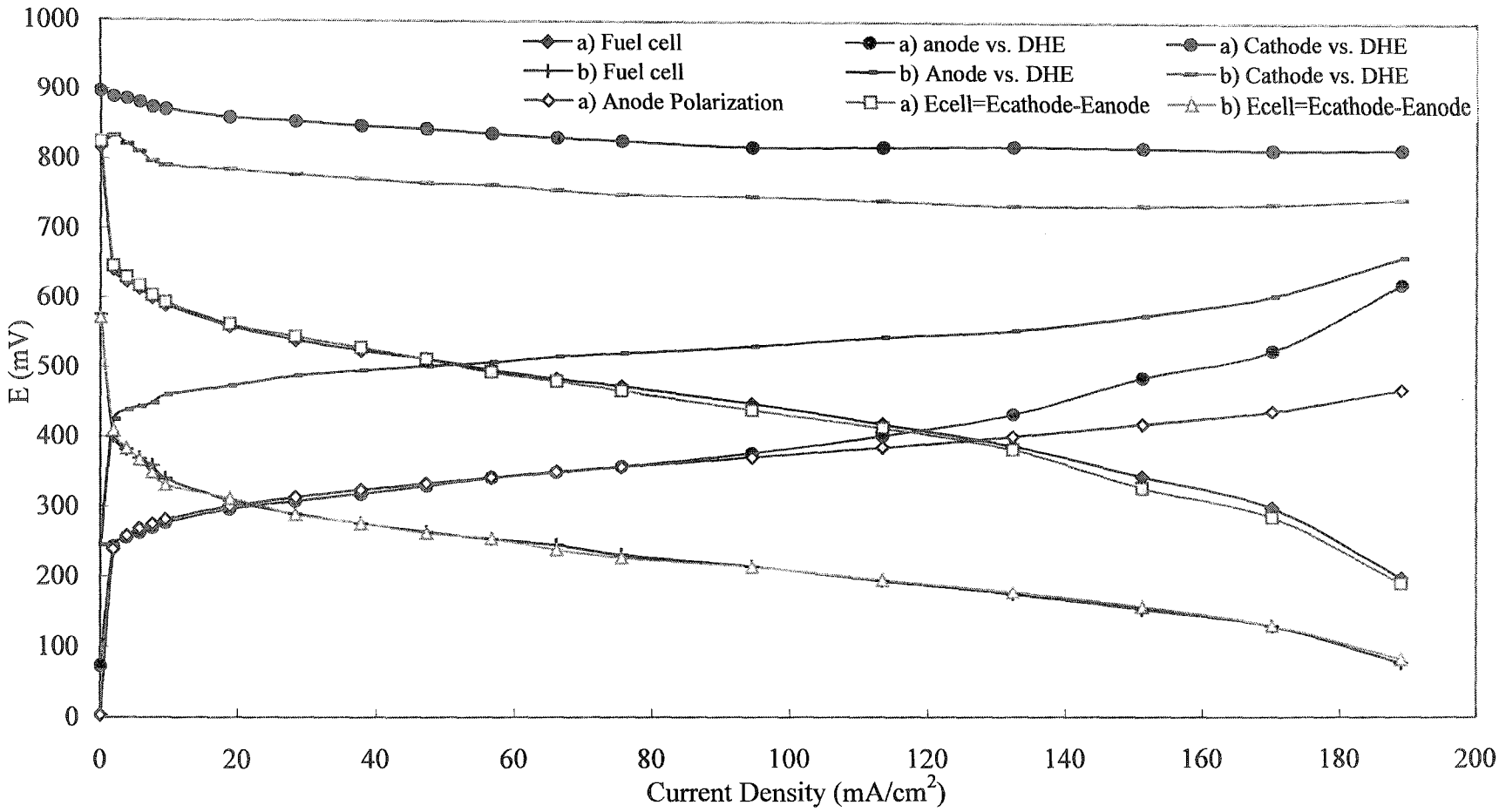

Fig. 5.7. Comparison of polarization curves for different MEAs in a 5cm^2 DMFC with a reference electrode at 60 °C. The cell was operated with 0.156 mL/min 1 M methanol solution and 73.1 mL/min air. a) $PtRu|Nafion115|Pt$; b) $Pt|Nafion115|Pt$.

5.4 Conclusions

A reference electrode that can monitor electrode performance during operation of a fuel cell is very important. In this chapter, an edge type Pt wire reference electrode was characterized by polarization measurements and impedance spectra measurements. Both experiments showed that the DHE reference electrode has some stability in a DMFC. It is easy to use and can provide good qualitative diagnostic information for DMFCs without modification of the cell hardware. However, the accuracy of this DHE reference electrode is questionable. The potential drift makes it inappropriate for long-term measurements. The DHE potential has to be adjusted frequently by passing H_2 through the anode or cathode frequently. A methanol tolerant reference, such as Ir/Ir oxide, is suggested.

References

[1] R. Jiang, C. Rong, D. Chu. *J. Power Sources*, 2004, 126: 119-124

[2] C. He, Z. Qi, M. Hollett, A. Kaufman. *Electrochem. Solid-State Lett.*, 2002, 5: A181-A183

[3] W. He, T. V. Nguyen. *J. Electrochem. Soc.* 2004, 151: A185-A195

[4] J. P. Diard, N. Glandut, P. Landaud, B. L. Gorrec, C. Montella. *Electrochimica Acta*, 2003, 48: 555-562

[5] F. N. Buchi, G. G. Scherer. *J. Electrochem. Soc.*, 2001, 148: A183

[6] A. P. Saab, F.H. Garzon, T. A. Zawoszinski. *J. Electrochem. Soc.*, 2003, 150: A214.

[7] A. Kuver, I. Vogel, W. Vielstich, *J. Power Sources,* 1994, 52: 77

[8] X. Ren, T.E. Springer, S. Gottesfeld, *J. Electrochem. Soc.* 2000, 147: 92-98

[9] S. C. Thomas, X. Ren, S. Gottesfeld, P. Zelenay. *Electrochim. Acta,* 2002, 47: 3741-3748

[10] R. Jiang, D. Chu. *J. Electrochem. Soc.* 2004, 151: A69-A76

[11] G. Li, P.G. Pickup. *Electrochimica Acta*, 2004, 49: 4119

[12] Z. Liu, J. S. Wainright, W. Huang, R. F. Savinell. *Electrochim. Acta,* 2004, 49: 923-935

[13] S. C. Thomas, X. Ren, S. Gottesfeld, P. Zelenay. *Electrochimica Acta*, 2002, 47: 3741-3748

[14] A. B. Geiger, R. Eckl, A. Wokaun, G. G. Scherer. *J. Electrochem. Soc.* 2004, 151: A394-A398

[15] M. M. Mench, C. Y. Wang. *J. Electrochem. Soc.* 2003, 150: A79-A85

Chapter 6

Summary

Methanol crossover through the Nafion proton conducting membrane is one of the two main factors that decrease the energy efficiency and limit the performance of direct methanol fuel cells. In this thesis, polypyrrole modified Nafion membranes were used to improve the fuel cell efficiency by decreasing methanol crossover.

Steps that compose of the modification procedure have been studied. The pyrrole loading is roughly proportional to the square root of the loading time, indicating a diffusion-controlled process. Polypyrrole is mainly formed inside the water filled pores in the Nafion membranes. The reduction of methanol crossover current is proportional to the amount of polypyrrole inside the Nafion membranes, which is due to the decrease of composite membranes' porosity. Higher polypyrrole contents produce lower methanol crossover rates. However, the membrane's resistance also increases with modification. An optimized modification procedure was determined as a compromise between the effects of increased membrane resistance and decreased methanol crossover.

The optimized polypyrrole/Nafion composite membranes were characterized in a DMFC. However, the presence of polypyrrole on the membrane surface caused poor interfacial bonding between the composite membranes and electrodes, and resulted in poor cell performance. After further surface cleaning of the polypyrrole on the surface with H_2O_2, the composite membranes showed superior performance than Nafion 115. In addition, this modification procedure has good reproducibility. The modified membranes decrease the methanol crossover by 40% relative to unmodified Nafion 115, but their

resistance is 70% higher. Polarization studies showed that the composite membranes usually reach their peak performance after running for three days. Anode polarization measurements and electrochemical impedance spectroscopy studies showed that the slow activation of the MEAs made from composite membranes can be attributed to two processes: the slow hydration of the modified membranes and activation of the cathode catalyst.

In order to take advantage of the low methanol crossover of composite membranes but avoid the offset of their high resistance, two alternative approaches were proposed by providing counter ions in the modification process or by using new pyrrole sulfonate monomer. The preliminary results showed the modified membranes prepared by these two methods are promising and warrant further research.

It is very important to introduce a reference electrode to acquire the performance behaviour of each electrode in an operating cell to improve cell performance. However, the DHE reference electrode used nowadays either requires a complex fuel cell design and construction, such as the external DHE, or needs major perturbation of the cell by passing H_2 through the anode or cathode compartment. A simple edge type Pt wire DHE reference electrode was introduced in this thesis. Both polarization experiments and impedance experiments have shown that this reference electrode has good short term stability in DMFCs and can provide good qualitative information. However, the DHE potential drifts over long time, making it inapplicable for long-term measurements.